

PERFORMANCE OF STONE MASTIC  
ASPHALT INCORPORATING NANO  
TITANIUM MODIFIED ASPHALT BINDER



NUR SYAFIQAH SHAMIMI BINTI MOHD  
ZALI

اونيورسيتي مليسيا قهغ

MASTER OF SCIENCE

UNIVERSITI MALAYSIA PAHANG

UNIVERSITI MALAYSIA PAHANG

## UNIVERSITI MALAYSIA PAHANG

### DECLARATION OF THESIS AND COPYRIGHT

Author's Full Name : NUR SYAFIQAH SHAMIMI BINTI MOHD ZALI  
Date of Birth : 19<sup>TH</sup> OCTOBER 1996  
Title : PERFORMANCE OF STONE MASTIC ASPHALT  
INCORPORATING NANO TITANIUM MODIFIED  
ASPHALT BINDER  
Academic Session : SEMESTER II 2021/2022

I declare that this thesis is classified as:

- CONFIDENTIAL (Contains confidential information under the Official Secret Act 1997)\*  
 RESTRICTED (Contains restricted information as specified by the organization where research was done)\*  
 OPEN ACCESS I agree that my thesis to be published as online open access (Full Text)

I acknowledge that Universiti Malaysia Pahang reserves the following rights:

1. The Thesis is the Property of Universiti Malaysia Pahang
2. The Library of Universiti Malaysia Pahang has the right to make copies of the thesis for the purpose of research only.
3. The Library has the right to make copies of the thesis for academic exchange.

Certified by:

Shamimi  
(Student's Signature)

[Signature]  
(Supervisor's Signature)

961019-05-5216  
New IC/Passport Number:  
Date: 11<sup>TH</sup> MARCH 2022

TS. DR KHAIRIL AZMAN BIN  
MASRI  
Name of Supervisor:  
Date: 11<sup>TH</sup> MARCH 2022

NOTE : \* If the thesis is CONFIDENTIAL or RESTRICTED, please attach a thesis declaration letter.

### SUPERVISOR'S DECLARATION

We hereby declare that we have checked this thesis and, in our opinion, this thesis is adequate in terms of scope and quality for the award of the degree of Master of Science.



(Supervisor's Signature)

Full Name : TS.DR KHAIRIL AZMAN BIN MASRI  
Position : SENIOR LECTURER  
Date : 11 MARCH 2022



(Co-supervisor's Signature)

Full Name : TS.DR MAZLAN BIN ABU SEMAN  
Position : SENIOR LECTURER  
Date : 11 MARCH 2022

## STUDENT'S DECLARATION

I hereby declare that the work in this thesis is based on my original work except for quotations and citations which have been duly acknowledged. I also declare that it has not been previously or concurrently submitted for any other degree at Universiti Malaysia Pahang or any other institutions.

*Shamimi*

(Student's Signature)

Full Name : NUR SYAFIQAH SHAMIMI BINTI MOHD ZALI

ID Number : MAG20003

Date : 11 MARCH 2022

UMP

اونيورسيتي ملايسيا قهغ

UNIVERSITI MALAYSIA PAHANG

PERFORMANCE OF STONE MASTIC ASPHALT INCORPORATING NANO  
TITANIUM MODIFIED BINDER



NUR SYAFIQAH SHAMIMI BINTI MOHD ZALI

**UMP**  
Thesis submitted in fulfillment of the requirements  
for the award of the degree of  
Master of Science

اونيورسيتي ملايسيا قهغ

**UNIVERSITI MALAYSIA PAHANG**

College of Engineering

UNIVERSITI MALAYSIA PAHANG

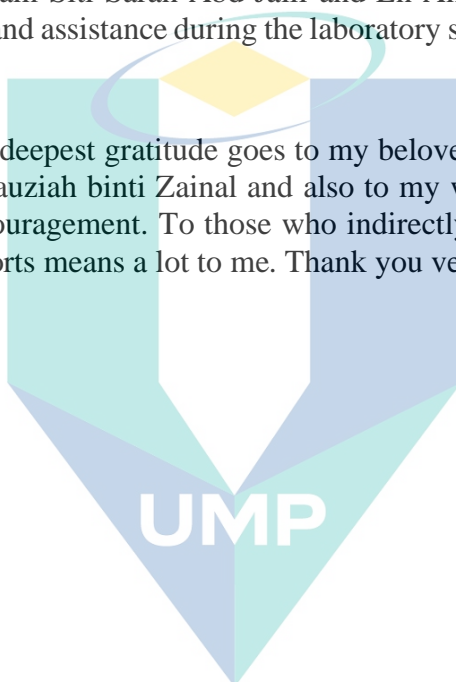
MARCH 2022

## ACKNOWLEDGEMENTS

In the name of Allah, the Most Gracious and the Most Merciful, Alhamdulillah, all praises to Allah for the strengths and His blessing in completing this thesis. I would also like to express my sincere thanks to my supervisor, Ts.Dr Khairil Azman Bin Masri and my co-supervisor Ts.Dr Mazlan bin Abu Seman for the continuous support during this research. Without their encouragement and help this thesis would not have been completed. I could not ask for a better supervisor and mentor for my study.

Special thanks to the Highway & Traffic Engineering Laboratory technicians, En Mohd Sani Mohd Noh, Madam Siti Sarah Abd Jalil and En Amir Asyraf Haji Idris for their never-ending support and assistance during the laboratory session takes place. They never fail to amaze us.

Last but not least, my deepest gratitude goes to my beloved parents; Mr. Mohd Zali bin Sopein, Mrs. Saliza Fauziah binti Zainal and also to my whole family for their endless love, prayers and encouragement. To those who indirectly contributed in this research, your kindness and efforts means a lot to me. Thank you very much



اونيورسيتي مليسيا قهغ

UNIVERSITI MALAYSIA PAHANG

## ABSTRAK

Batu mastik asfalt (SMA) adalah sejenis turapan fleksibel yang sesuai dengan kawasan lalu lintas tinggi. Oleh kerana itu, SMA dapat memenuhi jumlah trafik yang banyak. Selama bertahun-tahun, reka bentuk SMA terus bertambah baik dengan menambahkan penstabil, aditif, atau bahkan pengikat. Namun, pengubahsuaian ini kadang-kadang mahal dan tidak mesra alam. Di samping itu, kerana ciri penggredan jurang SMA di mana penggradan agregat tidak dinilai dengan baik (variasi ukuran agregat minimum), SMA mengalami beberapa kelemahan seperti pengikatan dan pengikatan pengikatan semasa pencampuran dan transportasi. Di antara bahan tambahan mungkin yang dapat meningkatkan kualitas nanomaterial. Nanomaterial dalam campuran aspal sejak kebelakangan ini menarik minat. Nanomaterial menunjukkan potensi pengubah yang dapat menghadapi masalah dalam campuran asfalt seperti ubah bentuk pramatang, busuk, dan keletihan. Oleh itu, titanium Nano digunakan dalam kajian ini dengan julat 1% hingga 5% berat bitumen dara. Bitumen yang diubah dapat diakses oleh sifat fizikalnya melalui ujian titik pelunakan, ujian penembusan dan putaran putaran, sementara untuk sifat kimia, FTIR dan XRD dilakukan, dan SEM-EDX untuk sifat morfologi. Makmal dilakukan lebih jauh dengan menilai prestasi mekanikal SMA yang diubah sesuai nano dengan modulus yang tahan lasak, kerentanan, dan ujian ujian dinamis. Dari hasilnya, pada penambahan 3% nano titanium, modulus berdaya tahan SMA menunjukkan peningkatan kekuatan 50% berbanding dengan sampel yang tidak diubah untuk suhu 20°C dan 50°C. Saluran pengikat juga menunjukkan pada sampel nano titanium 2% yang diubah suai, saluran pengikat turun dikurangkan sebanyak 91.5%. Perkara yang sama berlaku untuk pengikatan yang diubah pada 3% untuk SEM-EDX, yang menentukan pengikatan yang lebih baik tanpa pengikatan pengikatan bahan kimia yang sudah ada. Kesimpulannya, pengubahsuaian pengikat dengan titanium nano telah mempengaruhi komposisi pengikat yang membawa peningkatan dalam semua aspek bitumen yang mendorong prestasi mekanik campuran. Kajian ini dilakukan untuk meningkatkan prestasi mekanikal aspal batu mastik dengan pengikatan dengan nano titanium dengan harapan dapat memperoleh campuran SMA yang lebih baik yang dapat mempengaruhi lebih raya Malaysia

اونيورسيتي مليسيا فھق

UNIVERSITI MALAYSIA PAHANG

## ABSTRACT

Stone mastic asphalt (SMA) is a type of flexible pavement that suit to high traffic area. Therefore, SMA can cater high volume of traffic loads. Over the years, SMA design keeps improving by adding stabilizers, additives, or even modifying the binder. However, this modification sometimes costly and not environmentally friendly. In addition, due to gap graded characteristic of SMA where the aggregate gradation is not well graded (minimum aggregate size variation), SMA suffers a few drawbacks like bleeding and binder drain off during mixing and transporting. Among the potential additive that may improve the properties is nanomaterials. Nanomaterials in asphalt mixture have pique interest lately. Nanomaterials show a potential modifier that can encounter problems in asphalt mix like premature deformation, rutting, and fatigue. Thus, Nano titanium was used in this study with the range of 1% to 5% by weight of virgin bitumen. The modified bitumen is accessed by its physical properties through softening point test, penetration test and rotational viscosity, while for chemical properties, FTIR and XRD are carried out, and SEM-EDX for morphological properties. The laboratory is further performed by assessing the mechanical performance of nano-modified SMA by its resilient modulus, moisture susceptibility, and dynamic creep test. From the results, at 3% addition of nano titanium, the resilient modulus of SMA shows a 50% increasement in strength compared to the unmodified sample for both 25°C and 40°C. The binder drain down also shows at 2% nano titanium modified sample, the binder drains down is reduced by 91.5%. The same goes for modified binder at 3% for SEM-EDX, which shows more well-dispersed binder components without eliminating the chemical binder elements that are already present. In conclusion, the modification of the binder with nano titanium has influenced the composition of the binder which brings improvements in all aspect of the bitumen which promotes the mechanical performance of the mix. This study is done to improve the mechanical performance of stone mastic asphalt by modifying the binder with nano titanium in hope to obtain a more well enhanced SMA mixture that could contribute to the expressways of Malaysia.

اونيورسيتي ملايسيا قهغ

UNIVERSITI MALAYSIA PAHANG



## TABLE OF CONTENT

<b>DECLARATION</b>	
<b>TITLE PAGE</b>	
<b>ACKNOWLEDGEMENTS</b>	<b>ii</b>
<b>ABSTRAK</b>	<b>iii</b>
<b>ABSTRACT</b>	<b>iv</b>
<b>TABLE OF CONTENT</b>	<b>v</b>
<b>LIST OF TABLES</b>	<b>x</b>
<b>LIST OF FIGURES</b>	<b>xi</b>
<b>LIST OF SYMBOLS</b>	<b>xiv</b>
<b>LIST OF ABBREVIATIONS</b>	<b>xv</b>
<b>LIST OF APPENDICES</b>	<b>xvi</b>
<b>CHAPTER 1 INTRODUCTION</b>	<b>1</b>
1.1 Stone Mastic Asphalt	1
1.2 Problem statement	2
1.3 Objectives	3
1.4 Significance of study	4
1.5 Scope of study	5
1.6 Thesis outline	5
<b>CHAPTER 2 LITERATURE REVIEW</b>	<b>7</b>
2.1 Introduction	7
2.2 Binder	7
2.3 Materials used in binder modification	8
2.3.1 Waste materials	8
2.3.2 Reclaimed Asphalt Pavement (RAP)	15

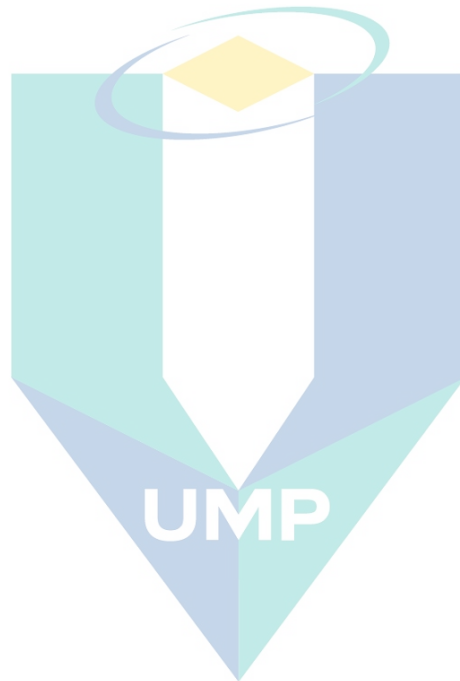
اونيورسيتي ملايسيا فاهغ  
UNIVERSITI MALAYSIA PAHANG

2.3.3	Crumb rubber	15
2.4	Polymer in binder modification	16
2.5	Morphological and Chemical properties	18
2.6	Stone Mastic Asphalt	24
2.6.1	Basic concept of pavement	24
2.6.2	Overview of Flexible pavement	25
2.7	Type of flexible pavement	25
2.7.1	Dense Graded Asphalt	25
2.7.2	Porous Asphalt	26
2.7.3	Polymer Modified Asphalt	27
2.8	History of SMA	27
2.8.1	Advantages of SMA	28
2.8.2	Disadvantages of SMA	33
2.8.3	Design requirement	35
2.9	Application of nanomaterials	37
2.10	Nano titanium dioxide (Nano TiO <sub>2</sub> )	46
2.11	Gap of Research	49
<b>CHAPTER 3 METHODOLOGY</b>		<b>53</b>
3.1	Introduction	53
3.2	Flow of research	53
3.3	Source of raw materials	55
3.4	Materials preparation	55
3.5	Materials properties	56
3.6	Materials testing methods	58
3.6.1	Sieve Analysis	58

3.6.2	LA Abrasion	59
3.6.3	Aggregate Impact Value	59
3.6.4	Aggregate Crushing Value	60
3.6.5	Bitumen	60
3.6.6	Nano titanium dioxide	61
3.6.7	Bitumen modification process by using binder mixer	61
3.6.8	Type of mixture	62
3.7	Physical properties test	62
3.7.1	Softening point test	62
3.7.2	Penetration test	64
3.7.3	Rotational Viscosity test	65
3.8	Morphological properties of nano titanium modified binder	66
3.8.1	X-Ray Diffraction Analysis (XRD)	66
3.8.2	Scanning Electron Microscope with Energy Dispersive X-Ray Analysis (SEM-EDX)	68
3.9	Chemical properties of nano titanium modified binder	69
3.9.1	Fourier Transform Infrared Spectroscopy (FTIR)	69
3.10	Mechanical properties of SMA	70
3.10.1	Volumetric properties (Marshall Stability)	70
3.10.2	Resilient Modulus	71
3.10.3	Dynamic creep	72
3.10.4	Moisture Susceptibility	73
3.11	Binder drain down	75
3.12	Summary of materials testing and sample	76
<b>CHAPTER 4 RESULTS AND DISCUSSION</b>		<b>78</b>
4.1	Introduction	78

4.2	Physical properties of aggregates	78
4.2.1	Sieve Analysis	78
4.2.2	LA Abrasion	79
4.2.3	Aggregate Impact Value	80
4.2.4	Aggregate Crushing Value	80
4.3	Physical properties of binder	81
4.3.1	Softening point	81
4.3.2	Penetration test	82
4.3.3	Rotational viscosity	83
4.4	Morphological and chemical properties	84
4.4.1	X-Ray Diffraction Analysis (XRD)	84
4.4.2	Scanning Electron Microscope with Energy Dispersive X-Ray Analysis (SEM-EDX)	86
4.4.3	Fourier Transform Infrared Spectroscopy (FTIR)	91
4.5	Volumetric properties of nano modified SMA	93
4.5.1	Stability	93
4.5.2	Flow	95
4.5.3	Stiffness	98
4.6	Mechanical properties of nano modified SMA	101
4.6.1	Resilient Modulus	101
4.6.2	Dynamic Creep	103
4.6.3	Moisture susceptibility	105
4.7	Binder drain down	107
4.8	Summary of results	108
	<b>CHAPTER 5 CONCLUSIONS</b>	<b>111</b>
5.1	Conclusion	111

5.2 Recommendation	112
<b>REFERENCES</b>	<b>114</b>
<b>APPENDICES</b>	<b>124</b>



اونيورسيتي ملايسيا قهغ

**UNIVERSITI MALAYSIA PAHANG**

## LIST OF TABLES

Table 2.1	Gradation for SMA20	35
Table 2.2	Summary of grade of bitumen used in previous research	36
Table 2.3	Some of the effects of using nanomaterials as observed in their research.	44
Table 2.4	Publications involving the related keywords starting from 1970 to 2021	50
Table 3.1	Aggregated gradation for SMA20 (JKR, 2008)	57
Table 3.2	Properties of bitumen	60
Table 3.3	Properties of nano titanium	61
Table 3.4	Summary of materials testing and sample	76
Table 4.1	LA Abrasion value results	79
Table 4.2	Aggregate Impact Value result	80
Table 4.3	Aggregate crushing value results	80
Table 4.4	Rotational viscosity results	84
Table 4.5	Unmodified and modified bitumen elements	90
Table 4.6	Ranking table for the mechanical tests on samples	109
Table 4.7	Ranking table for the tests on binder samples	109
Table 4.8	Objective parameters	110

اونيورسيتي ملايسيا قهغ

UNIVERSITI MALAYSIA PAHANG

## LIST OF FIGURES

Figure 2.1	Microstructure image of eggshell (ES) powder (a) 1000×(b) 5000×(c)10 000× (d)30 000×. The dotted lines shows the observation range at different multiples.	10
Figure 2.2	IR spectrum of asphalt binder	10
Figure 2.3	Penetration test, Softening point and Ductility test	11
Figure 2.4	Worlwide plastic waster, including PET from 1950-2015	12
Figure 2.5	Resilient modulus of modified mixtures	14
Figure 2.6	ITS values of mixtures	14
Figure 2.7	Fatigue life of mixtures	15
Figure 2.8	Viscosity values ar 135°C and 165°C	18
Figure 2.9	XRD patterns of base AP-5 asphalt and modified samples	22
Figure 2.10	Scanning electron microscope (SEM) micrographs with their corresponding EDXS spectra of unmodified and DCG-modified asphalts. (a) 0% DCG, (b) 3% (c) 6% (d) 9% DCG	23
Figure 2.11	AFM topography and friction images with their corresponding histograms on the right side highlighting the influence of DCG on base AP-5 asphalt micromorphology and friction.	24
Figure 2.12	Flexible pavement cross section	25
Figure 2.13	Example of typical dense graded asphalt cross-section	26
Figure 2.14	Example of porous pavement	26
Figure 2.15	EVA (%) against binder drain off (%)	29
Figure 2.16	Flow number valus of SMA-EVA modified mixes	30
Figure 2.17	Master curves for SMA mixtures	31
Figure 2.18	Fatigue parameter of SMA mixtures	32
Figure 2.19	Nano ZnO and Nano RGO used	33
Figure 2.20	FESEM images of nano modified binders at different mixing times	39
Figure 2.21	Publications involving type of pavement	51
Figure 2.22	Publications involving materials	51
Figure 2.23	Publications involving testing methods	52
Figure 3.1	Flow of laboratory experiments	54
Figure 3.2	Binder mixer machine	56
Figure 3.3	Aggregate sample	58
Figure 3.4	Sieve shaker machine	58
Figure 3.5	Binder mixing procedures	62
Figure 3.6	Samples after being cooled on ring apparatus	63

Figure 3.7	Samples falling when reaching softening point	64
Figure 3.8	Penetration test apparatus set up	65
Figure 3.9	Rotational viscometer machine	66
Figure 3.10	D8 Advance (Brand: Bunker)	67
Figure 3.11	Samples for XRD	67
Figure 3.12	Samples for SEM-EDX	68
Figure 3.13	FTIR machine	69
Figure 3.14	Sample for FTIR-Atr	69
Figure 3.15	Marshall stability set up	70
Figure 3.16	Resilient modulus set up	71
Figure 3.17	UTM Machine	72
Figure 3.18	Sample set up for dynamic creep	73
Figure 3.19	Indirect tensile machine	74
Figure 3.20	Samples in water bath at 25°C	75
Figure 3.21	Binder drain down basket	76
Figure 4.1	SMA20 aggregate gradation	79
Figure 4.2	Softening point results	82
Figure 4.3	Penetration test results	83
Figure 4.4	Rotational viscosity at 135 °C and 165 °C	84
Figure 4.5	XRD graphs for nano titanium modified binder	85
Figure 4.6	XRD graph for nano titanium powder	86
Figure 4.7	0% nano titanium modified bitumen	87
Figure 4.8	1% nano titanium modified bitumen	87
Figure 4.9	2% nano titanium modified bitumen	88
Figure 4.10	3% nano titanium modified bitumen	88
Figure 4.11	4% nano titanium modified bitumen	88
Figure 4.12	5% nano titanium modified bitumen	88
Figure 4.13	Control Sample	88
Figure 4.14	1% nano titanium modified bitumen	89
Figure 4.15	2% nano titanium modified bitumen	89
Figure 4.16	3% nano titanium modified bitumen	89
Figure 4.17	4% nano titanium modified bitumen	90
Figure 4.18	5% nano titanium modified bitumen	90
Figure 4.19	Transmittance (%) vs. wavenumbers (cm <sup>-1</sup> ) spectral interpretation of unmodified bitumen.	92



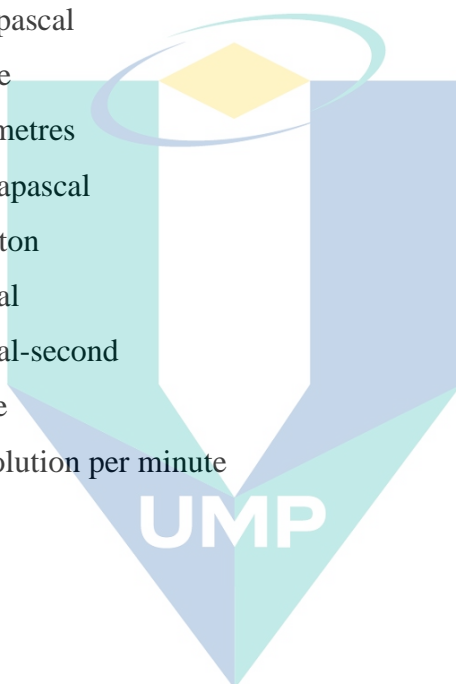
Figure 4.20	Transmittance peaks of unmodified bitumen.	92
Figure 4.21	Transmittance peaks of 3% nano titanium modified bitumen	93
Figure 4.22	Stability and density against nano titanium percentages	94
Figure 4.23	Stability and flow against nano titanium percentages	94
Figure 4.24	Stability and Density R <sup>2</sup> values	95
Figure 4.25	Stability and Flow R <sup>2</sup> values	95
Figure 4.26	Density and Flow against nano titanium percentage	96
Figure 4.27	Flow and stiffness against nano titanium percentages	97
Figure 4.28	Density and Flow R <sup>2</sup> values	97
Figure 4.29	Stiffness and Flow R <sup>2</sup> values	98
Figure 4.30	Stiffness and density against nano titanium percentages	99
Figure 4.31	Stability and stiffness against nano titanium percentages	99
Figure 4.32	Stiffness and Density R <sup>2</sup> values	100
Figure 4.33	Stability and Stiffness R <sup>2</sup> values	100
Figure 4.34	Resilient modulus vs Amount of Nano Titanium at 25°C	102
Figure 4.35	Resilient modulus vs Amount of Nano Titanium at 40°C	103
Figure 4.36	Permanent strain vs cycles	104
Figure 4.37	Creep stiffness values	105
Figure 4.38	ITS value vs Amount of Nano Titanium	106
Figure 4.39	TSR value vs Amount of Nano Titanium	107
Figure 4.40	Binder drain down vs Amount of Nano Titanium	108

اونيورسيتي ملايسيا قهغ

UNIVERSITI MALAYSIA PAHANG

## LIST OF SYMBOLS

°C	Celsius
cp	centipoise
cm	centimetres
dmm	decimillimetre
°F	Fahrenheit
K	Kelvin
KPa	Kilopascal
m	metre
mm	millimetres
Mpa	Megapascal
N	Newton
Pa	Pascal
Pa.s	Pascal-second
P	Poise
RPM	Revolution per minute



اونيورسيتي مليسيا قهغ

UNIVERSITI MALAYSIA PAHANG

## LIST OF ABBREVIATIONS

ASTM	American Society for Testing and Materials
AFM	Atomic Force Microscopy
BS	British Standard
DGA	Dense Graded Asphalt
EDX	Energy dispersive X-Ray
FTIr	Fourier Transform Infrared
HMA	Hot Mix Asphalt
JKR	Jabatan Kerja Raya
NP	Nano particles
NT	Nano Titanium
NS	Nano Silica
NC	Nano Clay
PA	Porous Asphalt
PMB	Polymer Modified Bitumen
PWD	Public Work Department
RV	Rotational Viscosity
SBS	Styrene-Butadiene-Styrene
SEM	Scanning Electron Microscope
SMA	Stone Mastic Asphalt
WMA	Warm Mix Asphalt
XRD	X-Ray Diffraction

اونیورسیتی ملیسیا فہم

UNIVERSITI MALAYSIA PAHANG

## LIST OF APPENDICES

Appendix A: Resilient Modulus of Nano titanium modified binder of SMA mix at 25°C & 40°C.	124
Appendix B: Graphs of Marshall properties	126
Appendix C: Graphs of Marshall properties	128
Appendix D: Images from scanning electron microscope (SEM) of unmodified bitumen	132
Appendix E: Images from scanning electron microscope (SEM) of 1% NT modified bitumen	133
Appendix F: Images from scanning electron microscope (SEM) of 2% NT modified bitumen	134
Appendix G: Images from scanning electron microscope (SEM) of 3% NT modified bitumen	135
Appendix H: Images from scanning electron microscope (SEM) of 4% NT modified bitumen	136
Appendix I: Images from scanning electron microscope (SEM) of 5% NT modified bitumen	137
Appendix J: FTIR Absorbance peaks for bitumen	138
Appendix K: FTIR Absorbance peaks for nano titanium	139
Appendix L: FTIR Absorbance peaks for 1% and 2%	140
Appendix M: FTIR Absorbance peaks for 3% and 4%	141
Appendix N: FTIR Absorbance peaks for 5%	142
Appendix O: FTIR Absorbance peaks stacking	143
Appendix P: FTIR Absorbance peaks overlay	143
Appendix Q: Spectral interpretation of bitumen	144
Appendix R: Spectral interpretation of nano titanium	144
Appendix S: Spectral interpretation 1% and 2%	145
Appendix T: Spectral interpretation 3% and 4%	146
Appendix U: Spectral interpretation 5%	147

# CHAPTER 1

## INTRODUCTION

### 1.1 Stone Mastic Asphalt

Stone mastic asphalt (SMA) appeared in Germany in the mid 1960's due to heavy loads from studded tires; SMA was made to resist those loads, and thus it was deemed to no longer be needed when the use of such tires was banned. However, it was found that SMA has excellent permanent deformation resistance, countries have begun using SMA for their general road pavements (Sadeghnejad & Shafabakhsh, 2017). SMA is a kind of hot mastic asphalt (HMA) consisting of two parts of large size aggregate and bitumen-filled mortar (bitumen mix, filler and stabilizing additives) (Liu et al., 2020). This constitution makes SMA have more durability, stability and more resistance to permanent deformation. Nanomaterials however could play a good role in improving SMA properties.

SMA offers a deformation-resistant, robust surface material that is ideal for high-traffic roads. SMA has been described as a sustainable asphalt surfacing alternative for residential streets and highways in Europe, Australia, the United States and Canada. SMA has a high gross aggregate content that interlocks to form a stone skeleton that prevents permanent deformation (Woodward et al., 2016). The stone skeleton is filled with bitumen mastic and filler to which the fibers are applied to provide sufficient bitumen stability and to prevent binder leakage during transport and placement (Korayem et al., 2020). SMA, properly designed and produced, has excellent properties.

Unfortunately, due to its gap graded structure when the filler is added it needs extra time to be filled and this could affect SMA productivity (Ameli et al., 2020). Not only that, but increased material cost are associated with SMA, as it needs higher asphalt binder and filler contents, as well as a fiber additive. Besides that, the fatigue life of SMA

is also affected when the load exerted exceeds its limit, since the real-life conditions differ from the production stage.

Recently there has been an increase in interest in using nanomaterials in the pavement industry to explore the performance of mixtures when nanomaterials are included as an additive. Several studies have been performed on the use of various forms of nano particles as a modification factor for bitumen and hot asphalt mixtures. Some of the evident advantages of using nanomaterials is increased aging resistance, improved moisture susceptibility and enhance mechanical performance. Among various nanomaterials, nano hydrated lime contributed the most in increasing the moisture damage resistance of hot mastic asphalt (HMA) mixes according to (Razavi & Kavussi, 2020).

This research is done to evaluate the performance of stone mastic asphalt with nano titanium incorporated as the asphalt modifying binder. With nano titanium properties that could improve asphalt aging properties and premature permanent deformation like fatigue and rutting, stone mastic asphalt could have longer fatigue life, more resistance to permanent deformation and stands higher loads for a longer period of time. The nano titanium modified binder would reduce the time taken for the filler to set properly into the mastic and increase the adhesion between the aggregates and binder in order to reduce binder drain down in the stone mastic asphalt. This study is done to provide a more suitable material to be used in SMA design to improve the condition of the road that is exposed to extreme weather and increasing traffic demand.

## **1.2 Problem statement**

Stone mastic asphalt has been used in highly trafficked roads as conventional pavement has less resistance to the increasing loads on pavement. With its high content of coarse aggregates, SMA provides more contact between the stones and thus makes the structure more durable (Arshad et al., 2017). Pavement always has a relationship with the climatic changes or the rainy season in some countries, but traffic conditions have been left out as one of the contributors to pavement distresses (Miranda et al., 2020). However, this high content of coarse aggregate makes the structure of SMA have gaps in between the aggregates. As a result, the gaps would enable the binder to flows from it. This would

happen during the mixing process as the temperature is high during that time. Additionally, it could also happen during the placing of the mix, before the mix consolidates are set. Binder drain-down is bound to happen, which is why there are stabilisers, additives and modifiers introduced in order to prevent excessive bleeding of bitumen from the SMA mix.

Binder is a viscous fluid and its properties like adhesion, durability, flow and resistance to water do affect the properties of the pavement. The binder that is being used in the pavement consists of a certain selected grade, and usually has a limitation depending on the process of mixing the material, the weather and the material properties itself. The binder may be adhesive in the early stage of life but after a certain period of time, the bitumen may experience conditions that may deteriorate the component of the mix itself. Since Malaysia has a rainy season and experiences floods, it could affect the pavement, as the binder is not very resistant to moisture damage. Moreover, the binder is used in a gap-graded mix, which has a higher chance of getting water into the voids of the pavement. This would then bring premature deformations to the road, since the material is already exposed to moisture. Some related permanent deformations that may occur because of this are rutting and potholes.

Stone mastic asphalt commonly uses polymers in order to strengthen the mix, but with recent developments in nanotechnology, nano materials drawing attention for their uses in pavement mixes to counter problems such as rutting, fatigue and binder drain-down in stone mastic asphalt. Nanomaterials like nano silica, nano clay and others are being implemented into the pavement, but usually the focus has been on the mix only. For this research nano titanium is chosen as the nanomaterial to be used in the binder, before being added into the mix. The physical, rheological and chemical properties of the binder are assessed and the mechanical performance of the mix is evaluated.

### **1.3 Objectives**

The objective of the study is to assess the overall performance of stone mastic asphalt with a nano titanium modified binder. Among the objectives are:



1. To determine the physical and rheological properties of a nano titanium modified asphalt binder.
2. To assess morphological and chemical characteristics of a nano titanium modified asphalt binder.
3. To evaluate the mechanical performance of a nano titanium modified stone mastic asphalt.

#### 1.4 Significance of study

Stone mastic asphalt has been used as a choice for high traffic pavements such as expressways, as it is able to withstand loads for a longer time. The instances of using stone mastic asphalt vary according to the countries involved or the anticipated usage, and some nations decide to include additives like polymers. Stone mastic asphalt is valued for its ability to resist high axle loads, but possesses problems with the excess drain-off of bitumen. This condition is called binder drain-down and is a common problem in SMA.

Because of that, various additives have been implemented, but still drain-down cannot be reduced significantly. Due to this, nanotechnology is being introduced and nanomaterials are being used in pavement mixes, with many choosing to use nanomaterials either as a stabiliser, additive or even modifier. The advantages of using nanomaterials include lower costs, enhanced performance, ease of procurement and many more. With its broad spectrum, the pavement industry has been looking to expand further regarding the use of nanomaterials.

Hence, the use of nano titanium in stone mastic asphalt could reduce its main problem that is always raised which is binder drain-down. The chosen nanomaterial is nano titanium. The properties of nano titanium could also improve other aspects of stone mastic asphalt like offering longer service life, increased durability and reduced moisture susceptibility.



## 1.5 Scope of study

For this study, SMA20 is used and the specifications are adopted from the Public Work Department of Malaysia (JKR, 2008). The bitumen used is of a 60/70 penetration grade. The bitumen is melted in the oven for about one to two hours approximately. The nano titanium is obtained in powder form and used from 1% to 5% by bitumen weight. Then, the binder mixer machine is operated at 165°C and for one hour for the mixing process. The nano titanium modified binder is prepared by mixing the required percentage of nano titanium from 1% to 5% with the bitumen.

The nano titanium modified bitumen would then be further evaluated for its physical and rheological properties. The tests involved are: softening point, penetration test and rotational viscosity. Next, the nano titanium modified bitumen is evaluated for its chemical and morphological properties, and among the tests involved are X-Ray Diffraction analysis (XRD) and Fourier Transform Infrared Spectroscopy (FTIR), which is completed using Atr-Ftir. The last test uses the Scanning Electron Microscope with Energy Dispersive X-Ray Analysis (SEM-EDX).

Finally, the mechanical properties of the stone mastic asphalt that has been incorporated with the nano titanium modified binder are evaluated by Marshall stability (Volumetric properties), Resilient modulus, Dynamic creep, moisture susceptibility and binder drain-down. For the volumetric properties, the following are observed: stability, flow and stiffness. Meanwhile the resilient modulus is assessed in two conditions, which are 135°C and 165°C. Moisture susceptibility is done in both wet and dry conditions. The optimum content of nano titanium would be finalised and is determined at the end of the study.

## 1.6 Thesis outline

The following are the summaries for each chapter included in this thesis. The chapters are explained briefly with each of their characteristics.

Chapter 1 starts with the introduction of the stone mastic asphalt material itself. The introduction briefly speaks about the history, usage, advantages and problems in

using stone mastic. Next is the problem statement, which covers what the previous research has found from using stone mastic asphalt and follows by expounding on the common problems that have not been solved. This is followed by stating the objectives in doing the research and explaining the significance of the study.

Chapter 2 is the literature review; it includes topics like the materials used in binder modification and pavement types. There is also a discussion of the properties of the asphalt and binder, alongside with the previous research conducted with their findings and concerns. The history of stone mastic asphalt, its advantages, disadvantages and application are also elaborated on. Nanomaterials, alongside with its application, are discussed in this chapter, together with nano titanium as the material chosen for the research.

Chapter 3 talks about the details of the research. The type of materials, specifications used and all testing done in the research are explained. There are three stages in the laboratory process, and each of the stages are explained in regard to the process involved. The procurement of the materials, and the amount of materials used are also covered in this chapter. The tests involved are referred to their own specifications and are completed with great care.

Chapter 4 presents the results and discussion on the tests that has been carried out on the materials. All the results are arranged according to each objective assigned to them. The physical and rheological properties start off first, followed by the chemical and morphology properties. Next, the mechanical properties of the stone mastic asphalt incorporated with nano titanium modified binder is covered. Lastly the optimum content of nano titanium is obtained at the end of the chapter.

Chapter 5 is the last chapter and it covers the conclusion of the research in regards to the objectives and recommendations for future research that offer future insights. This chapter concludes the study and contains areas of improvement to be used for future endeavours or related topics.

## CHAPTER 2

### LITERATURE REVIEW

#### 2.1 Introduction

This chapter presents the topics covered in this research; namely the binder itself, the materials used for binder modification, and the morphological and chemical characteristics that are involved in binder modifications. Stone mastic asphalt comes with its own history, advantages, disadvantages and design requirements. The types of flexible pavement which exists other than stone mastic asphalt are also briefly talked about. The application of several types of nanomaterials which, have been found in some research is discussed alongside with their effect and suggestions on the nanomaterials. The chosen nanomaterial used in this research which is nano titanium, is also elaborated on. The last subchapter is focused on the gap of research found in the study.

#### 2.2 Binder

For more than a century, binder has been employed in the creation of asphalt pavements. Binder, as a viscoelastic material, is crucial in defining many elements of road performance (Pipintakos et al., 2021). A bituminous mixture, for example, must be flexible enough to avoid pavement breaking at low temperatures and rigid enough to prevent rutting at high temperatures. These traditional binders, on the other hand, do not always function as planned primarily due to rising traffic volumes and increasing axle weights (Zhang et al., 2020).

As a result, the performance-related qualities of bitumen, such as resistance to permanent deformation, low temperature cracking, load-related fatigue, wear, stripping, and ageing, must be addressed for certain applications. This leads to more improvements being made to the binder, as a means of increasing its quality, and as a way to make the pavement last longer. Previously, some of the ingredients used in order to improve the

mix were waste materials, reclaimed asphalt pavement, and crumb rubber (Apostolidis et al., 2019).

Among the methods used, binder modification has been used in the pavement industry and due to the emergence of nanotechnology and nanomaterials it is getting more attention for possible modifications. The influence of different nanomaterials were being assessed in terms of their physical and rheology properties. But with nanomaterials, researchers were interested to see whether it could also affect the chemical and morphology properties of the bitumen. These modified forms of bitumen have a high chance of improving the asphalt pavement.

### **2.3 Materials used in binder modification**

Waste materials, in addition to cellulose fibre and polymers like styrene-butadiene-styrene (SBS), are being used as one of the elements which can be added to the stone mastic asphalt mix. This is compatible with ecologically friendly products and cost-cutting measures while utilising accessible natural resources, such as repurposing old asphalt pavement once it has been filtered (Amini & Imaninasab, 2018). In the asphalt pavement sector, reclaimed asphalt pavement (RAP) is one of the materials that is commonly explored with crumb rubber.

#### **2.3.1 Waste materials**

Waste materials are increasing in great numbers as the industry continues to progress. Instead of allowing excess production to go to waste, they are placed in asphalt mixtures as an aggregate replacement or filler; as recycling waste materials in asphalt mixtures have shown to make positive improvements on the roads (Rahman et al., 2020). Some of the waste materials are eggshell waste, waste rubber tires, waste engine oils, plastics, glass waste, steel slag and many more (Bamigboye et al., 2021). These waste materials are being used in a certain amount by bitumen weight or can be added up to 50% of the desired material. These could lead to more environment friendly, sustainable materials being available for future use.

Wang et al. (2021) incorporated bitumen with eggshell waste to make a material which is suitable for bio-roads construction and investigated the impact of biological eggshell powder on the high and low temperature characteristics of bitumen materials. The amounts of eggshell (ES) used were 5, 10, and 15% (mass percentage), and the shear rate was optimized. All of these were adopted from previous research and tests. The tests carried out included SEM, which revealed the eggshell powder microstructure. FT-IR was used to analyse the interaction between the egg powder and asphalt.

The high and low-temperature characteristics were investigated using conventional performance tests, which were the penetration test, softening point, and ductility index. Dynamic shear rheometer (DSR) and bending beam rheometer (BBR) experiments were also conducted. The results showed that eggshell powder has a rough and porous microstructure as seen in Figure 2.1, no apparent chemical reaction with asphalt and the consistency, hardness, and high-temperature characteristics were improved as seen in Figure 2.2 and 2.3. The research demonstrated that the application of eggshell powder in asphalt is feasible and has long-term resource and environmental advantages.

Overall, they achieved their aim to study the high and low-temperature characteristics of bitumen materials. However, they suggested to concentrate more on the interaction mechanism between biological waste and asphalt. They also encouraged researchers to develop a new composite biomaterial that can comprehensively improve the properties of bitumen.

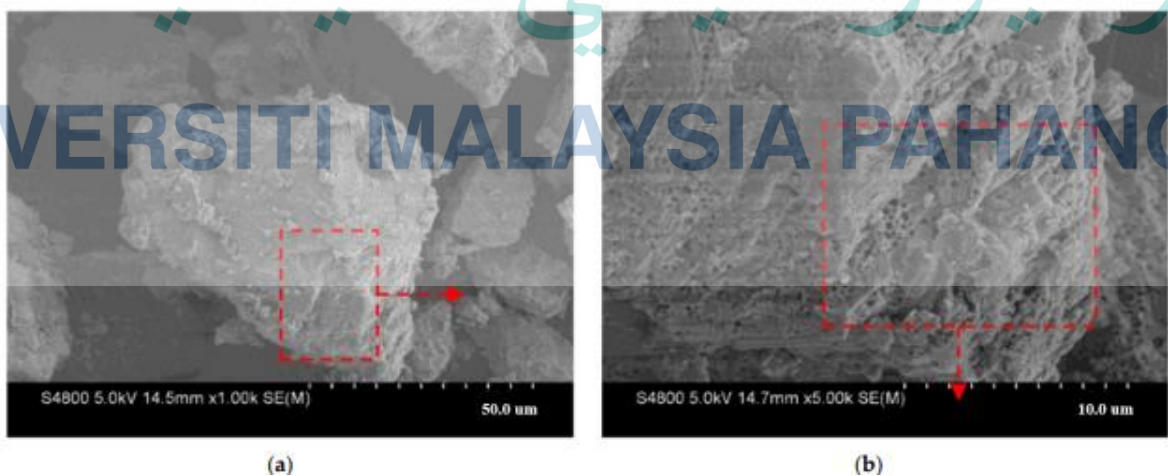




Figure 2.1 Microstructure image of eggshell (ES) powder (a) 1000×(b) 5000×(c)10 000× (d)30 000×. The dotted lines shows the observation range at different multiples.

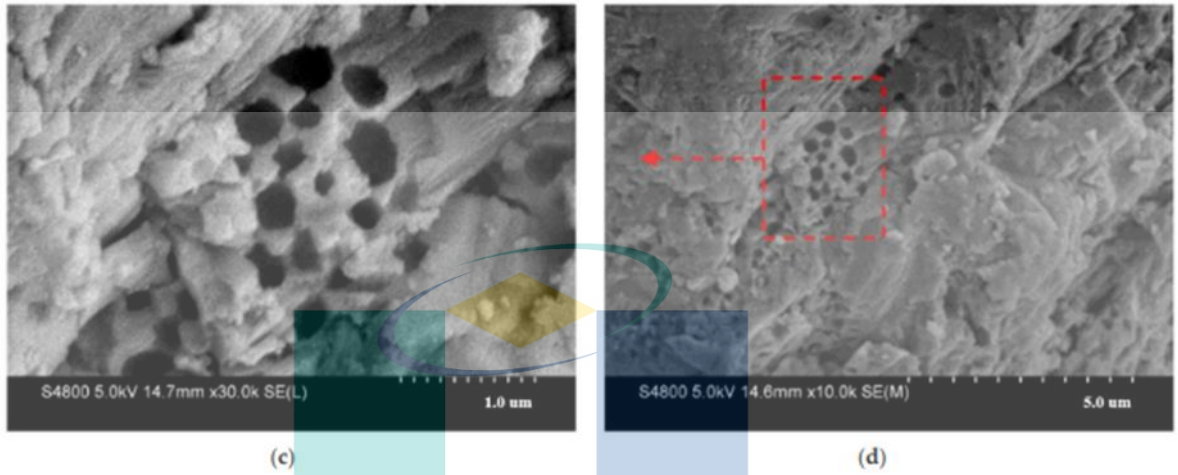


Figure 2.1 Continued  
Source: Wang et al. (2021)

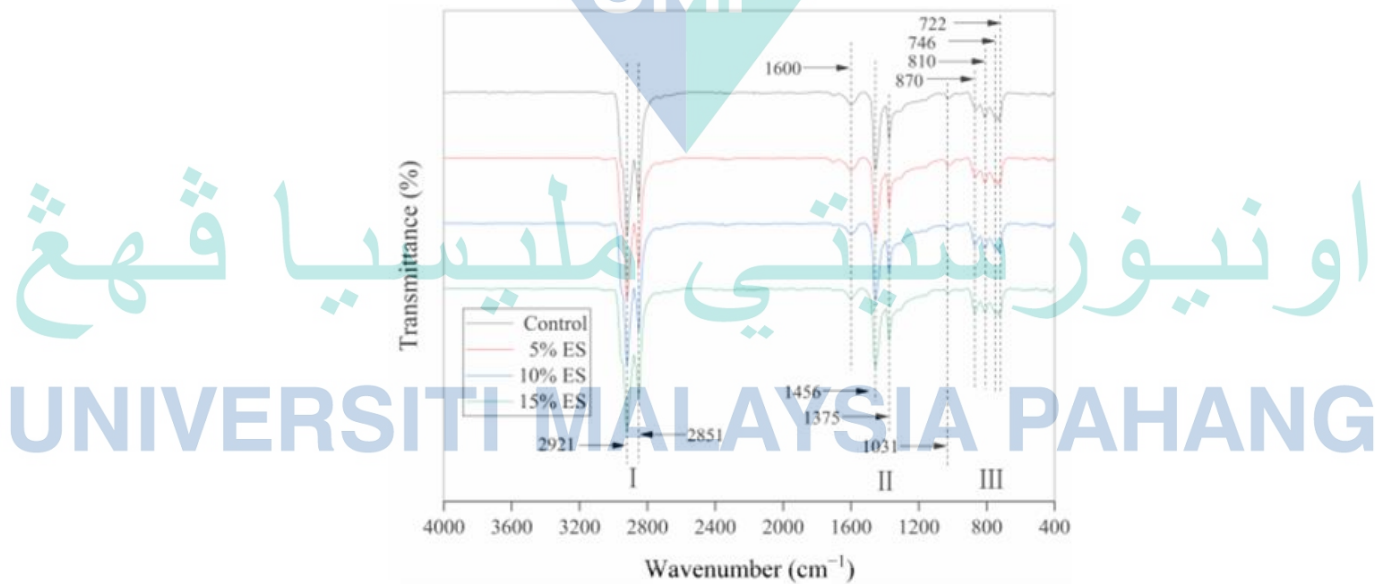


Figure 2.2 IR spectrum of asphalt binder  
Source: Wang et al. (2021)

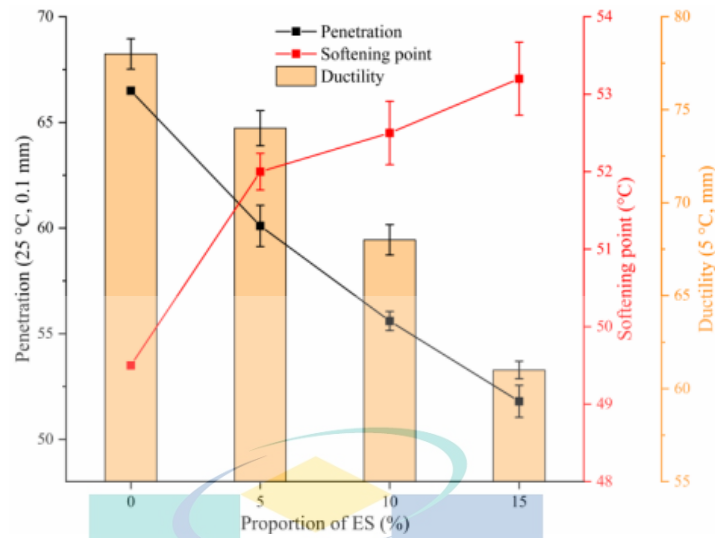


Figure 2.3 Penetration test, Softening point and Ductility test

Source: Wang et al. (2021)

Other than the materials mentioned, PET is the most common plastic waste pollutant, and according to UN Environment (2018), in every minute, about 1 million are purchased and 5 trillion plastic bags are used worldwide annually. This is because plastic has durability advantages, is lightweight and is also user-friendly (Perera et al., 2019). These waste materials can also be used as a binder modifier and rejuvenator as they improve the properties of the mix which they are replaced or added in, although not all are useful since different waste materials possess different properties. Figure 2.4 shows the numbers of plastic wastes generated from 1950-2015.

اونيورسيتي ملايسيا قهق

UNIVERSITI MALAYSIA PAHANG

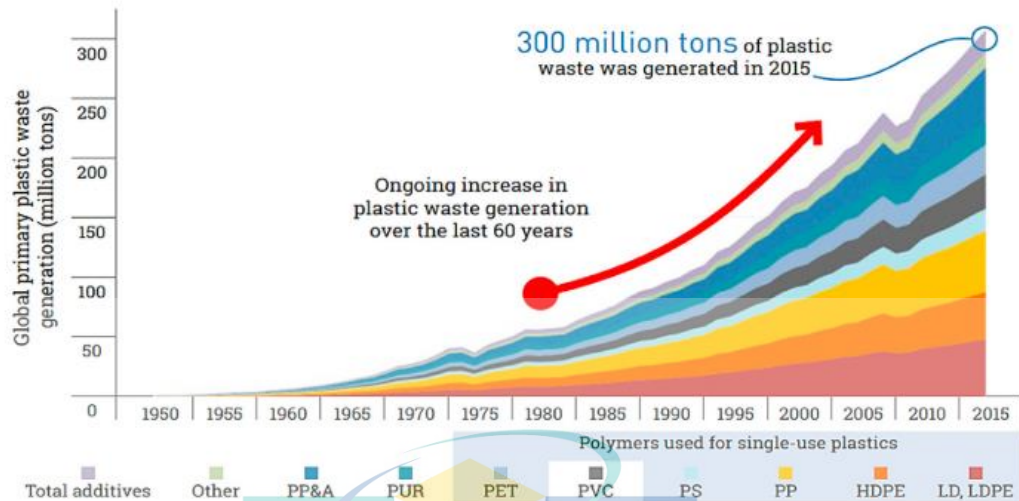


Figure 2.4 Worldwide plastic waster, including PET from 1950-2015  
Source: UNEP (2018)

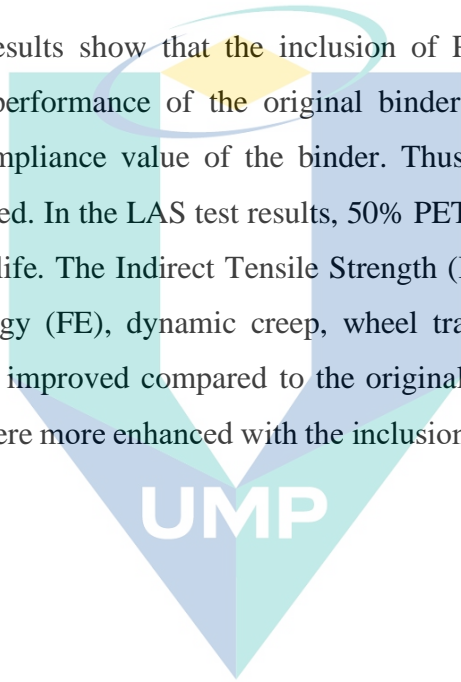
Ameli et al. (2020) carried out a study to assess the effect of Anti Stripping Agents (ASA), Ground Tire Rubber (GTR), and waste polyethylene terephthalate (PET) on the performance behaviour of binders and Stone Matrix Asphalt (SMA) mixtures. They stated that the study was needed because there had been too little research in the rheological properties of binders and the performance of CR/PET modified mixtures. They used three ASA's liquid as a modifier, which are ASA(A), ASA(B) and ASA(C). The bitumen used was of 85/100 penetration grade. The tests conducted in order to investigate the rheological properties were the Dynamic Shear Rheometer, Multi Stress Creep Recovery (MSCR), and Linear Amplitude Sweep (LAS) tests. While to evaluate the mechanical performance, Resilient Modulus, Tensile Strength, dynamic creep, wheel track, and four-point beam fatigue tests were done.

Figure 2.5 shows the resilient modulus value was enhanced as CR/PET was included. The sample with PC2B mixtures had the highest value of resilient modulus among the specimens which included ASA. The reason for this was that the ASA was able to stiffen the binder. While for the PET/CR, the addition up to 50% PET and 50% CR showed an increased value of resilient modulus. Based on Figure 2.5, the resilient modulus values of ASA-modified mixes (A) and (C) were increases up to 50%. PET, on the other hand, caused the Mr values to decline when higher percentages were used.



Figure 2.6 presents the ITS values from all of the modified samples. According to the ITS values, the usage of PET/CR and ASA increased and decreased the cohesion and adhesion of the binder to the aggregate, respectively. Figure 2.7 shows the fatigue behaviour of specimens: the results showed that using PET/CR improved the fatigue behaviour of specimens. All modified combinations have a longer fatigue life than the control mixture, with the addition of PET percentages up to 50% resulting in an ascending trend, but the addition of 75% PET resulted in a declining trend. This could be because the CR powder enhanced the negative characteristics of PET as a plastic component.

MCSR test results show that the inclusion of PET and crumb rubber (CR) enhance the rutting performance of the original binder since it decreased the non-recoverable creep compliance value of the binder. Thus, the permanent deformation resistance also increased. In the LAS test results, 50% PET and 50% crumb rubber (CR) improved the fatigue life. The Indirect Tensile Strength (ITS), Resilient Modulus (Mr) values, Fracture Energy (FE), dynamic creep, wheel track test and four-point beam fatigue test values all improved compared to the original. The fatigue life and rutting aspects of the SMA were more enhanced with the inclusion of PET/CR and ASA's in the binders and mixtures.



اونيورسيتي مليسيا قهغ

UNIVERSITI MALAYSIA PAHANG

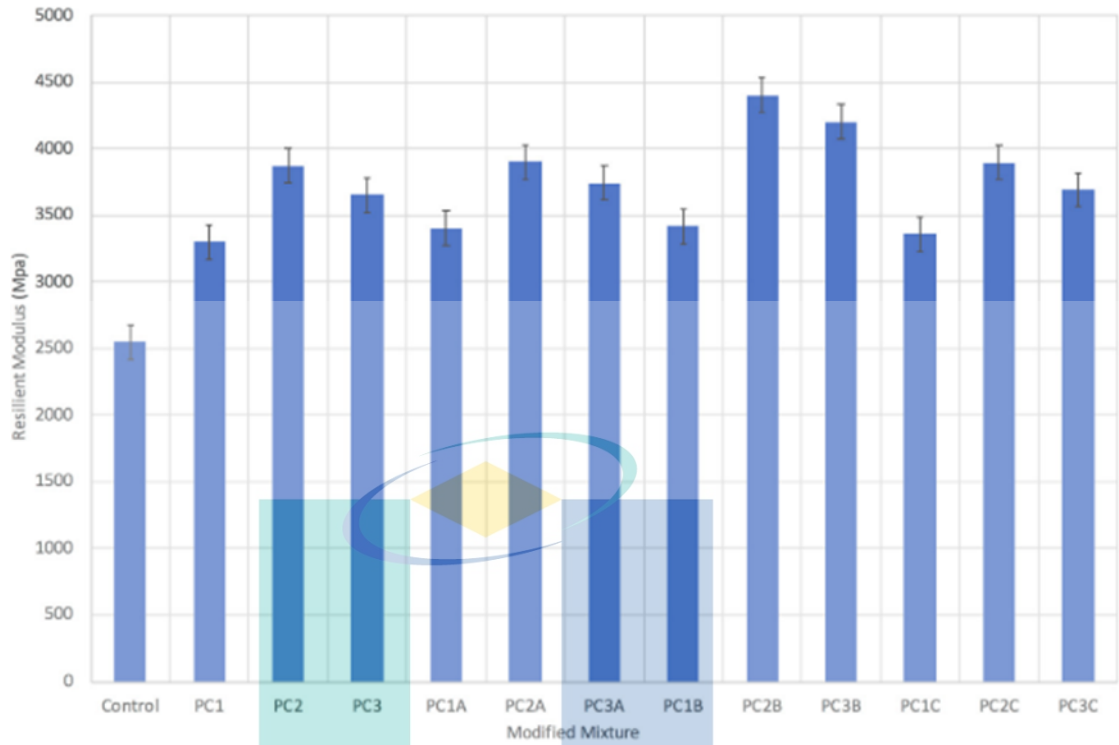


Figure 2.5 Resilient modulus of modified mixtures

Source: Ameli et al. (2020)

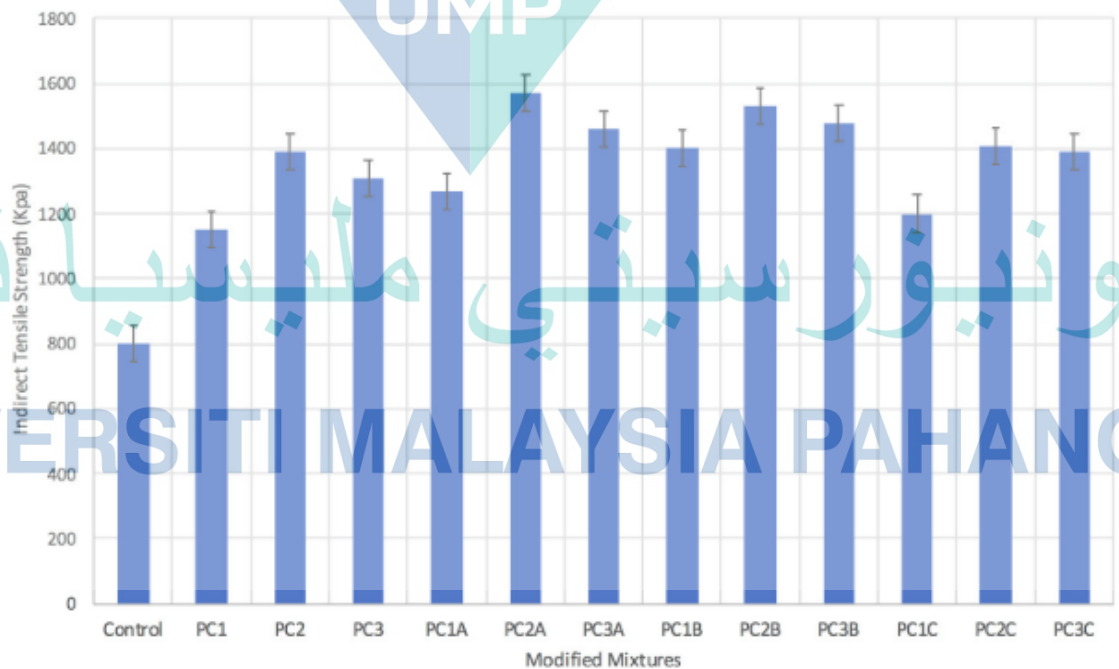


Figure 2.6 ITS values of mixtures

Source: Ameli et al. (2020)

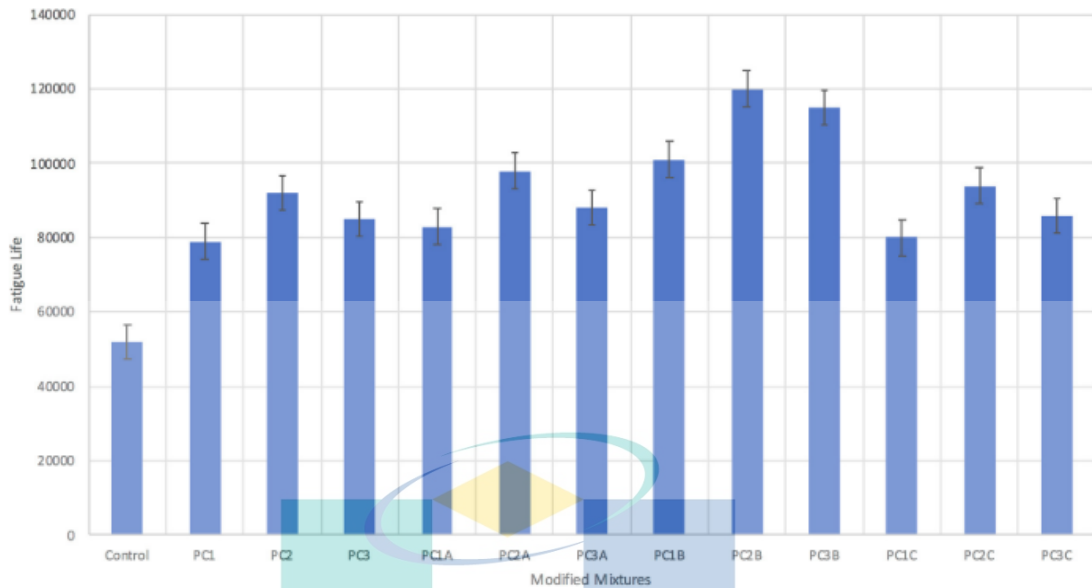


Figure 2.7 Fatigue life of mixtures

Source: Ameli et al. (2020)

### 2.3.2 Reclaimed Asphalt Pavement (RAP)

Reclaimed asphalt pavement is used in pavement construction as a method for saving costs and for also saving natural resources. RAP has been used in previous research with a 20% to 100% ratio in the asphalt mix (Orešković et al., 2020). Reclaimed asphalt pavement (RAP) is a substance created when asphalt pavements are removed for repair, resurfacing, or access to buried utilities. The usage of RAP in asphalt pavement has proven to increase the performance of asphalt in both strength and stability (Choudhary et al., 2020).

The paving industry has a high rate of emission for carbon dioxide, and the high demands it places on natural resources is also worrying. Without change, the situation could become unsustainable for future generations, making it far more important to use RAP in order to save natural resources from further depletion (Fernandes et al., 2019).

### 2.3.3 Crumb rubber

Crumb rubber is made up of elastomeric compounds, steel and fabric. It is generated from end-of-life vehicles and lorry tires, which cannot be disposed of

completely without any treatment, which add to the number of waste tires accumulating in the landfills (Rodríguez-Fernández et al., 2020). These waste tires are traditionally eliminated by burning, but the excessive number of waste tires making it increasingly hazardous as they release harmful gases like carbon dioxide which leads to environmental pollution. There are three processes involved in producing asphalt rubber from crumb rubber which are the wet process (ARwet), dry process (ARdry), and terminal process (ARtb) (Picado-Santos et al., 2020).

Crumb rubber is suggested for use in asphalt mixtures as an additive, partial aggregate replacement and modifier (Mohammed et al., 2018). The structure of crumb rubber determines the performance of the crumb rubber modified asphalt, as when it is added into the asphalt mix, the mix forms a honeycomb structure which enhances the adhesion between the aggregates as compared to the mix without crumb rubber (Chen et al., 2019). This makes crumb rubber one of the promising alternatives which can be added into any asphalt mix to enhance some of the resulting mechanical performance.

#### **2.4 Polymer in binder modification**

In the past years, a demand for high-quality bitumen has arisen in order to create more durable pavement that requires less maintenance and has less of a rehabilitation concern. The most widely used method to date is the use of polymer modified bitumen (PMB). Some of the most used polymers are polyethylene (PE), polypropylene (PP), ethylene-vinyl acetate (EVA) and styrene-butadiene-styrene (SBS) (Ameli et al., 2020). Although none of these mentioned polymers were initially meant for bitumen modification, they seem to produce a satisfying effect on some of the properties of bitumen, like increasing the stiffness at higher temperatures, improving cracking at low temperatures or even allowing for longer fatigue life (Eskandarsefat et al., 2019). It may seem that everything is going well with the modification by using polymers, but they also exhibit some drawbacks. Some mentioned drawbacks are their high cost, high temperature sensitivity, poor storage stability and limited improvement in elasticity (Ren et al., 2020).

These polymers are not easily obtained, and getting your hands on them would involve a relatively high expense depending on what type of polymers you wanted to use

(Lin et al., 2019). Next, they are sensitive to high temperatures, although they also promotes the improvement of bitumen at high temperatures (Yusoff et al., 2019). The major concern however regarding PMBs would be their poor storage stability.

Mirsepahi et al. (2020) in their study, which aimed at modifying polymer bitumen with a combination of nano clay and nano lime sought to address rutting as one of the major problems in pavement. PG 58-16 bitumen was used and modified with nano clay and nano lime. Three samples with different percentages by bitumen weight were used. The optimal percentage of each of the nanomaterials, nano clay and nano lime, was 4% based on protocols from previous studies. In order to produce a modified bitumen with specifications similar to PG 58-16, 3% of SBS was added to PG 64-22 pure bitumen. Rotational viscosity tests were performed to determine the viscosity parameter. The results showed that the viscosity of the polymer bitumen when added with nanomaterials at a constant temperature, increased and the stiffness changed accordingly.

Figure 2.8 shows the viscosity values at 135°C and 165°C. At a constant temperature, the addition of nanomaterials to the polymer bitumen increased the viscosity and the stiffness of the bitumen was also modified accordingly. At 135°C, comparing NL4NC4 with the control sample, it was found that the addition of a NC and NL compound to a polymer bitumen resulted in an increase in viscosity due to nanomaterials. The cumulative strain decreased compared to the control sample, and this decrease, continue to grow by increasing the percentage of NL and NC modifiers up to 6%. On the other hand, they concluded that an increase in temperature has a negative effect on the cumulative strain but by increasing the percentage of NL and NC modifiers the impact could change.

The results revealed that the addition of modifiers to polymer bitumen increased the stiffness of the bitumen and improved the rutting characteristics at zero shear viscosity due to the rise in viscosity (ZSV). In this investigation, the effect of nano-lime on improved rutting resistance was much greater than that of nano-clay in all three studies.

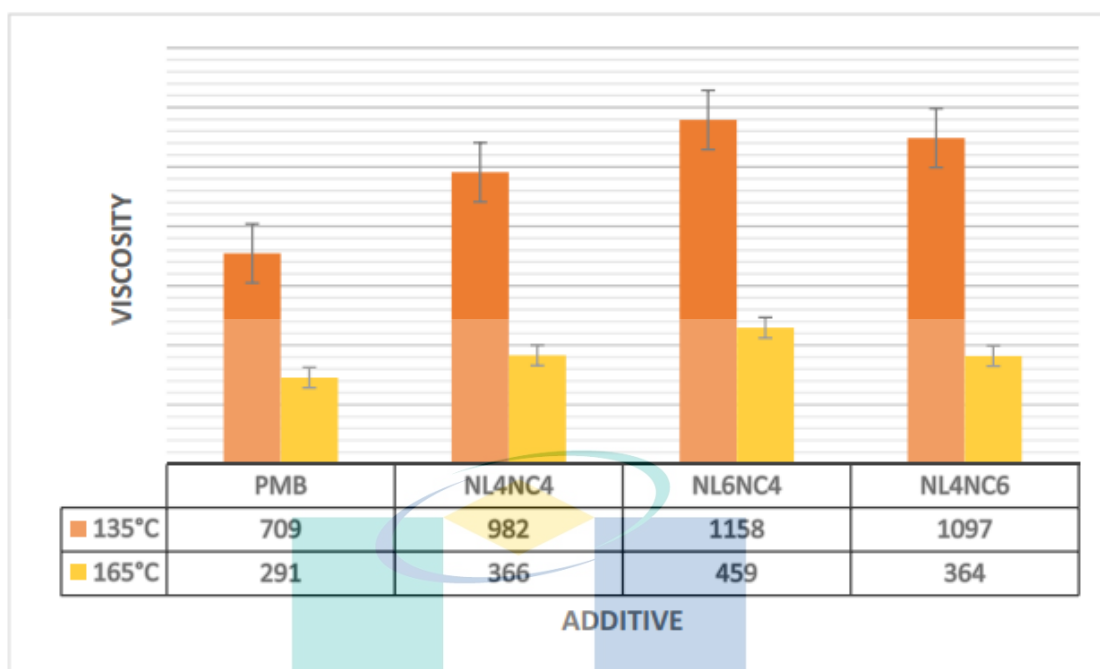


Figure 2.8 Viscosity values at 135°C and 165°C

Source: Mirsepahi et al. (2020)

The rutting parameters of non-recoverable creep compliance ( $J_{nr}$ ) and the recovered creep (R%) were also evaluated, along with the effect of nano-silica on the improvement of these parameters at high temperatures, which was assessed by simulating dynamic loading using a Dynamic Shear Rheometer (DSR) and performing the MSCR test at 3 temperatures of 58, 64 and 70 °C. Then, the influence of nano-clay and nano-lime hybrids on rutting parameters was evaluated in two nonlinear and linear viscoelastic states.

Overall, the results from all of the experiments showed that the viscosity increased due to the addition of modifiers to polymer bitumen, which resulted in more stiffness for the bitumen and an improvement of the rutting parameters at zero shear viscosity (ZSV). In all three experiments, the effect of nano-lime was significantly higher than that of nano-clay on increasing the resistance to rutting in this study.

## 2.5 Morphological and Chemical properties

For many years, optical microscopy (OM) and its derivatives (e.g. fluorescence OM) have been widely employed to research the morphology of bituminous materials.



However the technique's resolution, and therefore the length scales of the bitumen structure which are examinable, are limited. This limitation of OM is overcome by atomic force microscopy (AFM) (Ozdemir et al., 2021). Indeed it is well known that the method which is always associated with morphological investigations is atomic force microscopy (AFM) and this was used by (Blom et al., 2018), (Rosyidi et al., 2020), (Xing et al., 2020), (Blom et al., 2021) and many more.

Rahmad et al. (2021) used Rediset LQ1106 as an additive in warm mix asphalt and PG76 as the binder. The additive was added in different percentage of 1%, 2%, 3%, 4%, and 5%, and all six samples including the control samples were assessed in terms of viscosity, stripping characteristics, stability, bonding formation and morphology. Among the test involved were rotational viscosity, Vialit Adhesion and Boiling Water tests while for the morphology characteristics the concept of Atomic Force Microscopy (AFM) was used.

For viscosity, the tests were done at two temperatures, which were 165°C and 195°C. The mixture that included Rediset in the first place showed a great reduction of viscosity and the results showed that higher viscosity reduction efficiency signifies higher effectiveness of the blend. Rediset contains an amine compound type that could act as an anti-stripping agent, and although it improved the adhesion between the mix, it had virtually no effect on the viscosity of the asphalt binder actually. Normally, polar molecules were necessary in the asphalt binder system like water so that the surfactant will work, because asphalt is nonpolar.

Therefore, the initial reason why all the samples experienced reduced viscosity was the effect of the Rediset element in it that was able to make the viscosity reduced. Rediset is comprised of a mix of emulsifying agents and surfactants that can reduce the internal friction forces resulting in decreased viscosity. As a result, by having an increased content of Rediset, the viscosity-reduction material also increases the resulting thinning of the asphalt binder and lowers viscosity.

As for the water boiling test and vialit adhesion, they presented a decent result for the adhesive properties between asphalt aggregates and asphalt binders as a consequence of the Rediset anti-stripping agent which had improved the adhesiveness properties of the

blending. The binder's cohesive characteristic that promoted the strength of the asphalt mix together with the interlocking and frictional resistance of the aggregates had been observed to be reliable. The cohesion of the binder was able to be achieved with the presence of a good bond between the aggregates and the asphalt binder. This test showed that by adding Rediset LQ into PG76, the adhesion properties were well maintained. The bond between the binder and the aggregates, did not diminish, which would have caused ravelling or stripping.

Other than that, mechanical bonding also played a role alongside the chemical bonding in adhesion improvement, since the surface of the aggregates involved, or surface geometry as per name, provides a lot of intertwining effects between the aggregates and the binder. The mechanical bonding is also a substantial characteristic for the adhesion properties when comparing with the chemical bonding, because of the characterization of the physical features of aggregates, since surface unevenness of the aggregate was widely accepted to be important for the adhesion. While all of the improved materials' adhesive and peeling capabilities were successfully retained in the vialit adhesion test, the previously described properties were unfortunately affected by water and temperature in the boiling water test. Thus, the Rediset-PG76 binders in this investigation was able to withstand physical impact, but it is impacted by moisture and temperature increases.

Thermal analysis results show that the new materials decomposed at temperature more than 350 °C. Based on the TGA analysis for this study, the effect of adding Rediset into PG76 was not obvious during the earlier phase. The effect of Rediset, even though not consistent with the weight percentages can be seen in the second and third phase, when the total weight loss of Rediset-PG76 was found to be less with 2% to 4% Rediset added. However, the decrement was not a constant trend. As the process advanced to stage three, all the decomposition processes reached a steady state. These results indicate that even though the WMA additive had an influence in lowering the compacting and mixing temperatures, the materials were not susceptible to high temperature.

Through microscopic observation, it was discovered that any adjustment made to the controlled binder by adding varying amounts of Rediset can be clearly recognised by



the forms and dispersal of the "bee-like" structures. This discovery indicates that Rediset had a physical impact on PG76. This assertion is confirmed by grain dispersion information in the samples. The surface roughness study revealed projecting spikes on the binder's surface that matched with the "bees" structures.

Nciri et al. (2021) carried out a study to discover the potential benefits of discarded chewing gum (DCG) as a performance enhancing modifier for road pavement applications, and its influence on the asphalt binder's attributes was thoroughly examined. The base asphalt AP-5 (PG 70–22) was used along with various fractions of DCG (3%, 6% and 9% by weight of bitumen). The tests involved were Fourier transform-infrared spectroscopy (FT-IR), X-ray diffraction (XRD), thin-layer chromatography-flame ionization detection (TLC-FID), scanning electron microscopy (SEM), atomic force microscopy (AFM), thermogravimetric analysis (TGA), and differential scanning calorimetry (DSC). To inspect the physical and rheological changes of the asphalt cement after DCG incorporation the Brookfield viscometer, ring and ball softening point, needle penetration, and dynamic shear rheometer (DSR) tests were carried out.

FT-IR inspection revealed that the gum-asphalt interaction was not chemical but was more physical. Meanwhile, XRD showed that the microcrystalline phase was not affected, and instead the amorphous phase of the asphalt was slightly affected as seen in Figure 2.9. This was due to the existence of talc filler in DCG which may affect the properties of the bitumen. Iatroscan analysis revealed that the aromatics and resin behaved differently in response to the inclusion of waste gum into the binder, while the saturates and asphaltenes content remained unchanged.

From Figure 2.10, the SEM shows that due to higher doses of DCG, it has completely assimilated with the bitumen matrix which in turn becomes rougher. Figure 2.11 (a) until (d) of AFM reveals that the size of the bee-shaped microstructure expanded, peri-phase domains contracted and the para-phase domain is completely abolished. TGA/DTGA/DSC data highlighted that the high-temperature stable additive slightly influence the thermal properties of the blends. DSR and empirical rheological tests showed that the waste gum made the bitumen less vulnerable to heat and tender, thereby boosting its resistance against fatigue cracking at intermediate service temperatures. On

top of that, DCG widened the thermal window of the bitumen performance grade (PG), and preserved its viscosity at standard temperatures, leading to it maintaining an appropriate workability for asphalt mix.

Overall, the use of DCG as a bitumen modifier is economical viable and can reduce the issue of plastic pollution, while empowering hot-asphalt mix performance and making longer-lasting roads. The authors suggest researchers to conduct additional laboratory tests like the bending beam rheometer test, storage stability test, toughness and tenacity test, wheel tracking test, direct tension test, etc. Giving special attention to the rutting distress factor and adopting a special pre-processing to the gum waste before use would effectively ensure the ability to achieve outstanding performance.

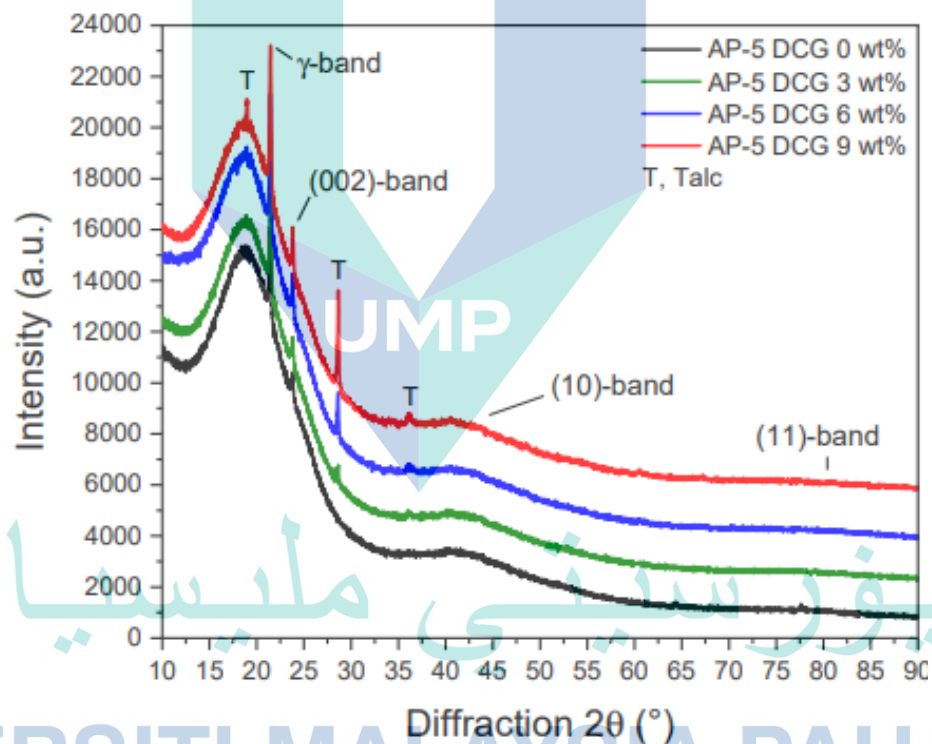


Figure 2.9 XRD patterns of base AP-5 asphalt and modified samples

Source: Nciri et al. (2021)

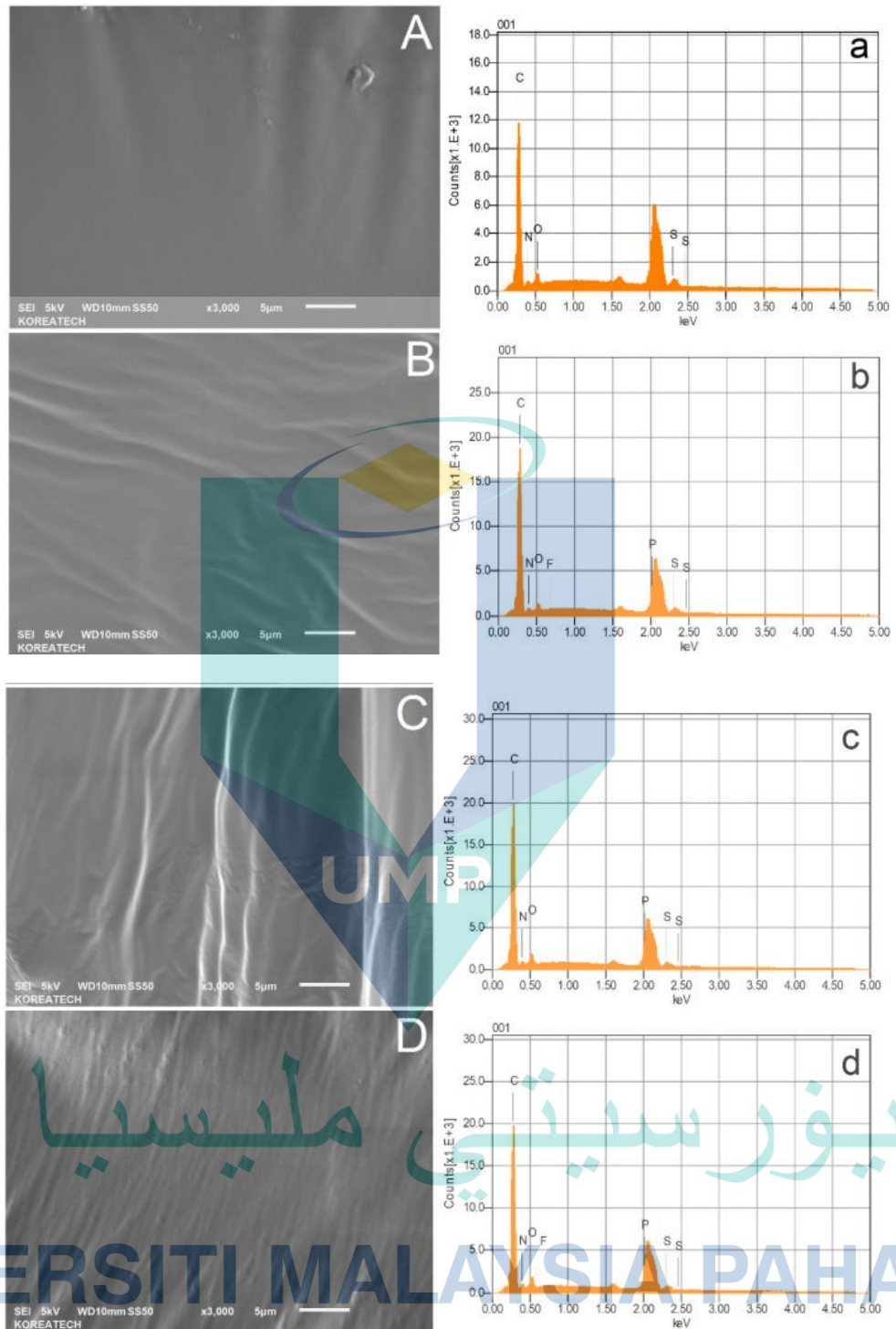


Figure 2.10 Scanning electron microscope (SEM) micrographs with their corresponding EDXS spectra of unmodified and DCG-modified asphalts. (a) 0% DCG, (b) 3% (c) 6% (d) 9% DCG

Source: Nciri et al. (2021)

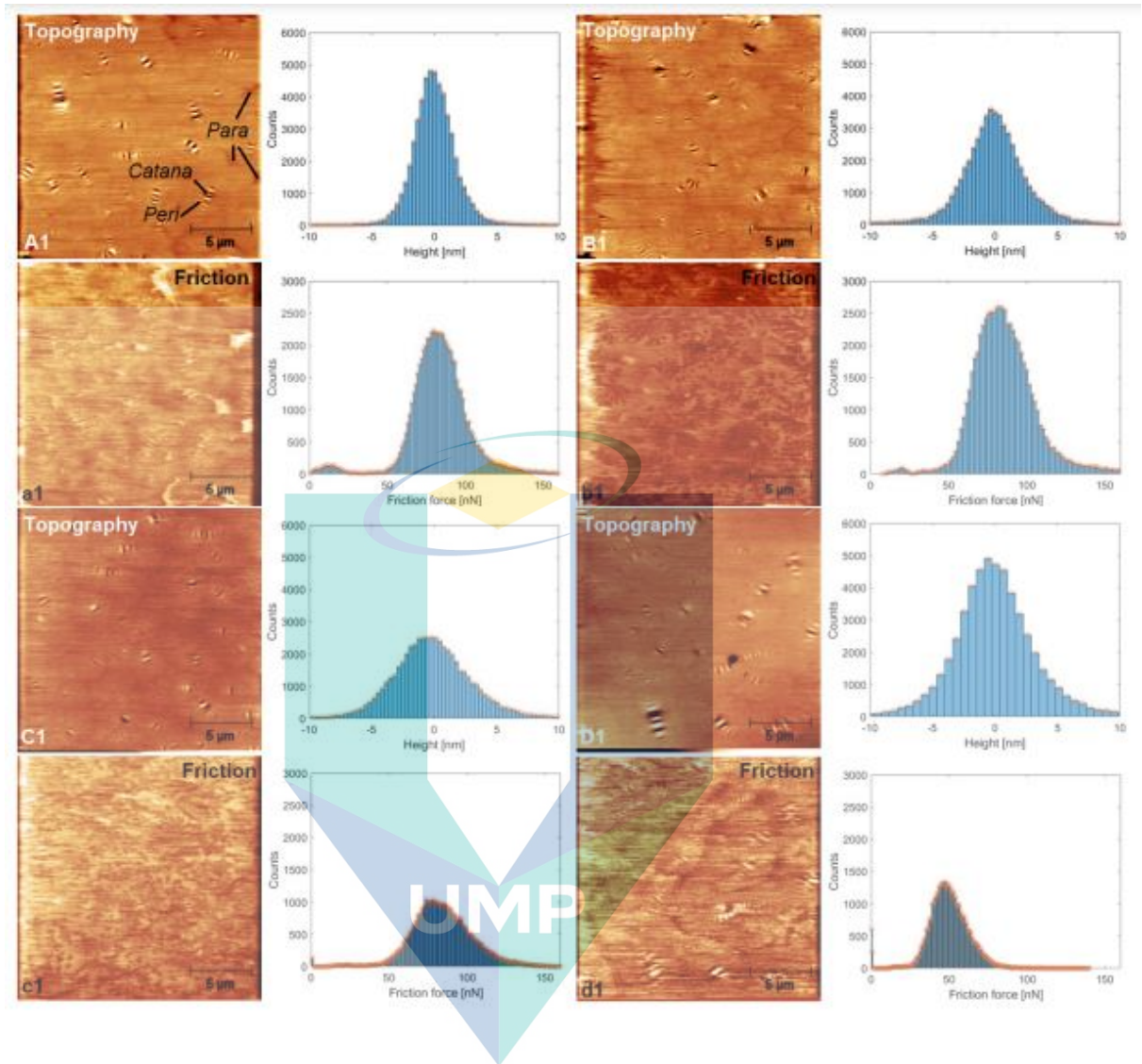


Figure 2.11 AFM topography and friction images with their corresponding histograms on the right side highlighting the influence of DCG on base AP-5 asphalt micromorphology and friction.

Source: Nciri et al. (2021)

## 2.6 Stone Mastic Asphalt

### 2.6.1 Basic concept of pavement

The type of binder used differentiates the two types of pavement, which are flexible pavement and rigid pavement. These types of pavements are commonly encountered and each are applied according to their own speciality. Given the right specifications and materials each of these pavements serve their purpose in a good way.



## 2.6.2 Overview of Flexible pavement

Flexible pavement is made up of asphaltic or bituminous materials spread over the surface course, and the largest part of flexible pavement is made up of a mix of both fine and coarse aggregates (Peng et al., 2020; You et al., 2020). As the name implies, this pavement acts like a sheet of paper and when a load is exerted on the pavement the structure will bend and then return back to its original nature after the load has been released ( Ghavami et al., 2019). Since flexible pavement possess low flexural strength, overexertion of load may lead to pavement deformation. Some deformations, like rutting and fatigue are encountered by flexible pavement all around the world as a result of various factors (Huang et al., 2021).

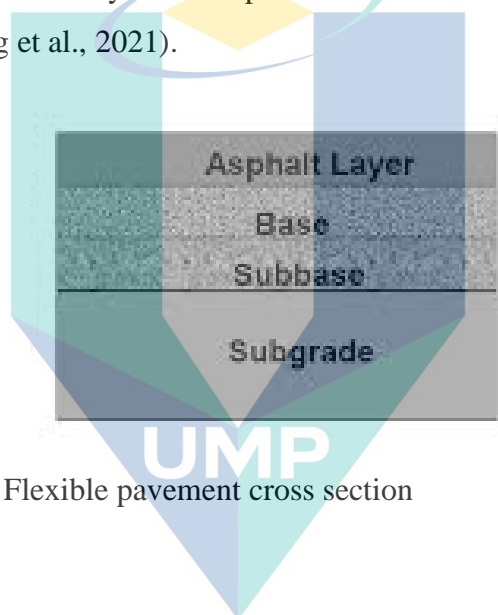


Figure 2.12 Flexible pavement cross section

## 2.7 Type of flexible pavement

There are several different types of flexible pavement available, which are Dense Graded Asphalt, Porous Asphalt, Polymer Modified Asphalt and Stone Mastic Asphalt.

### 2.7.1 Dense Graded Asphalt

Dense graded asphalt is the most common type of pavement that is well graded and has been among the top choices to be used in the pavement industry. Dense graded asphalt, also known as hot mastic asphalt (HMA), is used in the construction industry and could be a mix of coarse and fine aggregates (Ganji et al., 2019). This type of pavement needs to be maintained regularly and requires inspections from time to time, as permanent

deformations like cracking and fatigue could affect the pavement's condition and thus could bring harm to the users of the road (Lima & Thives, 2020).

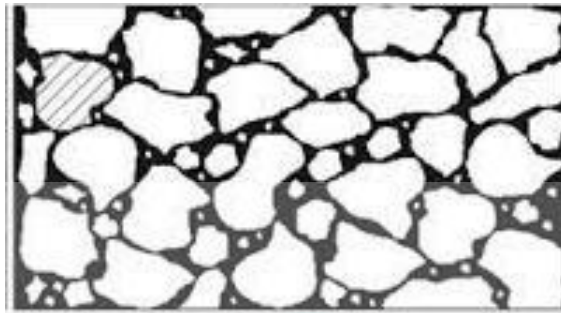


Figure 2.13 Example of typical dense graded asphalt cross-section

### 2.7.2 Porous Asphalt

Porous asphalt (PA), or open graded friction courses (OGFC), are hot mix asphalts with a high air voids content (Chen et al., 2020). These porous asphalts are usually used for structures like driveways, sidewalks, drains, pathway shoulders, friction courses for highway pavements, permeable sub bases under the conventional flexible or rigid pavements and low volume roads, since they provide safety and environmental benefits (Qian et al., 2020; Yang et al., 2019). These benefits are due to their porous nature which enables rainwater to flow out from the pavement instantly, reducing the presence of moisture on the pavement (Yan et al., 2020). They differ from traditional asphalt in that as the structure build up allows water to pass freely through it, it reduces or controls the amount of run-off from the surrounding area.



Figure 2.14 Example of porous pavement

### 2.7.3 Polymer Modified Asphalt

Polymer modified asphalt is an asphalt mixture which incorporates one or more polymers in the mix. Modification of asphalt binders is usually performed with polymers in order to improve one or more of the basic asphalt properties, including rigidity, elasticity, brittleness, storage stability and durability, along with resistance to accumulated damage (Wang et al., 2020). Styrene-butadiene styrene (SBS) is one of the polymers that is mentioned in the production of polymer modified asphalt (Ren et al., 2020). Since asphalt pavements are easily exposed to low temperature cracking, SBS has been observed to provide an enhancement in the asphalt mix as SBS degrades over a long period of time, which makes it suitable to use in the asphalt mix (Ren et al., 2020).

### 2.8 History of SMA

Stone mastic asphalt (SMA) or stone matrix asphalt first appeared in the 1960s in Germany (Arshad et al., 2019). Back then, Germany uses studded tyres in their lorries and because of the load the tyres exerted on the pavement, SMA was developed to withstand the pressure from the tyres. However, when those tyres ceased to be in use, SMA also slowly disappeared. However, SMA resurfaced back in the 1990s to 2000s as countries like the USA and those in Europe were developing their own SMA pavements and started using it for their highly trafficked roads (Parimita, 2020). This led other countries, including Malaysia, to revise their SMA specifications so that it could be arranged for use depending on the condition of the roads which were suitable for their own country.

Stone mastic asphalt is a gap graded asphalt, as the two main component are the high content of coarse aggregate which is approximately 70% to 80 % of the whole mix alongside high content of bitumen as the filler. Since SMA is made up of mostly aggregates with changing gradations, the content of the coarse aggregate is increased. As a result, SMA has an enhanced ability for bearing wheel loads in pavement. The high bitumen content completes the mix with an additive like cellulose fiber in order to prevent problems like bleeding in the mix. The coarse aggregate content provides stone on stone contact, making SMA more durable than conventional pavement (Liu et al., 2017). The



specification used for SMA are from the Malaysian Public Work Department for roads (JKR, 2008).

### 2.8.1 Advantages of SMA

Stone mastic asphalt has a gap graded structure with a significant amount of coarse aggregates; these aggregates make a skeleton-like structure which thus provides a durable structure. Chegenizadeh et al. (2021) also mentioned that SMA is able to resist deformation and fatigue better and longer than the traditional asphalt mix. Other advantages of stone mastic asphalt include its stability at high temperatures, increased wearing resistance, malleability at low temperatures and increased adhesion which helps it inhibit the separation of particles.

In order to make a more enhanced SMA mix, they resorted to add Ethylene-Vinyl Acetate (EVA) in the SMA and focusing on SMA fatigue and rutting behaviour. EVA and C320 bitumen were prepared by wet techniques, before EVA was added at 2% to 6% by bitumen weight. Dynamic modulus, drain off, flow number test, 4-point flexural beam test, and wheel tracking tests were run to evaluate the performance of the ordinary and EVA modified SMA blends.

Figure 2.15 displays the binder drain off when added with EVA. The binder drain off was reduced with more EVA included in the mix. Because of its fantastic grip and the union generated with its base bitumen, the natural effects of the mix of EVA in SMA blends are not only effective for preventing blend drainage, but also for balancing out added substances other than plastomers.

Figure 2.16 shows the flow number values of SMA-EVA modified mixtures. The results reveal that FN varied with the percentage of EVA. Rutting resistance was related to the FN value. The FN increment indicated an increase in rutting resistance. As can be observed, the sample containing 6% EVA had a higher FN value and thus a stronger rutting resistance. The FN value of the sample without EVA was 490, while the FN value of the sample with 6% EVA added was 702.

They concluded that by increasing the EVA percentage, the flow number increased likewise, while the binder drains down decreased. The fatigue life of the EVA/SMA mix showed a satisfactory enhancement at a 6% inclusion along with the initial flexural stiffness.

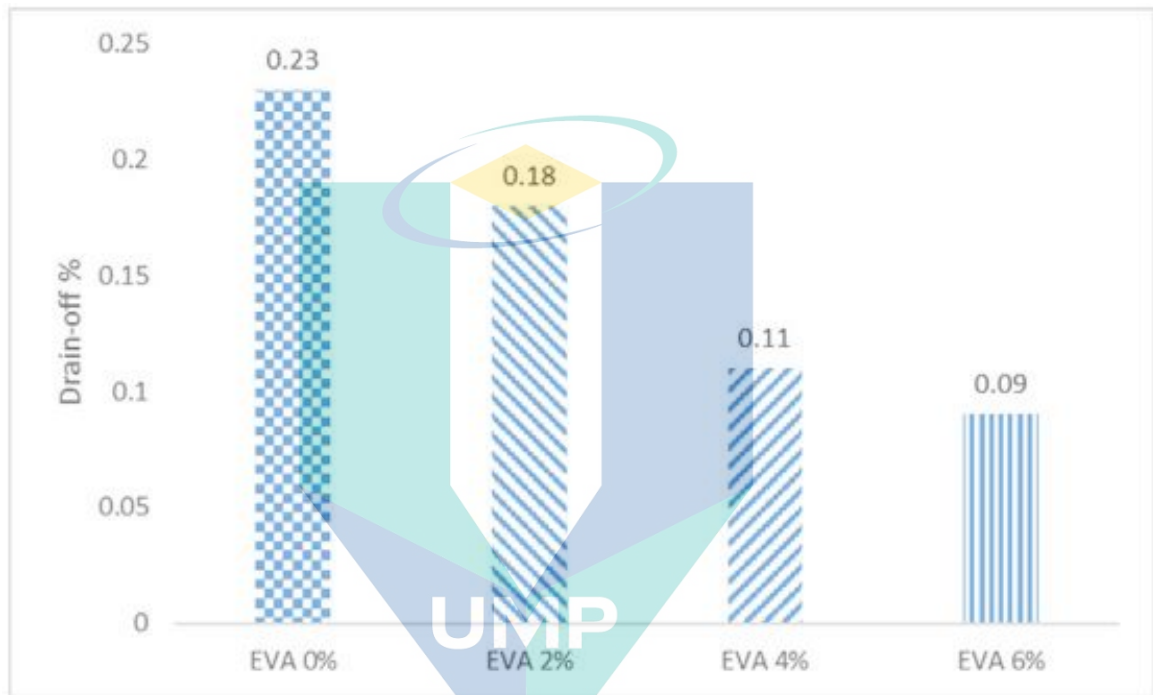


Figure 2.15 EVA (%) against binder drain off (%)

Source: Chegenizadeh et al. (2021)

اونيورسيتي ملايسيا قهق

UNIVERSITI MALAYSIA PAHANG

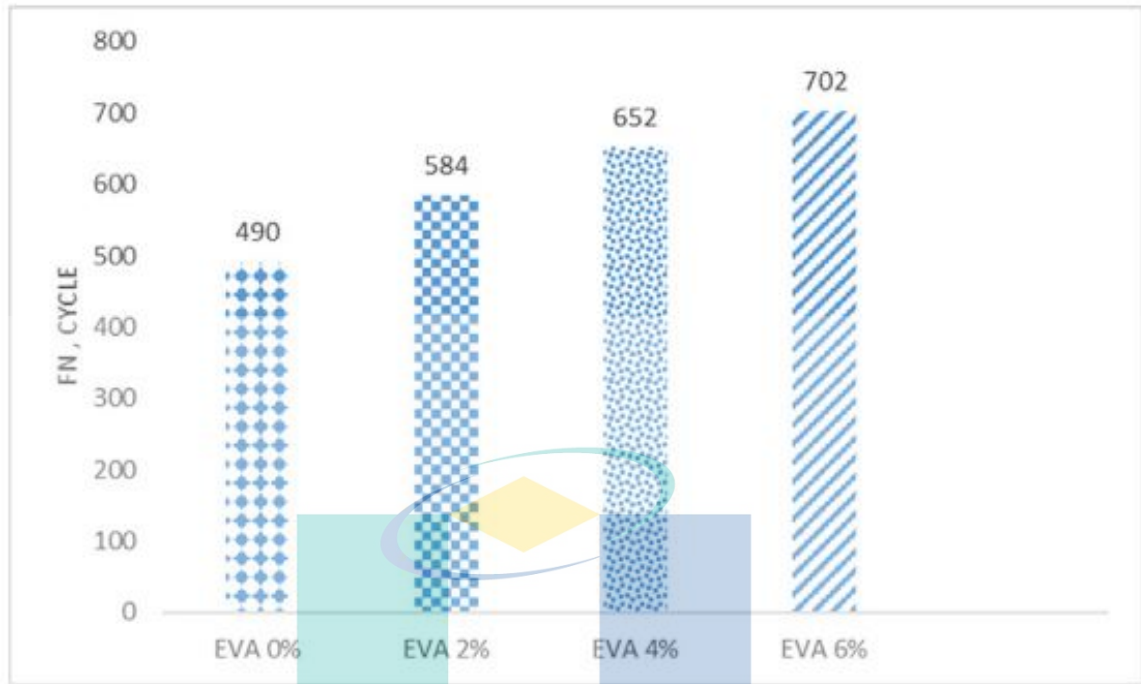


Figure 2.16 Flow number value of SMA-EVA modified mixes  
 Source: Chegenizadeh et al. (2021)

Other than that, stone mastic asphalt reduces skidding, has less noise, and helps to enhance night vision. This type of mix is suitable for heavy traffic areas as heavy loads are a stone mastic asphalt speciality. Heavy traffic will impose more load on the road, and stone mastic asphalt could endure the loads because of the strong adhesion between the bitumen and aggregate (Kumar & Ravitheja, 2019).

Irfan et al. (2019) conducted a research study on the effects of varying the nominal maximum aggregate size (NMAS) with cellulose fiber added to the stone mastic asphalt mixture. 0.3% cellulose fiber was added according to the weight of the aggregates; the NMAS used were 19.5, 12.5 and 9.5mm and a 60/70 grade of bitumen. The samples were prepared by the Superpave Gyrotory method and the dynamic modulus and flow tests (flow number and flow time) were observed.

Figure 2.17 shows that the 25 mm SMA mixture has the highest dynamic modulus values at all frequencies, whereas the 12.5 mm mixture has the lowest dynamic modulus values. Meanwhile Figure 2.18 shows that at a temperature of 21°C, the samples exhibited fatigue behaviours and the crack resistance of various SMA gradations using

the principles of dynamic modulus and phase angle. The 25 mm SMA mix has the greatest fatigue parameter value, which correlates to the lowest fatigue resistance, whereas the 12.5 mm SMA mix performs significantly better among the evaluated gradations and has a stronger fatigue cracking resistance.

The results were overall assessed for each of the mixes stress-dependant curves and the 25mm NMAAS demonstrated that it exhibited great strength against fatigue while the phase angle and dynamic response result highlighted the 12.5 mm NMAAS. In the end, 25 mm NMAA was chosen, as the flow test results and statistical models displayed a better stone to stone contact between the aggregates as compared to the 12.5 mm.

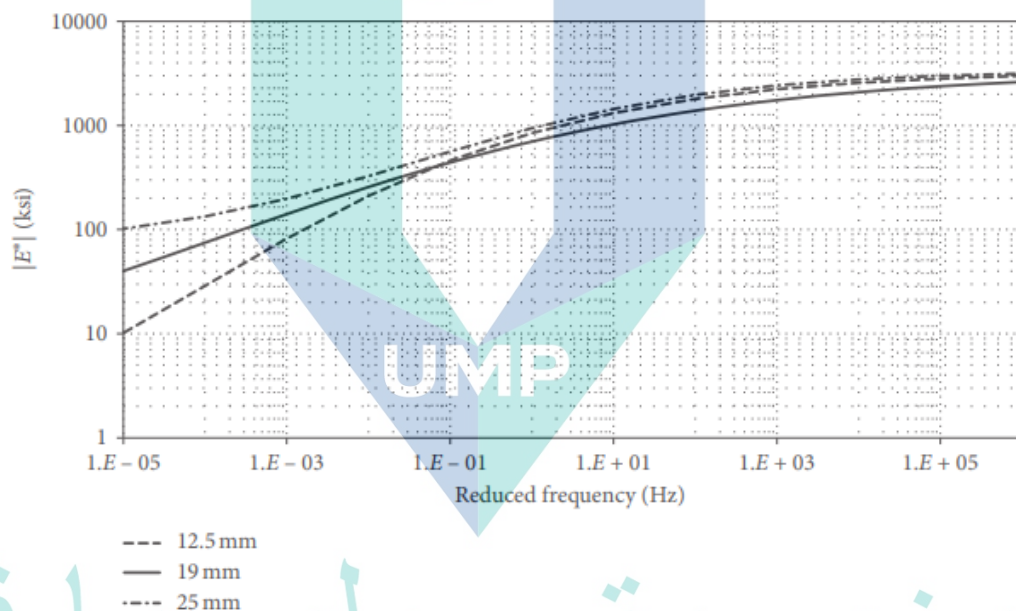


Figure 2.17 Master curves for SMA mixtures

Source: Irfan et al. (2019)

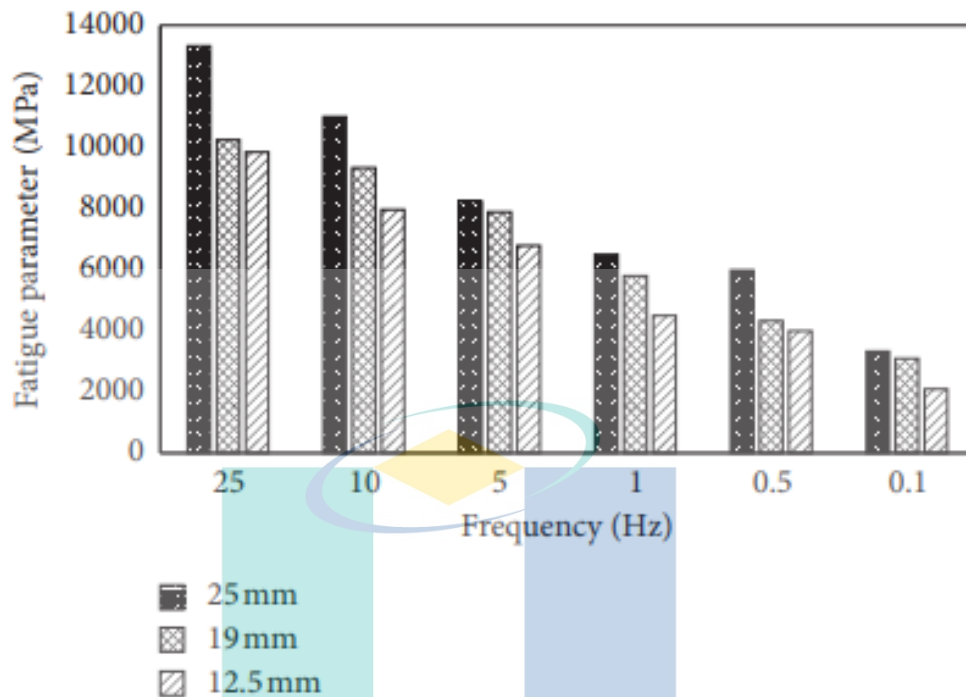


Figure 2.18 Fatigue parameter of SMA mixtures

Source: Irfan et al. (2019)

Fakhri & Shahryari (2021) carried out a study on the effects of nano zinc oxide (ZnO) and nano reduced graphene oxide (RGO) for the moisture susceptibility property of stone mastic asphalt (SMA). They mentioned that moisture damage was among the main sources of distresses in pavements. For this study, the test methods for evaluating the moisture damage which were carried out were the immersion Marshall test, indirect tensile strength test, boiling water test, static creep test, pull-off adhesion test, and Semi-circular bending (SCB) fracture test. Figure 2.19 displays the materials used for the study.

Nano ZnO and Nano RGO were used in 0.2%, 0.4% and 0.6% amounts by weight of the binder. The results show that the softening point and viscosity increased, while the penetration and ductility decreased. The mechanical test results revealed that an increase in the percentage of Nano ZnO and RGO make the Marshall Stability, indirect tensile strength, accumulated strain, pull-off adhesion strength, and fracture energy all increases. The bitumen coating on aggregates in SMA was also improved.



The Nano ZnO and Nano RGO enhanced the moisture susceptibility of stone mastic asphalt. The moisture susceptibility was next assessed by the ITS, pull-off, and Semi-circular bending (SCB) fracture test which all exhibited good results. In general, the ANOVA test verified that Nano ZnO has a more significant effect than Nano RGO. The authors recommended using Nano ZNO instead of Nano RGO.

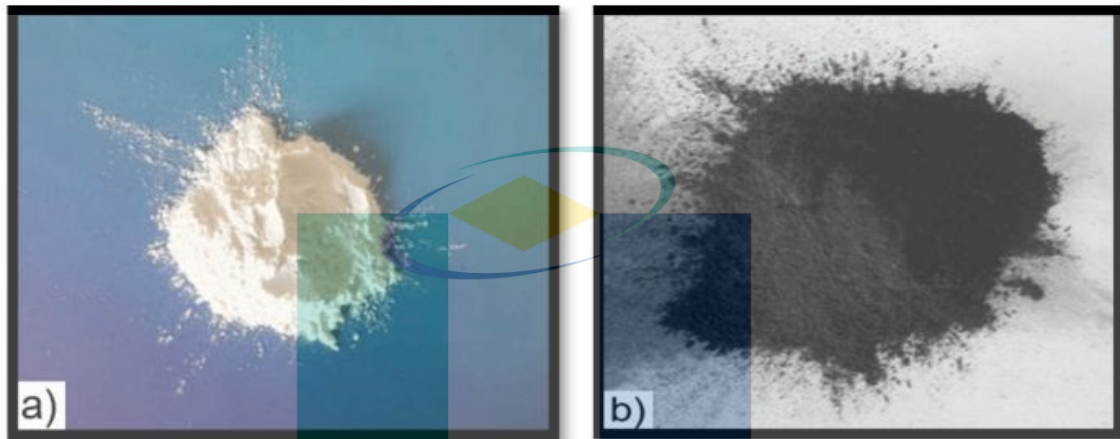


Figure 2.19 Nano ZnO and Nano RGO used  
Source: Fakhri & Shahryari (2021)

### 2.8.2 Disadvantages of SMA

Stone mastic asphalt possesses a few disadvantages. Some common problems that have been raised are binder drain down, the high cost of production, rutting and moisture susceptibility (Guo et al., 2020). Binder drain down refers to when the binder flows out from the asphalt mixture, or in other words, when the binder drains off from the aggregates to the bottom during placing, production, and storage (Devulapalli et al., 2019). Compared to a dense graded asphalt, this problem is most likely to occur in a gap graded asphalt since there would be voids between the aggregates, along with the presence of a high volume of binder in the SMA mix.

With this, the binder is prone to flow between the voids and this is why SMA has stabilisers like cellulose fiber and polymers in order to prevent the binder from coming off the mixture (Jain et al., 2020). Stone mastic asphalt need to be mixed at a fairly high temperature, so the high temperature will also influence the binder drain down of the mixture. As for the high production cost, it is mainly concerned with the materials in

SMA since SMA uses a high amount of coarse aggregates, which means the cost to obtain the material needed is high,

The effect of water on the reduction of the adhesiveness between the aggregates and binder in the asphalt mixtures has been investigated for a long time, and the related terms deal with the materials cohesion or adhesion (Alam & Aggarwal, 2020; Nobakht et al., 2020). The adhesive and cohesive properties are involved with three components in SMA, which are the binder (bitumen) itself, aggregates and the filler used. Moisture susceptibility is one of the problems related to asphalt pavements, and it could be defined as the loss of adhesion between the binder and aggregates in the asphalt mixture due to the presence of moisture (Ameli et al., 2020).

This loss of adhesion makes the asphalt mixture lose its strength and this will lead to common problems like stripping and ravelling (Soenen et al., 2020). SMA is made up of coarse aggregates which means that it has voids, and this is where the problem lies as the voids are permeable to moisture (Khedmati et al., 2017). Usually the heavy rainfall season is a disaster for the pavement, as during that time there is a high exposure to moisture over a prolonged time, and after the rainy season there are many deformations visible on the road as a result.

Potholes are one of the moisture damage related distresses which happen when the underlying soil of the pavement has been softened with a large amount of moisture (Li et al., 2019). The appearance of this problem is like a hollow curve on the road with various shapes and sizes. The soil from beneath the pavement, when exposed to moisture for a long time, will lead to premature cracking, and with time this premature distress grows into a permanent issue given the road is not being taken care of properly and is not maintained.

The next issue is rutting, which is one of the forms of road deformation that can happen to flexible road pavements too. Rutting occurs in the form of a longitudinal depression in an affected area of the pavement that looks like an accumulated consolidation (Zhang et al., 2020). It can look like a wheel that has just been over the pavement, but instead of withstanding the load from the tires, the pavement deforms and doesn't go back to the original shape as it was before. Eventually, this permanent



deformation results in a rutting of the road, as aggregates and the binder each have their own share of the blame for causing deformations in the flexible pavement (Guo et al., 2020).

Deformations may also occur if the pavement design was not done according to the requirements, making the established pavement have less resistance to the loads exerted on the pavement (Saboo et al., 2019). It could also happen when the pavement is not compacted properly, as insufficient asphalt thickness and the presence of water alongside with exposure to high temperatures for a prolonged time damage the pavement (Alkaissi, 2020).

When the asphalt is placed, it needs approximately 24 hours before the mix is properly set into the ground, but nowadays the consolidation time may often not be fully achieved. Workers may try to make the mix faster which results in deformations due to the shorter period of time. Thus, nano materials seem to have a positive influence in improving the rutting resistance when included in asphalt.

### 2.8.3 Design requirement

Stone mastic asphalt design requirements are taken from Malaysia Public Work of Department - Flexible Pavement. SMA20 is used for this research.

Table 2.1 Gradation for SMA20

Sieve Size (mm)	Percentage by weight passing sieve
19.0	100
12.5	85 – 95
9.5	65 - 75
4.75	20 – 28
2.36	16 – 24
0.600	12-16
0.300	12-15
0.075	8-10

Source: Jabatan Kerja Raya (JKR), (2008)

The table below shows some previous research with the grade of bitumen which is used in stone mastic asphalt.

Table 2.2 Summary of grade of bitumen used in previous research

Title	Grade of bitumen	Source
Mechanical performance of stone mastic asphalt incorporating steel fiber	60/70	(Jasni et al., 2020)
Rutting and fatigue properties of cellulose fiber-added stone mastic asphalt	60/70	(Irfan et al., 2019)
Laboratory evaluation of stone mastic asphalt containing amorphous carbon powder as filler material	60/70	(Korayem et al., 2020)
Investigation on moisture susceptibility and rutting resistance of asphalt mixtures incorporating nano silica modified binder	60/70	(Arshad et al., 2017)
The role of nanomaterials in reducing moisture damage in asphalt mixes	60/70	(Razavi & Kavussi, 2020)

From Table 2.2, it can be seen that most of the design of stone mastic asphalt uses the 60/70 grade of bitumen and previous researchers also used the same grade of bitumen.

## 2.9 Application of nanomaterials

Previous studies proved that there are various kinds of materials that have been used in asphalt as modifiers, stabilisers, additives and so on in order to improve the performance of the binder or the mix. These performance metrics include resilience, permanent deformation, stability, moisture susceptibility, binder drain down and many others. From all of the materials encountered, polymers were the most widely used in binder modification.

However, the flaw in using pure polymer modifiers is that most of them are thermodynamically inharmonious with the asphalt binder due to a large contrast in density, molecular weight and solubility between the polymer and the asphalt binder. This could result in changes in the composite material during its storage, which is not exposed to sight and then affects the materials when used. Therefore, more researchers have concentrated on the introduction of nanomaterials as the modifier due to the rapid development of nanotechnology in the pavement industry, so that this issue with polymers could find a solution.

Nanomaterials are chemical compounds or products that are processed and used on a very small scale. The size of nanomaterials is between 1 to 100 nanometres (nm) (Caputo et al., 2020). A few examples of nanomaterials are titanium dioxide, silica oxide, graphene oxide and aluminium oxide. Nanomaterials had previously been used in the healthcare industry, beauty products and biology related fields; they have also been previously used in construction before transitioning to the pavement industry (Mazari et al., 2021).

Due to nanomaterials high surface area and very small size as compared to normal additives, they exhibit special characteristics when used in a mixture at an optimum ratio. There are two methods of producing nanomaterials, namely, the top-down approach and the bottom-up approach (Rawtani et al., 2020). The top-down approach consists of two methods. In the first, bigger structures are diminished in size until these reach the nano scale, while the second approach consists of deconstruction into their composite parts (Zhou et al., 2020). Nanomaterials have different characteristics according to their type; thus, it is imperative for researchers to study more into them and discover their individual

properties. Some asphalt mix pavements that have been added with nanomaterials either as a modifier, additive or rejuvenator have seen the properties of the asphalt mix improved tremendously.

In a study by Razavi & Kavussi (2020) they investigated the role of nanomaterials in reducing moisture damage to asphalt mixes. They proposed a cost-effective method in producing nano hydrated lime, which was the planetary ball milling process. They also mentioned that the addition of nanomaterials reduces the moisture damage to HMA mixes. There were four types of nanomaterials involved which were the nano  $\text{CaCO}_3$ , nano hydrated lime, nano bentonite and nano silica; and there were two types of anti-stripping fillers that were chosen namely hydrated lime and  $\text{CaCO}_3$ .

The minimum particle size of the nano hydrated lime was obtained through a Scanning Electron microscope (SEM) and Dynamic Light Scattering (DLS) tests were done at 125 and 208 nm. The Field Emission Scanning Electron Microscopy (FE-SEM) technique was used to verify the homogeneity of the distribution of additive in the 60/70 grade bitumen. The images of the modified samples can be seen in Figure 2.20. Moisture damage was evaluated by the Modified Lottman test for different Freeze Thaw (F-T) cycles and Indirect Tensile Strength (ITS) values were reduced appreciably at the first cycle.

It shows that 4% nano hydrated lime exhibited the most resistance to F-T cycles. In addition, the Indirect Tensile Stiffness Modulus (ITSM) were performed at 25°C. From these tests, the Tensile Strength Ratio (TSR) and Index of Retained Resilient Modulus ( $\text{IRM}_r$ ) parameters were determined. The  $\text{IRM}_r$  values of mixes containing 20% hydrated lime filler and 4% nano hydrated lime increased to 56% and 60% respectively while in the case of using  $\text{CaCO}_3$  filler and nano  $\text{CaCO}_3$ , the  $\text{IRM}_r$  values increased to 48% and 54%.

The results of their study showed that among all the materials that they used, nano hydrated lime improved the resistance against moisture damage the most in asphalt mixes. They also recommended that the application of nanomaterials need to be in lower percentages rather than using high amounts of conventional antistripping fillers in order to increase water resistance on bituminous mixtures.

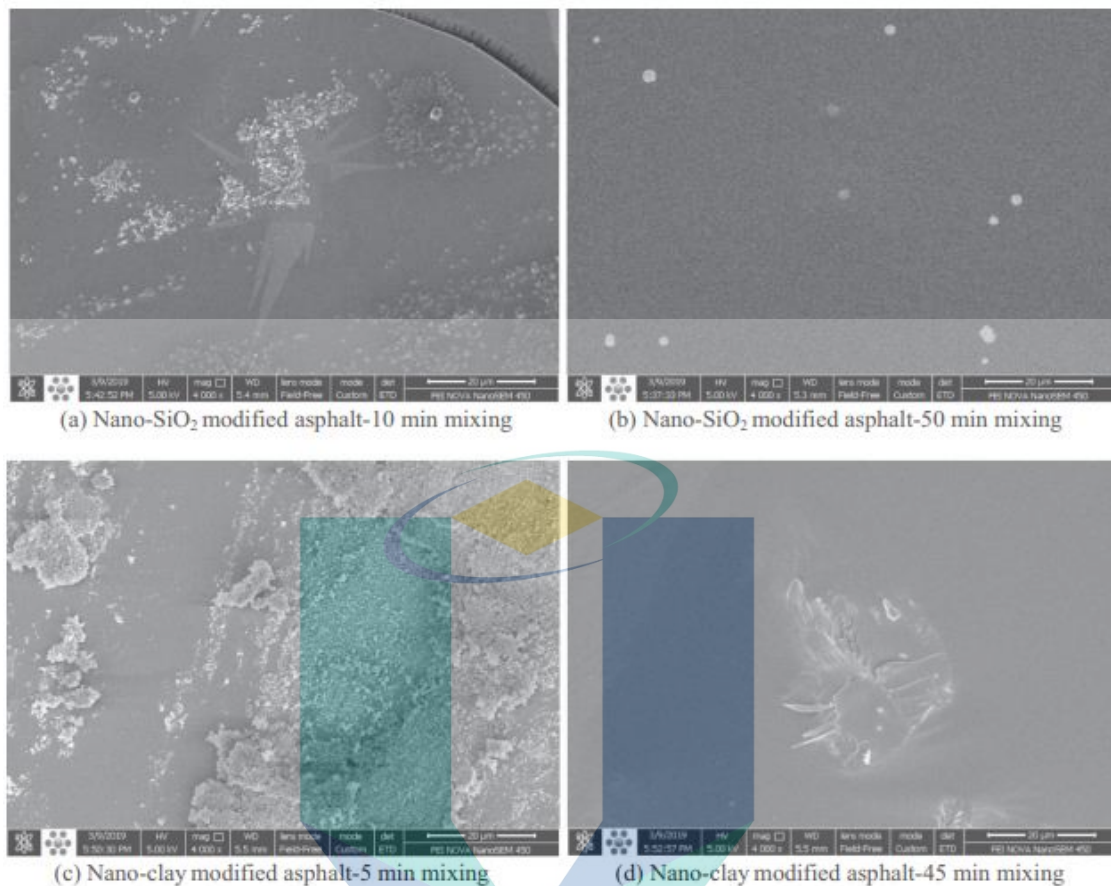


Figure 2.20 FESEM images of nano modified binders at different mixing times  
Source: Razavi & Kavussi (2020)

Nanomaterials have many types of applications depending on their respective type and size. Some of the commonly used nano materials that are always encountered are nano clay, nano silica (He et al., 2021), as well as nano sized metals like copper, zinc and aluminium oxide (Shafabakhsh et al., 2020). Aging is a concern of asphalt mixtures and there are two types, which are thermal oxidative aging and photo oxidative aging. This is an area where the surface modified nanomaterials like nano silica, nano zinc oxide and nano titanium act as though they could improve the anti-aging behaviour of asphalt (Hong et al., 2020).

Nano clay is a naturally occurring minerals and its purity could affect the final nanocomposite properties. Due to their low cost of production, it is commonly used, as it has the potential to improve mechanical and thermal binder properties (Ramadhansyah et al., 2020). Nano possesses properties like good stability, affordable cost, high surface



area, chemical purity and good dispersing ability which has made it one of the most used materials over the years in improving the mechanical performance of asphalt with issues such as aging, fatigue and cracking (Snehal et al., 2020). The following Table 2.3 shows some of the effects of using nano materials.

Cheraghian & Wistuba (2020) conducted a study on bitumen modified by a composite of clay and fumed silica nanoparticles which they exposed to ultraviolet (UV) light in the laboratory. They evaluated the surface morphology, rheological and chemical properties. The content of nanoparticles used was from 1% to 3%, with temperatures of 30 to 70°C. The testing involved was field emission scanning electron microscopy (FESEM), dynamic shear rheometer (DSR), and Fourier transform infrared (FT-IR) spectroscopy and they focused on the surface morphology, rheological and chemical properties of the modified binder.

The clay and fumed silica nanoparticles (CS-NPs) were 10–30 nm in size. CS-NPs offer rich binder contents in asphalt mixtures due to their improved surface area to volume ratio as compared to ordinary filler particles. Their broad surface (20–500 m<sup>2</sup>/g) is a distinguishing feature that increases particle contact, which has a significant effect on the rheological and anti-aging properties of the modified binders while also enhancing bond strength at the aggregate-bitumen interface.

It was discovered that bitumen modification with clay and fused silica nanoparticles significantly modified the final binder characteristics. The carbonyl index and oxidation degree decreased, and the clay and fumed silica nanoparticles significantly increased ageing resistance to ultraviolet (UV) light. The results show that the specific concentration of clay and fumed silica nanoparticles has a significant impact on the mechanical stability of the modified bitumen.

The researchers found that clay and fumed silica nanoparticles might be used as effective UV-shielding coatings in asphalt pavements. The addition of clay and fumed silica nanoparticles to bitumen significantly lowered stiffness and enhanced resistance to permanent deformation. The results show that the specific concentration of clay and fumed silica nanoparticles has a large influence on the mechanical stability of the modified bitumen.



According to the DSR and FT-IR data, increasing the content of NPs by more than 0.2 wt. % significantly increased UV ageing resistance. Furthermore, deformation resistance demonstrated that bitumen modification with CS-NPs minimises increase the stiffness for bitumen samples subjected to UV ageing and retards the bitumen hardening as a result of ageing.

Bitumen modification with clay and fused silica nanoparticles is an intriguing low-cost technology in asphalt pavement engineering that offers unique insights on making asphalt materials more durable. From a broader viewpoint, our discoveries of molecular interactions between nanoparticles and bitumen will pave the way for a new direction in the topic of nanotechnology for asphalt.

Taherkhani and Tajdini (2019) studied the effect of nano silica (NS) and hydrated lime (HL) on the asphalt concrete. The contents of NS involved were 2%, 4%, and 6% by bitumen weight, while the contents for HL were 1.5%, 2% and 2.5% by the weight of total aggregate. The content of the NS and HL was chosen based on studies by (Enieb & Diab, 2017) and (Yusoff et al.,2014). Among the tests involved were indirect tensile strength (ITS), resilient modulus, and fatigue tests. The ITS test was done with subject of conditioned and unconditioned samples along with one, three, and five freeze-thaw cycles. Resilient modulus was done at 5, 25 and 45°C.

The results showed that for ITS, 6% of NS shows 10% more improvement as compared to 2.5% for HL. The results indicated that increasing the content for NS and HL, made the stiffness also increase which resulted in the mixture being able to hold more tensile stress before experiencing failure. Additionally, NS was more effective than HL in the resistance against freeze-thaw cycles. The highest loss of ITS occurred to the unmodified sample after the conditioning under the first freeze-thaw cycle, followed by the HL modified sample. However, with increasing percentage of the additives could decrease the loss in ITS for nano silica (NS) samples. This shows that NS was able to have more resistance to moisture damage as compared to HL.

As for the resilient modulus test, it was clear that with the increasing NS and HL, the resilient modulus also increased. The stiffening effect for each material was because HL has a higher inside porosity and NS has a higher surface area. The large surface area

leads to more interaction between the binder and more absorption of oil in the asphalt cement. The resilient modulus of NS was better as compared to the HL while the difference in stiffness for them was more prominent at low temperature rather than high temperatures.

For the fatigue test, they were evaluated in terms of fatigue cracking and NS was slightly better in reducing fatigue cracking as compared to HL. But due to limited studies in the fatigue behaviour of HL it also reduces fatigue cracking, and NS improvement was not that significant. Overall, the author concludes that using HL was more economical than using NS for modification.

Jin et al. (2019) studied the modified bitumen with metal doped nano TiO<sub>2</sub> pillared montmorillonite. The photocatalytic activity of regular TiO<sub>2</sub> is not good enough to alleviate the ageing of asphalt pavement and degrade automobile exhaust, thus TiO<sub>2</sub> pillared montmorillonite (T/M) modifiers have been researched to alleviate the ageing of asphalt pavement and degrade automotive exhaust.

Different metal (Ce, Cu, Fe) doped modifiers based on T/M were prepared in this study to improve the photocatalytic performance of T/M. The sol-gel technique was used to produce metal doped TiO<sub>2</sub> pillared montmorillonite. X-ray diffraction (XRD) and an ultraviolet visible (UV-Vis) spectrophotometer was used to assess the modifier. The findings reveal that TiO<sub>2</sub> bearing various metal ions successfully infiltrated the organic montmorillonite (OMMT) layer to form a pillared structure. The optical absorption edge of the metal doped TiO<sub>2</sub> pillared montmorillonite (T/M) exhibits an apparent red shift when compared to the undoped TiO<sub>2</sub> pillared montmorillonite (T/M).

Furthermore, the effects of various modifier content on the characteristics of the original bitumen and catalytic capacities for automotive exhaust were analysed. The results demonstrate that Ce doped TiO<sub>2</sub> (Ce-T/M) pillared montmorillonite increases bitumen's high temperature performance and UV resistance the most. They conclude that according to the degradation rate of NO and HC gas, Cu-T/M > Ce-T/M > Fe-T/M > T/M. In conclusion, Cu-T/M exhibits the best improvement. Hence, these three kinds of metal ions effectively improve the photocatalytic degradation efficiency of T/M.

Xu et al. (2019) studied the physical properties and anti-aging characteristics of asphalt modified with nano zinc oxide powder. They reported that incorporation of nano zinc oxide has a good effect on the anti-aging property of asphalt. Not only that, the storage stability, penetration (25 °C), softening point, and ductility (5 °C) of nano ZnO modified asphalt was investigated in this study. Next, the rheological properties of modified asphalt, before and after ageing, was used to investigate the effect of nano ZnO on the rheological properties of asphalt. The fatigue properties of asphalt with various nano ZnO dosages was also investigated using the linear amplitude sweep (LAS) test. The thin film oven test (TFOT) and ultraviolet ageing (UV-ageing) test were used to assess the anti-aging properties of nano ZnO modified asphalt, and the UV–visible–infrared absorption test was used to explain the process.

The findings revealed that nano ZnO has an impact on asphalt penetration (25 °C), softening point, ductility (5 °C), and storage stability. nano ZnO can help with complicated shear modulus ( $G^*$ ), phase angle ( $\delta$ ), and fatigue. The addition of nano ZnO to asphalt improves its anti-UV ageing performance and allows for some viscosity recovery during the ageing process. They found that nano ZnO has a high absorption rate of ultraviolet radiation, with more than 95% absorption, demonstrating its superiority as an anti-UV ageing modifier for asphalt. The UV absorption intensity of nano ZnO modified asphalt is several times higher than that of original asphalt, and at 3%, it can reach its maximum value and display no change as the nano ZnO dosage is increased. They concluded that asphalt modified with a suitable nano ZnO dosage exhibits strong anti-aging properties.

Zhan et al. (2020) studied the Synergetic Effect of nano ZnO and Trinidad Lake Asphalt for Antiaging Properties of SBS-Modified Asphalt. They proposed a composite of nano zinc oxide (nano ZnO) and Trinidad Lake Asphalt (TLA) be incorporated in the SBS-modified asphalt.

Among the tests conducted were the rotary film oven test (RTFOT), ultraviolet aging (UV), and the pressure aging vessel test (PAV). Not only that, but the conventional physical index, rheological index, and four-component content of SBS-modified asphalt before and after three aging modes were also tested, and the characteristic functional

groups in SBS-modified asphalt were tracked and analysed by the Fourier transform infrared spectroscopy (FTIR).

The results showed that adding different proportions of nano ZnO and TLA in the process of thermal oxygen ageing and the ultraviolet ageing test clearly reduces the effects of ageing on the rheological properties of SBS-modified asphalt, and the antiaging ability of SBS-modified asphalt is clearly improved.

By combining the changes in physical and rheological properties before and after RTOFT, PAV, and UV ageing, the recommended proportion ratio of 3 % nano ZnO + 25% TLA was confirmed. Concurrently, the rate of heavy components increased, while the change index of the colloidal instability index in the SBS-modified asphalt under the blending ratio was significantly lower than in the blank SBS-modified asphalt samples for the same ageing mode. Meanwhile the FTIR spectra showed that SBS-modified asphalt performance deterioration was mainly caused by ultraviolet aging and long-term aging.

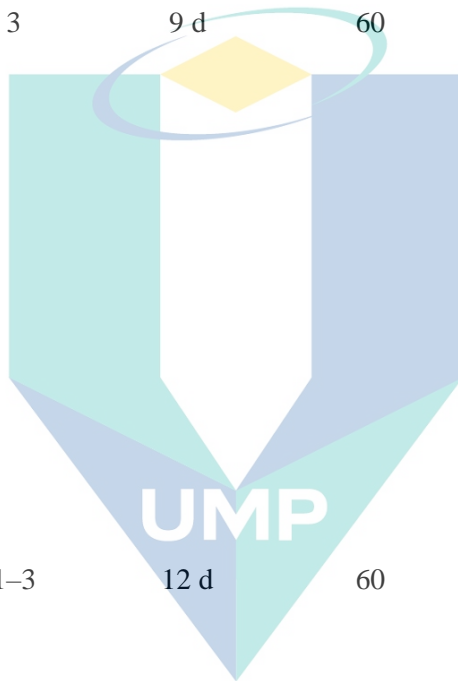
The addition of nano ZnO and TLA effectively reduced the increase of carbonyl groups and the breakage of the C double bond in butadiene, and synergistically improved the comprehensive aging resistance of SBS-modified asphalt. Overall, they found that this is an effective method to solve the aging problem in SBS modified asphalt.

Table 2.3 Some of the effects of using nanomaterials as observed in their research.

Nanomaterials	Content (%)	Ageing Time	Ageing Temperature (°C)	Observed Effect	References
Titanium dioxide/montmorillonite	4–6	336 h	-	5 % is the best UV aging resistance for the bitumen	(Jin et al., 2019)

Table 2.3 Continued

Nanomaterials	Content (%)	Aging Time	Aging Temperature (°C)	Observed Effect	References
Zinc oxide	2-3	6 d	80	3 % shows the best anti-aging performance	(Zhan et al., 2020)
Mg-Al-CO <sub>3</sub> layered double hydroxides	3	9 d	60	Layered double hydroxides with 180 nm possess the strongest ability to absorb and reflect UV light	(Cao et al., 2019)
Clay	1-3	12 d	60	2% improved the anti-aging resistance	(Cheraghian & Wistuba, 2020)
Zinc oxide	1-5 wt.-%	400 h	-	3% ZnO is the optimum content	(Xu et al., 2019)



اوتنيسور سديتي ملايسيا قهغ  
 UNIVERSITI MALAYSIA PAHANG

## 2.10 Nano titanium dioxide (Nano TiO<sub>2</sub>)

Nano titanium dioxide or Nano TiO<sub>2</sub> belongs to the transition metal oxides family. Titanium dioxide (TiO<sub>2</sub>) is a molecule which fundamentally consists of one atom of titanium and two atoms of oxygen. It is only found in about 0.6% approximately of the earth's crust alongside iron, copper and other metal oxides (He et al., 2021). Nano titanium dioxide is synthesized with the sol-gel method, which possesses self-cleaning and self-sanitizing properties since it is considered as an active photo-catalyst (Jameel et al., 2019).

The primary structure of Nano TiO<sub>2</sub> is octahedral, in which there is a three TiO<sub>2</sub> crystal structure (TiO<sub>6</sub>). The structure is temperature dependant, meaning its modes of arrangement and the links are different. Nano titanium existence in general is as a powder, sol or slurry form. It is either spherical or ellipsoidal (Li et al., 2018). Moreover, there are three forms of nano titanium with the first being anatase with a band gap of 3.2 eV. This form exists as an octahedral structure. Next is rutile with a 3.00 eV band gap, and a tetragonal structure. Lastly brookite has a 3.26eV band gap, with an orthorhombic structure.

According to Jayaraman et al. (2021) Titanium dioxide is highly beneficial in sunscreens since it absorbs UV light. It is one of the most commonly produced nanomaterials on a global scale. It is also the most often utilised photocatalytic substance since it performs best under sunshine. Titanium dioxide nanoparticles aid researchers in the development of photocatalysts that are more effective than others due to their increased surface area which is available for reaction with other molecules.

It can also be utilised in creams and coatings that absorb UV radiation without leaving a white coating in nanoparticle form, which is an advantage. Various approaches for utilising the photocatalytic capabilities of TiO<sub>2</sub> nanoparticles are currently being researched. The most photocatalytic form is the anatase form which has the most photocatalytic behaviour.

Since UV oxidation affects asphalt in high altitude regions, a nano titanium dioxide application could counter asphalt aging faster than other nanomaterials thanks to



its photocatalytic features. Features of nano titanium also include its high hardness, high dielectric constant, shielding ultraviolet radiation, weather ability and antimicrobial properties. nano titanium dioxide can also be applied in dental care as implants since it enhances protein adsorption, cell differentiation and surface bioactivity (Yang & Huang., 2019). Food simulants are involved with nano titanium dioxide as it is one of the materials involved in making food packaging (Yang et al., 2019).

Additionally, carbon-based nanomaterials are also being modified since nanomodification processes are being developed and have become an interest. Carbon nanotubes and graphene oxides are being investigated in terms of thermal characteristics for the asphalt binder in a study by (Wang et al.,2020). Wang et al. (2020) conducted a study to find out whether adding CNTs or graphene oxide would produce a change in the physical properties and chemical constitution of the modified binder.

It has been seen that compared to the original structure of the graphene, graphene oxide possesses more suitable characteristics like its layered structure that helps block gases and heat in the air. There are also more oxygen-functional groups where it helps the binder to be more compatible with GO. Both materials show improvement in terms of cohesiveness of the bitumen and the adhesion between the aggregates.

Cadorin et al. (2021) studied the asphalt nanocomposite with titanium dioxide for: mechanical, rheological and photocatalytic efficiency. They wanted to see how different percentages of titanium dioxide (TiO<sub>2</sub>) nanoparticles affected the mechanical and rheological properties, as well as the photocatalytic efficiency of a conventional asphalt binder. Different percentages of nano titanium were used with a three-percentage-point increment, ranging from 3% to 6%, 9%, 12%, and 15%.

The bitumen used had a penetration of  $60 \times 10^{-1}$  mm. The incorporation range (0–15%) comprised all study contents developed on the subject thus far, taking into account both the incorporation method via spraying and directly into the binder, which use up to 10% incorporation. However each study mentioned above investigated a different parameter, so there are no studies which used a comprehensive approach.

The experimental tests were carried out at two different temperatures: high and intermediate. The effect of nano titanium on the matrix was evaluated in several ways, including susceptibility to permanent deformation, fatigue damage tolerance, oxidative ageing resistance, apparent viscosity, and changes in dynamic shear modulus and phase angle. For the apparent viscosity, the nanocomposites asphalt binder had a higher viscosity compared to the normal binder, and as the content of nano titanium increases, the flow resistance also increases for all mixtures and temperatures.

The variation in the parameters in this study is due to the nature of the nanomaterial, which is not viscous. Furthermore, the small size (10 nm) and high specific surface area ( $60 \text{ m}^2/\text{g}$ ) of nano  $\text{TiO}_2$  allow it to reinforce and reach the complete asphalt matrix nanostructure. According to XRD, FTIR, and TGA, another factor is the crystallinity of the particles and the absence of amorphous impurities in the powder, which gives the nanomaterial a high mechanical resistance and structural stability even at high temperatures, which positively contributes to the structural reinforcement of the matrix at the nanoscale.

The photocatalytic efficiency was investigated in a continuous flow photoreactor with a  $\text{NO}_x$ -polluted atmosphere (nitrogen oxides). The results show that incorporating nano  $\text{TiO}_2$  into the asphalt binder influences the matrix's mechanical and rheological behaviour, providing greater resistance to permanent deformation, stiffness, fatigue damage tolerance at certain stress/strain levels, and resistance to oxidative ageing. However, photocatalytic nanocomposites are less susceptible to permanent deformation.

In terms of mechanical and rheological performance at intermediate temperatures, nano  $\text{TiO}_2$  incorporation results in: increased fatigue damage tolerance up to strain ranges of 7.7 percent and performance loss above this limit, characterised by greater sensitivity to the deformation level; as well as increased dynamic shear modulus and phase angle maintenance, i.e. increased material stiffness.

The nanomaterial increases the matrix's resistance to oxidative ageing, which contributes to fatigue cracking resistance. As long as the surface course of the pavement construction is limited to the performance of specified stress/strain levels, nano  $\text{TiO}_2$  can be useful in terms of boosting the fatigue resistance of the asphalt matrix. Overall

however, the photocatalytic semiconductor does not satisfy the mechanical and rheological performance expected in the study.

The 15% nano TiO<sub>2</sub> shows low efficiency in the photocatalytic activity as compared to photocatalytic cement matrices as the asphalt binder was covered by a portion of nanoparticles. The researchers suggested that further studies need to be carried out to increase the photocatalytic aspect of these matrices and to reduce the incorporated levels. The aspect that needs to be highlighted is the method of incorporating the nano titanium into the binder in order to get an ideal incorporation content of nano titanium.

### **2.11 Gap of Research**

Stone mastic asphalt has always been modified according to the changing conditions and parameters. Although it can be enhanced with additives like polymers, it does not satisfy the main problem which is associated with it, namely binder drain down. Additives may solve problems associated with the mechanical performance of the mix, but they do not address the properties of the binder. In this study, the physical, rheological and chemical properties of the modified binder are addressed prior to mixing it with the aggregates. Later on, the mechanical performance is also evaluated in regards to the binder modification.

Even though the usage of modified bitumen over recent years has dramatically improved bitumen properties, in order to foster higher quality and safe pavements, the use of a lower content of nanoparticles with better performance will improve the pavement industry. With the advance of nanomaterials in the pavement industry, nanomaterials are valued for their properties which can greatly enhance the mix depending on the type of nanomaterial used. For this study, nano titanium was chosen. nano titanium is valued for its small size particles, photocatalytic properties and ability to prolong fatigue life.

Some researchers recommended to add more tests in assessing the effect nanomaterials have on bitumen. The appropriate content of nanomaterials is recommended for use since higher contents of nanomaterials above 5% do not show a satisfactory change in the binder properties. Hence 1% to 5% nano titanium by bitumen

weight was used. Other than that, polymer modified mix has been found to have physical alterations but no chemical reaction. That is why, the study also intended to focus on the chemical properties of the bitumen after modification with nano titanium.

Table 2.4 shows studies performed in the previous 50 years in relation to the binder modification. These studies occurred between 1987 and 2021, and were found on the Scopus website by using the keywords “flexible pavement” AND “binder modification”, as well as “stone mastic asphalt” AND “binder”. A total of 1107 papers have been published regarding binder modification which have been identified. Of these, 175 papers matched up to the binder modification keywords. The trend shows a steady increase in the number of publications starting from 2009 to this day. It shows that more researchers are inclined to explore in the binder modification field as time goes on.

These publications were further arranged according to the related keywords as shown in Figure 2.21 until Figure 2.23. Among the keywords used were “applications”, “testing methods” and “materials”. Although the number of publications does seem to increase, there are more aspects that still need to be addressed in the binder modification area.

Table 2.4 Publications involving the related keywords starting from 1970 to 2021

Year	Publication	Year	Publication
1987	1	2008	7
1990	1	2009	16
1991	1	2010	16
1995	1	2011	22
1996	6	2012	28
1997	2	2013	35
1998	2	2014	36
2000	1	2015	51
2001	1	2016	74
2003	2	2017	95
2004	4	2018	107
2005	2	2019	140

Table 2.4 Continued

Year	Publication	Year	Publication
2006	7	2020	259
2007	15	2021	175

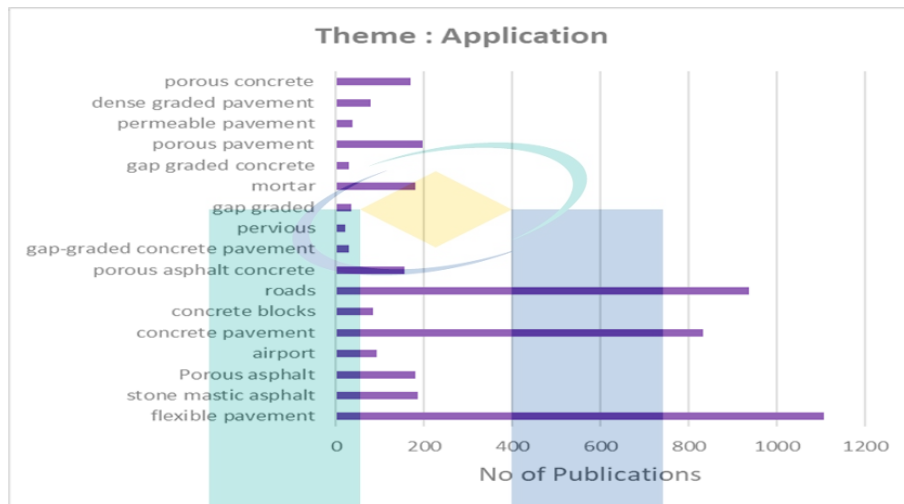


Figure 2.21 Publications involving type of pavement

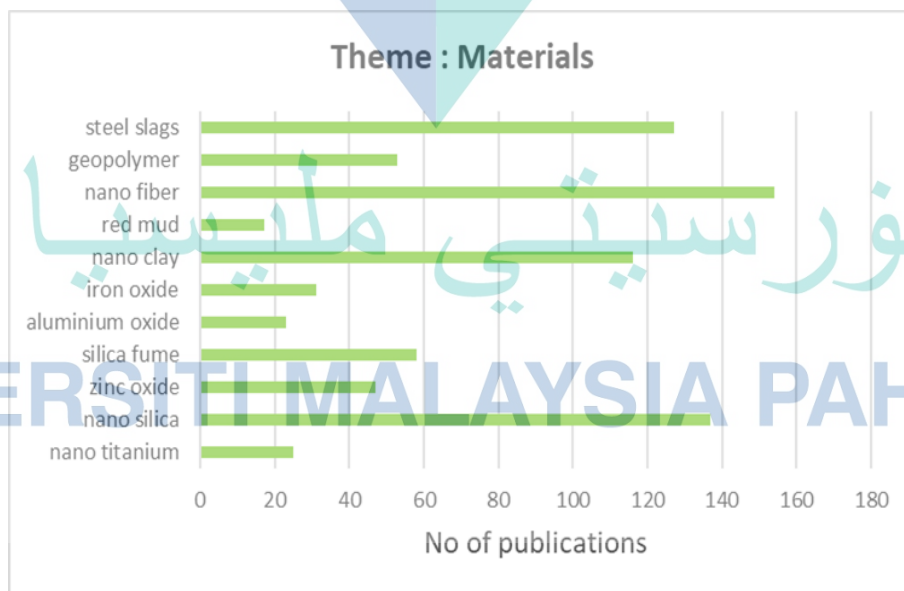


Figure 2.22 Publications involving materials

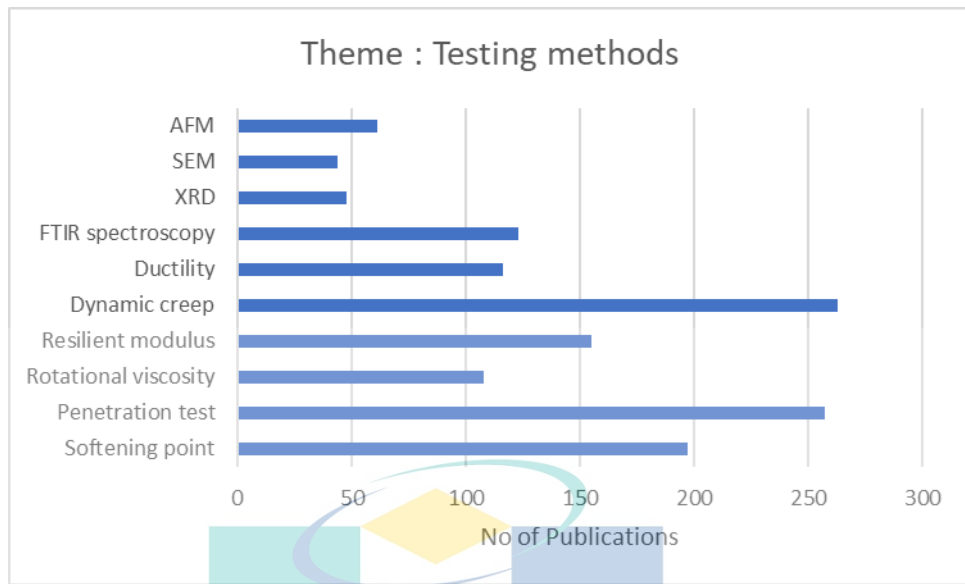
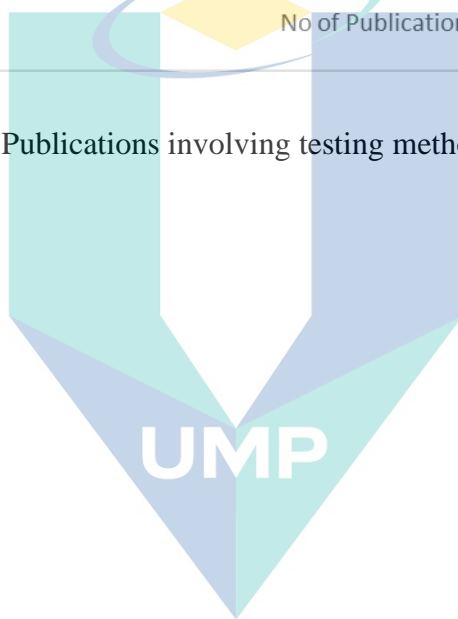


Figure 2.23 Publications involving testing methods



اونیورسیتی ملیسیا قہق

UNIVERSITI MALAYSIA PAHANG



## CHAPTER 3

### METHODOLOGY

#### 3.1 Introduction

This chapter is about the related tests which are involved with the samples. Starting from the aggregate's sample preparation and going to the binder's physical, morphological, rheological and chemical properties. The binder modification process is used to mix the binder and nano titanium. Meanwhile the Marshall mix method is used to make the Marshall samples, and lastly the mechanical performance is evaluated. The specifications used in this research were adapted from the Malaysian Public Work Department for road works.

#### 3.2 Flow of research

From Figure 3.1, the materials used are bitumen with a 60/70 penetration grade, aggregates according to the design requirements of SMA20 and nano titanium in powder form. The aggregates were sieved according to the specifications from the Malaysia Public Work Department: Flexible Pavement of SMA20 (JKR, 2008)

اونيورسيتي ملايسيا قهغ

UNIVERSITI MALAYSIA PAHANG

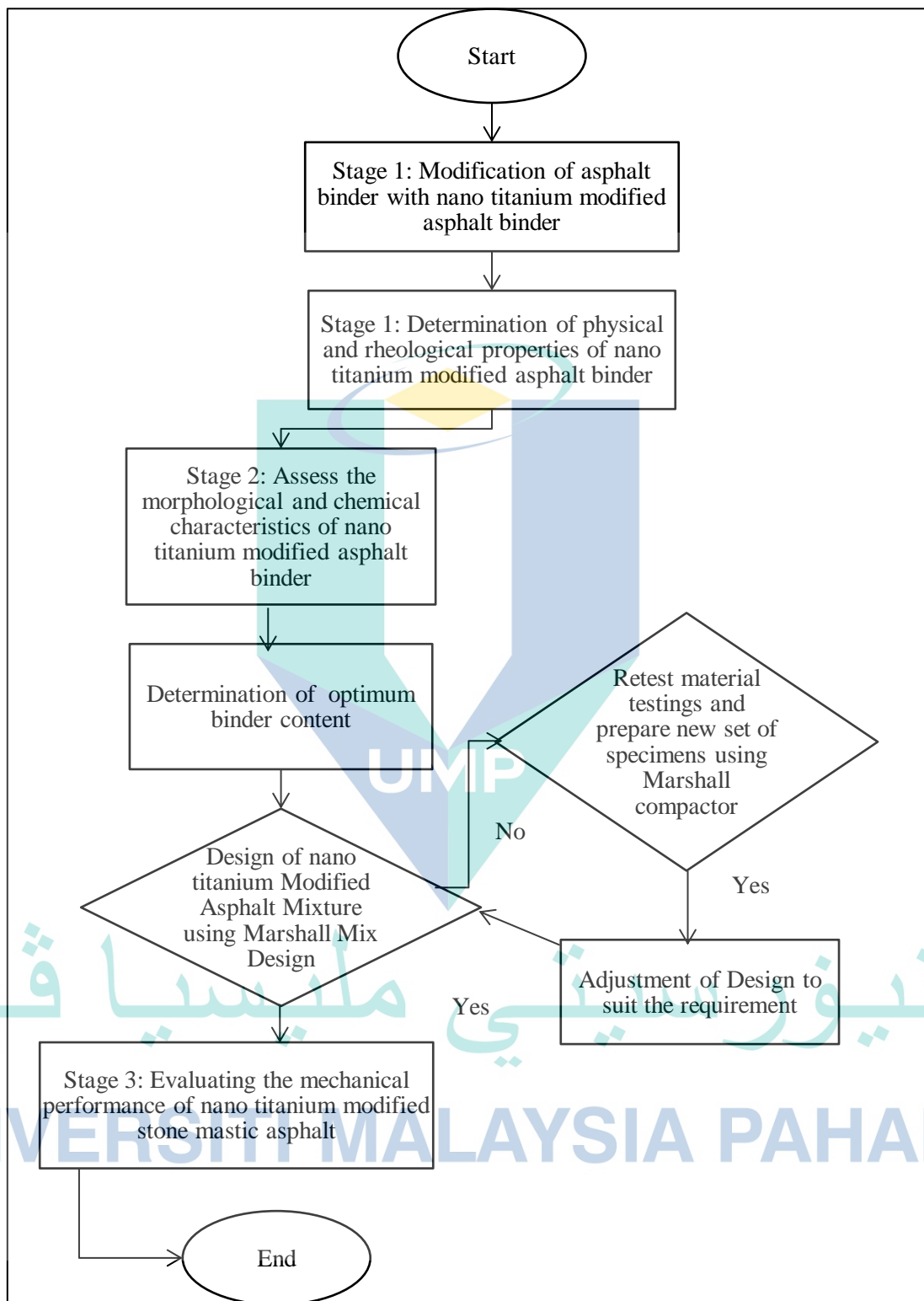


Figure 3.1 Flow of laboratory experiments

### 3.3 Source of raw materials

The granite used in this research was coarse and fine aggregates obtained from the Bekelah quarry, in Kuantan. The nano titanium powder was purchased from Gardner Global.

### 3.4 Materials preparation

For the preparation of the samples, the coarse aggregates were sieved first and after that the fine aggregates. The fine aggregates must be dried in the oven overnight before they were cooled and sieved. Then tests like the Sieve analysis, LA Abrasion and Aggregate Impact value were carried out. For the stone mastic asphalt samples, the samples prepared were 1200g of SMA20 specified aggregates for each sample and the nano titanium modified bitumen was then added from 1% to 5%. The samples were compacted by the Marshall compactor machine with 50 blows for both faces.

As for the nano titanium modified bitumen, the binder mixer machine was used for the mixing process of the nano titanium with the bitumen. Firstly, chunks of bitumen that had been placed in a steel cup were melted by putting them into the oven at the temperature of 140°C for about 1 hour and 30 minutes. Next the bitumen was weighed for about 500g and the nano titanium was prepared in intervals of 1 to 5g addition of nano titanium. The binder mixer machine was conditioned at 160°C prior to mixing and 1500 rpm was used for the mixing. The nano titanium was added gradually for the first 30 minutes and continued to be mixed for another 30 minutes in order for the mix to become homogenous. After modifying the bitumen, samples were collected and tested. The best percentage of nano titanium modification was determined after assessing the improvement of the mechanical properties of the samples. Figure 3.2 shows the binder mixer machine used.



Figure 3.2 Binder mixer machine

اونيورسيتي ملايسيا قهق

### 3.5 Materials properties

# UNIVERSITY MALAYSIA PAHANG

For the coarse aggregate, it was screened crushed hard rock and retained at a 5.0 mm sieve opening angular in shape and free from dust, clay, vegetative and other organic matter, and other deleterious substances. While for the fine aggregates, they were non-plastic and free from clay, loam, aggregations of material, vegetative and other organic matter, and other deleterious substances. For this research, SMA 20 was used. Table 3.1

below shows the gradation of SMA20 and Figure 3.2 is the retained aggregates for the 1200g sample.

Table 3.1 Aggregated gradation for SMA20 (JKR, 2008)

Sieve Size (mm)	Percentage by weight passing sieve (%)	Retained (%)	Retained (g)
19	100	0	0
12.5	85 – 95	10	120
9.5	65 – 75	20	240
4.75	20 – 28	46	552
2.36	16 – 24	4	48
0.6	12-16	6	72
0.3	12-15	0.5	6
0.075	8-10	4.5	54
Pan	-	7	84
lime	-	3	24

اونيورسيتي ملايسيا قهغ

UNIVERSITI MALAYSIA PAHANG



Figure 3.3 Aggregate sample

### 3.6 Materials testing methods

#### 3.6.1 Sieve Analysis

Sieve analysis was done according to ASTM C136/C136M-19 (ASTM, 2019) to determine the gradation sizes of the aggregates. The required sieve size was assembled together and coarse aggregates were loaded into the sieve. Then the sieve was positioned in the sieve shaker and operated for about 10 to 15 minutes.



Figure 3.4 Sieve shaker machine



### 3.6.2 LA Abrasion

LA Abrasion according to ASTM C131M-20 (ASTM, 2020) was done to obtain the Los Angeles number in the form of percentage wear of aggregates which reflects their resistance to degradation using the Los Angeles testing machine. The percentage of loss calculated followed Equation 3.1

$$\% \text{ of Loss} = (\text{Mass final} - \text{Mass Initial}) / \text{Mass Initial} \times 100 \quad 3.1$$

For the sample involved, the weight before was recorded along with the average sample height and diameter. There were 3000 revolutions, and the reading was taken and recorded for each 1000 revolutions.

### 3.6.3 Aggregate Impact Value

The objective of the experiment was to determine the aggregate impact value of road stone in the laboratory. It was done according to BS812-112 (BS,1990). The aggregates were sieved, the portion which passed the 14mm and was retained on the 10mm sieve was obtained. These aggregates were washed and dried at a constant temperature between 105°C and 110°C. These aggregates weight was recorded as an initial weight (M1) and then they were filled in the cylindrical measures in 3 layers, each layer was tapped 25 times with the tamping rod. The aggregates in the measure were weighed and were used as a duplicate test on the same material. From the cylindrical measure, the aggregates were transferred to the cup, also in 3 layers by tamping 25 strokes with the tamping rod. The hammer from the impact testing machine was released to fall freely on the aggregate. The sample was subjected to a total of 15 blows. The aggregates were then removed from the cup and sieved through a 2.36mm sieve. The weight was measured as weight loss (M3) as shown in Equation 3.2.

$$\text{AIV} (\%) = \text{Weight loss (M3)} / \text{Initial weight (M1)} \times 100\% \quad 3.2$$

### 3.6.4 Aggregate Crushing Value

The test was done to determine the mechanical strength of the aggregate. It was done according to BS812-110 (BS,1990). The aggregates were sieved and the portion which passed 14mm and was retained on the 10mm sieve was taken. The aggregates were then filled into the cylinder in thirds, in which each third was subjected to 25 blows. The initial sample weight was noted as M1. The surface cylinder was levelled and the plunger was inserted while the sample was placed between the plates of the testing machine. The load was then released and the crushed aggregates were removed. The crushed aggregates were sieved through a 2.36 mm sieve and weighed. The final weight was noted as M3. The aggregate crushing value was calculated as shown in Equation 3.3.

$$\text{ACV (\%)} = \text{Weight loss (M3)} / \text{Initial weight (M1)} \times 100\% \quad 3.3$$

### 3.6.5 Bitumen

The bitumen used was of a 60/70 penetration grade as stone mastic asphalt had been associated with it according to the Public Work Department (JKR, 2008) specification of bitumen types to be used in stone mastic asphalt mixes. The optimum binder content is 6.16% adopted from (Arshad et al., 2019).

Table 3.2 Properties of bitumen

Properties	Descriptions
Specific gravity @25°C	1.01/1.06 Kg/cm <sup>3</sup>
Penetration @25°C	60-70 mm
Softening Point @25°C	49-56 °C
Ductility @25°C	100 cm
Specific gravity @25°C	1.01/1.06 Kg/cm <sup>3</sup>
Penetration @25°C	60-70 mm
Softening Point @25°C	49-56 °C

### 3.6.6 Nano titanium dioxide

Nano titanium dioxide was chosen due to its properties like higher reactivity with bitumen due to its small size. It possesses photocatalytic properties which could help in eliminating hazardous gases like nitrogen monoxide. This promotes the environmentally friendly character of the asphalt pavement. Nano titanium dioxide also improves the asphalt aging properties. Not only that, nano titanium could reduce binder drain down properties by increasing the adhesion between aggregates and bitumen when added into the mix. The high number of nano particles is able to fill the voids that exist and make the structure more packed.

Nano titanium was used in 1%, 2%, 3%, 4% and 5% amounts by bitumen weight, as there is no exact amount of nanomaterial which has been specified and each amount also varies according to their own purposes. However, since the previous study by (Razavi & Kavussi, 2020) mentioned that including more than 5% nanomaterials does not influence the bitumen properties effectively, the amounts of 1% to 5% increments were chosen for this study.

Table 3.3 Properties of nano titanium

Properties	Descriptions
Colour	White
Purity	99.9%
Primary Particle Size	20nm
Structure	Anatase, Rutile, Brookite
Melting Point	1843°C
Boiling Point	2972°C
Relative Density at 25°C	4.26g/cm <sup>3</sup>

### 3.6.7 Bitumen modification process by using binder mixer

Binder modification process parameters were adjusted from the previous research, and the procedures of the binder modification are shown in the Figure 3.5 below:

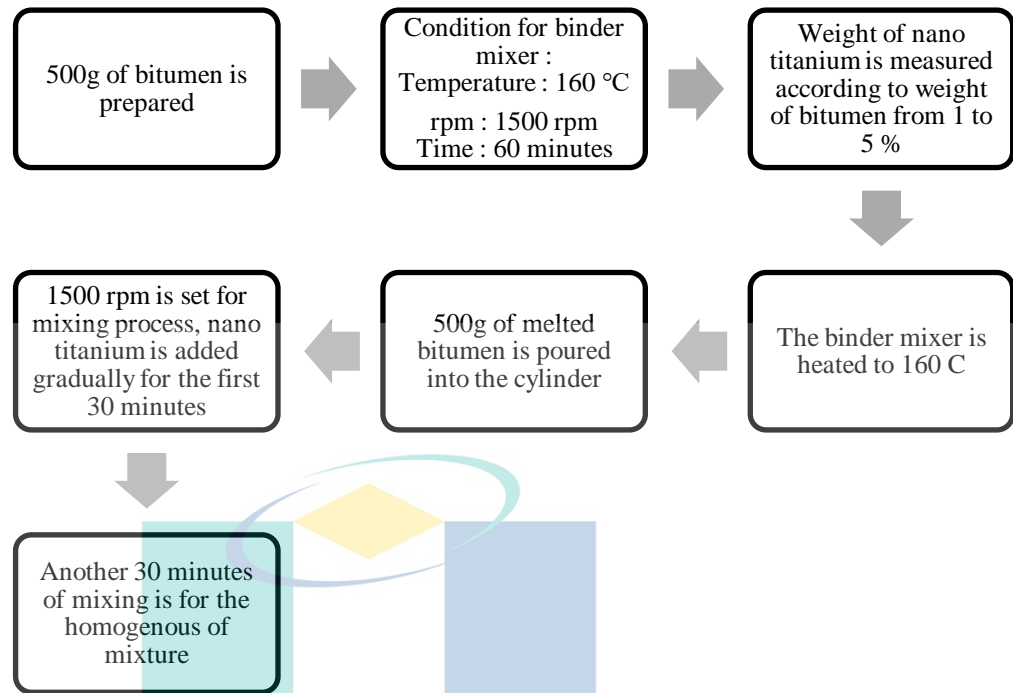


Figure 3.5 Binder mixing procedures

### 3.6.8 Type of mixture

Common SMA composition consists of 70–80% coarse aggregate, 8–12% filler, 6–7% bitumen, and 0.3 per cent fibre. Compared to the conventional mix, which contains about 40-60% aggregates, SMA possesses a higher content of coarse aggregate, as it increases the interlocking attributes of the aggregates and provides better stone to stone contact, which serves as a load carrying mechanism in SMA and hence provides better rut resistance and durability. The optimum binder content (OBC) of 6.16% was adopted from previous research by (Arshad et al., 2019).

## 3.7 Physical properties test

### 3.7.1 Softening point test

The objective of the experiment was to determine the temperature at which the given bitumen reaches a degree of softness according to ASTM D36 / D36M (ASTM, 2020). The bitumen was melted and poured into a pair of rings placed on a plate that have been previously applied with Vaseline. After the specimen has cooled, the ring was

suspended in the distilled water in the beaker at  $5^{\circ}\text{C} \pm 2^{\circ}\text{C}$  along with the steel balls. The temperature was maintained for 15 minutes. The steel balls were put on the surface of the bitumen in the ring. Then, the bath liquid was stirred and heated to  $5^{\circ}\text{C} \pm 2^{\circ}\text{C}$  per minute. The thermometer was placed in the middle of the ring holder and was levelled with the bottom of the ring. When the ball passed and dropped into the base plate, the temperature was recorded.



Figure 3.6 Samples after being cooled on ring apparatus

Figure 3.6 shows the samples that have been poured into the ring and left to be cooled for 30 to 60 minutes.



Figure 3.7 Samples falling when reaching softening point

Figure 3.7 shows the samples falling after reaching a certain temperature. When the balls reach the flat surface, the test was stopped and the temperature is recorded.

### 3.7.2 Penetration test

To determine the hardness and consistency of the bitumen before it was applied to the road according to ASTM D5 (ASTM, 2020) the specimens were prepared in a sample container as specified, and then placed in a water bath at room temperature about 1 to 1.5 hours prior to the test. Then, the penetrometer dial reading was set to zero. The penetration needle was cleaned and fixed into the holder and guide. For the normal test, the precisely dimensioned needle was loaded to  $100 \pm 0.05\text{g}$ . Next, the needle was slowly lowered until its tip just made contact with its image on the surface of the sample at right angles. The needle holder was released to penetrate the bitumen for  $5 \pm 0.1\text{s}$ , while its temperature was maintained at  $25^\circ\text{C} \pm 0.1^\circ\text{C}$ . The penetration was measured in terms of millimetres (mm). The depth of penetration was read and recorded. At least three



determinations on specimens were made at different points and the needle was cleaned before repeating the test. Figure 3.8 shows the set up for the penetration test. The needle was set to zero because if it was not, the reading would be wrong.

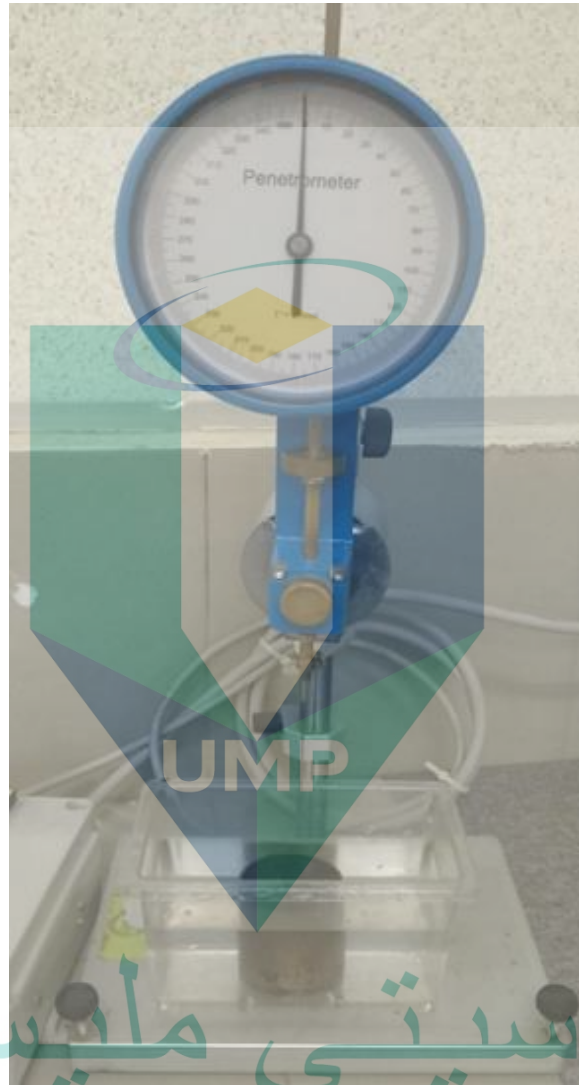


Figure 3.8 Penetration test apparatus set up

اونيفورسيتي ماليسيا قهغ  
UNIVERSITI MALAYSIA PAHANG

### 3.7.3 Rotational Viscosity test

This test basically measures the torque of the bitumen. The nano titanium modified sample was conditioned for 1 hour at the desired temperature. For this test, two temperatures: 135°C and 165°C were used. Figure 3.9 shows the rotational viscometer machine. The spindle size was determined according to the viscosity of the fluid used.

For bitumen, usually size #27 was used with 20 rotations per minute (RPM). Smaller spindle sizes were used according to the desired RPM speed as included in the manual which came along with the machine. This test is a combination of AASHTO T 316 (AASHTO.,2019) and ASTM D 4402 (ASTM, 2015). After getting the torque displayed as a percentage, the value just needs to be converted into pascals (Pa), as shown in Equation 3.4.

$$cP \times 0.001 = Pa. s$$

3.4



Figure 3.9 Rotational viscometer machine

UNIVERSITI MALAYSIA PAHANG

### 3.8 Morphological properties of nano titanium modified binder

#### 3.8.1 X-Ray Diffraction Analysis (XRD)

X-Ray Diffraction, frequently abbreviated as XRD, is known as a non-destructive test method used to analyse the structure of crystalline materials. XRD analysis, by way

of the study of the crystal structure, was used to identify the crystalline phases present in the material and thereby reveal the chemical composition information.



Figure 3.10 D8 Advance (Brand: Bunker)



Figure 3.11 Samples for XRD

The machine used was the D8 Advance from Bunker in 2016. The type of samples available to be assessed by this machine were in powder and thin film form. For the

powder sample, the sample required was less than 3g and the recommended size was between 30 $\mu$ m~10 $\mu$ m.

Huge chunks of bitumen were melted and mixed with an appropriate content of nano titanium before being cooled off. After the sample cooled off, the sample was formed into a small sphere. The sample was in a small sphere form state as the test only needs a small portion of the sample.

### 3.8.2 Scanning Electron Microscope with Energy Dispersive X-Ray Analysis (SEM-EDX)

Scanning Electron Microscopy (SEM) with Energy Dispersive X-Ray Analysis (SEM-EDX) provides detailed high-resolution images of the sample by reprojection of a focused electron beam across the surface and detecting secondary or backscattered electron signals.

The preparation of the sample was done by mixing the needed content of nano titanium with the preferred amount of bitumen. The sample was prepared by cooling the bitumen until it hardened and the bitumen was then scrapped into a small portion to be put under the microscope. The sample was then assessed by the machine and the results were generated.



Figure 3.12 Samples for SEM-EDX

### 3.9 Chemical properties of nano titanium modified binder

#### 3.9.1 Fourier Transform Infrared Spectroscopy (FTIR)

Fourier Transform Infrared Spectroscopy, also known as FTIR Analysis or FTIR Spectroscopy, is an analytical technique used to identify organic, polymeric, and, in some cases, inorganic materials. The FTIR analysis method used infrared light to scan test samples and observe their chemical properties.

For the bitumen, samples were prepared in a small steel container for about 50 - 100 g, and the bitumen was left to cool at room temperature. Then, the sample was made in the form of a small ball. A diluting agent was used according to the sample type. For this type of sample, FTIR-ATR was used. The wavelength was observed on the monitor display and certain peaks were observed and recorded. The results were then extracted from the software and analysed.



Figure 3.13 FTIR machine



Figure 3.14 Sample for FTIR-Atr

### 3.10 Mechanical properties of SMA

#### 3.10.1 Volumetric properties (Marshall Stability)

This test was done to prepare standard specimens of asphalt mixture for the determination of stability and flow in the Marshall apparatus, and to determine density, percentage air voids and percentages of aggregate voids filled with binder according to ASTM D 6927-15 (ASTM, 2015).



Figure 3.15 Marshall stability set up

This test was conducted on 8 samples with two samples for each percentage of 0%, 2%, 3%, and 4%. Prior to testing, the samples were conditioned by placing them in a water bath at a temperature of 60°C for 30 minutes. The samples were then placed on the Marshall stability machine as shown in Figure 3.15, and loaded with the amount of force required to break the sample. The values measured were taken as the Marshall Stability. The results appeared on the monitor of the machine and would be recorded. The volumetric properties like density, stability, flow and stiffness were obtained from this test.



### 3.10.2 Resilient Modulus

This test aims to determine the material stiffness under different conditions according to ASTM D7369-20 (ASTM, 2020). The test was conducted at two different temperatures which were 25°C and 40°C. The temperatures indicated low and high temperature condition. The Universal Testing Machine (UTM) was controlled from the computer and the software used was ITS-Resilient Modulus. Before running the software, the Axial force must be offset to zero to prevent the knob from going upward by itself.

The linear variable differential transducers 1 (LVDT1) and linear variable differential transducers 2 (LVDT2) cannot have negative values prior to the test, so as to prevent inaccurate readings. The test took approximately 3 hours for 3 samples, having a total of 6 samples for each temperature. The samples were tested in two positions which were the 0 and 90-degree positions. The average reading was taken for each sample.

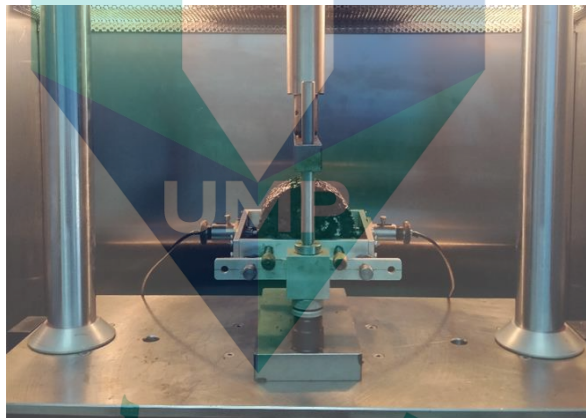


Figure 3.16 Resilient modulus set up



Figure 3.17 UTM Machine

### 3.10.3 Dynamic creep

This test is done to evaluate the rutting resistance of asphalt pavements according to ASTM D704-15 (ASTM, 2015). This test was completed using the UTM machine and a software for permanent deformation on the computer. The samples were conditioned at a temperature of 40°C in the machine before being placed into the dynamic creep apparatus. The testing occurred for about 2 hours, before the end results were produced on the computer.

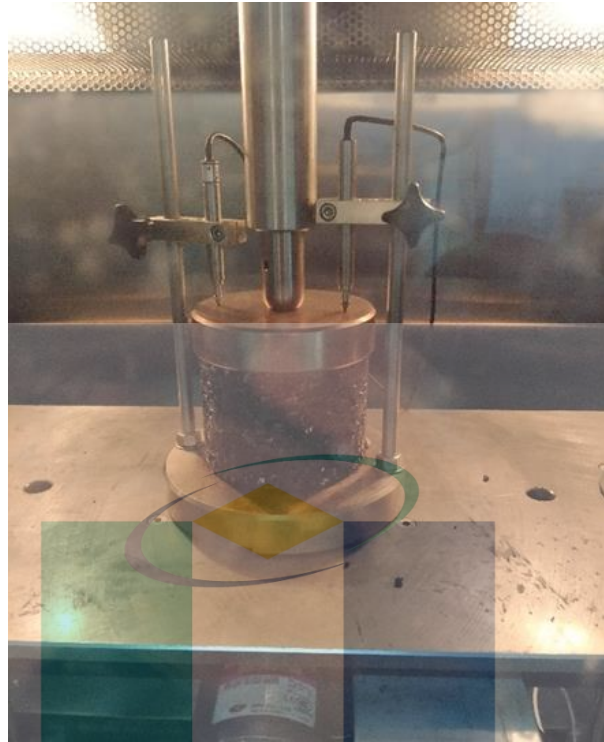


Figure 3.18 Sample set up for dynamic creep

### 3.10.4 Moisture Susceptibility **UMP**

The test was done according to AASHTO T-283 (AASHTO.,2014). All the samples had the same diameter with different heights. The samples were prepared in two conditions which were wet and dry conditions. There were a total of 16 samples, 8 for dry conditions and 8 for wet conditions. The dry samples were conditioned for 2 hours at 25°C while the wet samples were left in a water bath for 24 hours at 60°C and continued for 2 hours at 25°C. The samples were then tested by using the machine and the results were taken as shown in Equation 3.5 and 3.6

$$S_t = 2P/\mu D_t \quad 3.5$$

Where:

$S_t$  = Tensile Strength (KPa)

P = Applied Load (N)

t = Thickness of Specimen (mm)

D<sub>t</sub> = Diameter of Specimen (mm)

$$\text{TSR} = (S_t \text{ wet}/S_t \text{ dry}) \times 100 \quad 3.6$$

Where:

S<sub>t</sub> wet = Average Tensile Strength of Wet Conditioned Subset (KPa)

S<sub>t</sub> dry = Average Tensile Strength of Dry Subset in (KPa)



Figure 3.19 Indirect tensile machine



Figure 3.20 Samples in water bath at 25°C

### 3.11 Binder drain down

The method for this was adopted from (Masri et al., 2016). The samples involved were 0%, 2%, 3% and 4% of nano titanium modified bitumen. A loose sample of 1200g of stone mastic asphalt was heated in the oven for about 24 hours prior to the test. The sample was then mixed with each respective amount of nano titanium modified bitumen and then was put into a square basket. The basket was put into the oven for approximately 3 hours. The weight before and after was recorded and observed. The loss of weight was noted as the binder drain down and calculated as shown in Equation 3.7.

$$\text{Drain down, (\%)} = (B-A)/C \times 100 \quad 3.7$$

where,

A = Initial mass of sample with basket (g)

B = After mass of Wire Basket & Sample (g)

C = Total of accumulated binder loss (g)





Figure 3.21 Binder drain down basket

### 3.12 Summary of materials testing and sample

Table 3.4 shows the overall testing, number of samples and content of nano titanium involved. The testing which was arranged was the physical and rheology test, chemical and morphology test and mechanical performance tests.

Table 3.4 Summary of materials testing and sample

Test	Sample						NP
	Percentage of Nano Titanium						
	0 %	1% NTMB	2% NTMB	3% NTMB	4% NTMB	5% NTMB	
Penetration Test	2	2	2	2	2	2	
Softening Point	2	2	2	2	2	2	
Rotational Viscosity	2	2	2	2	2	2	
Total	6	6	6	6	6	6	



Table 3.4 Continued

Test	Sample						
	Percentage of Nano Titanium						
	0 %	1% NTMB	2% NTMB	3% NTMB	4% NTMB	5% NTMB	NP
FTIR	2	2	2	2	2	2	1
XRD	2	2	2	2	2	2	1
SEM-EDX	2	2	2	2	2	2	1
Total	6	6	6	6	6	6	3
Resilient Modulus	2		2		2	2	
Dynamic Creep	2		2		2	2	
Moisture susceptibility	4		4		4	4	
Binder drain down	2		2		2	2	
Total	10	0	10	0	10	10	
Total of all samples							115

اونیورسیتی ملیسیا قہق

UNIVERSITI MALAYSIA PAHANG

## CHAPTER 4

### RESULTS AND DISCUSSION

#### 4.1 Introduction

This chapter discusses the results which were obtained from the experiments conducted. It begins with the physical properties of the aggregates, and is followed by the physical properties of the binder and the morphological and chemical properties. Next, the volumetric properties of the stone mastic asphalt (SMA) and the mechanical properties of SMA with a nano titanium modified binder are discussed. Binder drain down results are also available to review and a summary of results is at the end of this chapter.

#### 4.2 Physical properties of aggregates

##### 4.2.1 Sieve Analysis

A Sieve analysis was done to obtain the required mass of the aggregates to be used, and it fell into the targeted specification as shown in Figure 4.1. The sieve sizes used were 19.0 mm, 12.5 mm, 9.5 mm, 4.75 mm, 2.36 mm, 0.6 mm, 0.3 mm and 0.075 mm. The retained aggregates weight fell on the range between the maximum and minimum levels and passed the specification according to (JKR, 2008).

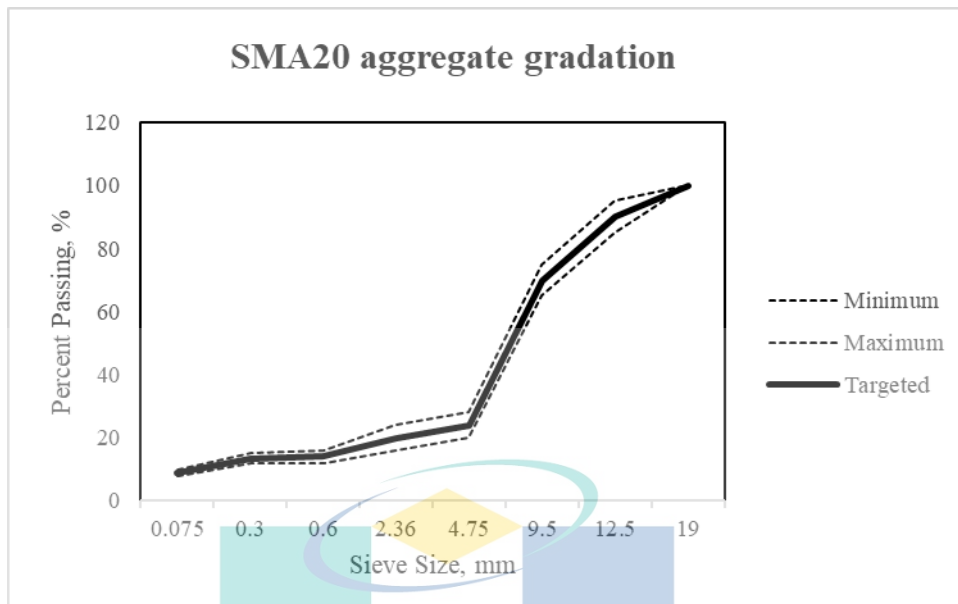


Figure 4.1 SMA20 aggregate gradation

#### 4.2.2 LA Abrasion

This test shows a result of about 21%, showing it passes the limit of the LA Abrasion value, which must be below 25%. This test shows the aggregates toughness and the abrasion importance. The percentage of wear due to the rubbing action of the steel balls and aggregates is used as the abrasive charge. The aggregates are shown to be suitable to be used in the experiment.

Table 4.1 LA Abrasion value results

Sample	Aggregate size (mm)	Weight of Crushed Aggregate (g)			% Loss
		Before (m1)	After (m2)	Loss (m3)	
	20	5001.4	3941.77	1059.63	21.18

$$\text{LA Abrasion Value (\%)} = (\text{weight loss}/\text{initial weight}) \times 100$$

$$\text{LA Abrasion Value (\%)} = (1059.63/5001.4) \times 100 = 21.18 \%$$

### 4.2.3 Aggregate Impact Value

The percentage of loss obtained from this test was 15%. This value indicates the resistance value of the aggregates to sudden shock or impact. Thus, the aggregates toughness is measured as strong and demonstrates sufficient strength. The aggregates are able to resist the loads exerted on them.

Table 4.2 Aggregate Impact Value result

Sample	Aggregate Size(mm)	Weight of Aggregate (g)			
		Before Test (m1)	Retain at 2.36mm sieve (m2)	Passing at 2.36mm sieve (m3)	% loss
A	10	293.66	251.6	43	15

### 4.2.4 Aggregate Crushing Value

Both of the samples show results below the aggregate crushing value limit, which is 25%. This shows that the aggregates could resist crushing under a gradually applied load. Crushing value is also a measure of the aggregate strength, thus these aggregates are qualified for use.

Table 4.3 Aggregate crushing value results

Sample	Aggregate Size(mm)	Weight of Aggregate before (g) m1	Weight Pass Sieve 2.36mm (g) m2	Aggregate Crushing Value (%)
A	20-14	3001.6	453.02	15.09
B	14-10	3000.24	358.83	11.96

### 4.3 Physical properties of binder

#### 4.3.1 Softening point

As shown in Figure 4.2, the softening point is at the highest at 3% nano titanium at 48.6°C as compared to 0% nano titanium which is only recorded at 44.4°C. Further addition of nano titanium beyond this makes the softening point drop lower than the initial recorded reading. The highest softening point being at 3% implies that the resistance of the bitumen to heat is increased and shows that there is a low probability that the bitumen will soften under high temperatures, which is a parallel for hot weather. This makes the bitumen less vulnerable to temperature changes. Rutting is one of the deformations which happens in related high temperatures. With the increase in the softening point, the rutting developments would be reduced.

Other than that, the 1% nano titanium modified binder showed a higher softening point too, but it did not satisfy the requirements of the standard softening point temperature. This may be a result of not enough nano titanium particles being present to influence the bitumen sample. This indicates that it needs more than 1% of nano titanium, hence the range of nano titanium was described as going up to 5%. The same could be said for the 2% nano titanium modified binder, which experienced a fall in the softening point of the binder. However, the 4% and 5% binders did experience the same trend, showing that a lower or higher than 3% addition of nano titanium did not manage to influence the temperature of the softening point. These results show that they are much less sensitive to temperature, especially at high temperatures (Geçkil, 2019).

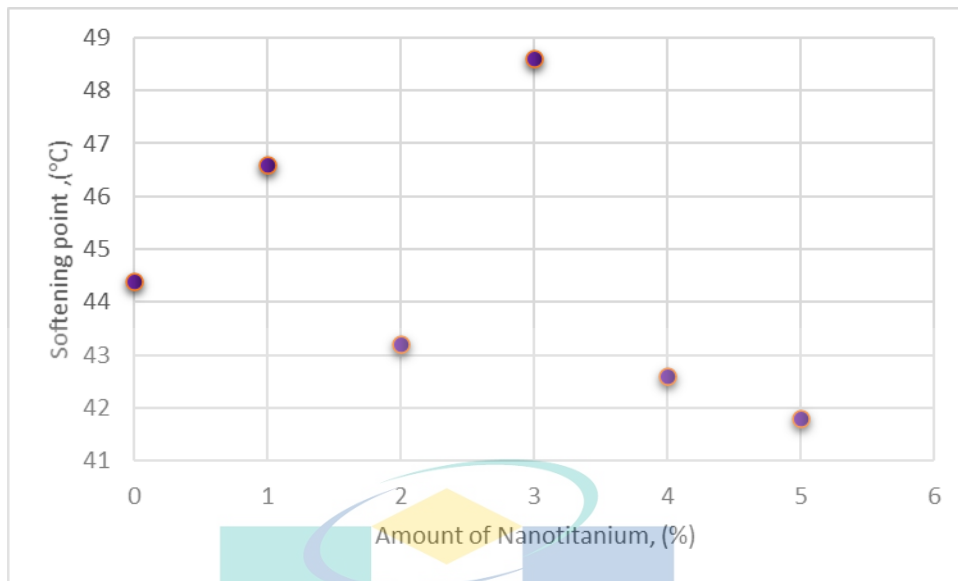


Figure 4.2 Softening point results

#### 4.3.2 Penetration test

The results in Figure 4.3 show that the bitumen penetration at 25°C varies with different nano titanium percentages, with a decreasing trend. This decreasing trend was also observed on earlier research conducted by (Crucho et al., 2018) and (Xu et al., 2019). The decreasing trend shows that the different nano titanium content levels have different influences on the bitumen, hence the bitumen elasticity is different for each percentage. The penetration for nano titanium mixtures between 1 to 5% is 73 mm, 61.5 mm, 60.5 mm, 55.5 mm, 54.5 mm, and 62.5 mm respectively. Since the penetration grade used is 60/70, the penetration values should also fall between 60 to 70 mm.

The consistency of the bitumen is harder at 3% and 4% nano titanium as compared with the 0% nano titanium sample which is more flexible. The addition of nano titanium caused the bitumen to be more consistent, harder and stiffer. It also improves the high temperature resistance of the mixtures (Ameli et al., 2020). The results show that the incorporation of nano titanium not only makes the binder stiffer, which makes the penetration decrease, but it also improves the temperature sensitivity of the original asphalt proportionally within a certain range of the nano titanium dosage. In conclusion, 4% nano titanium modified bitumen is chosen as the most suitable dosage.



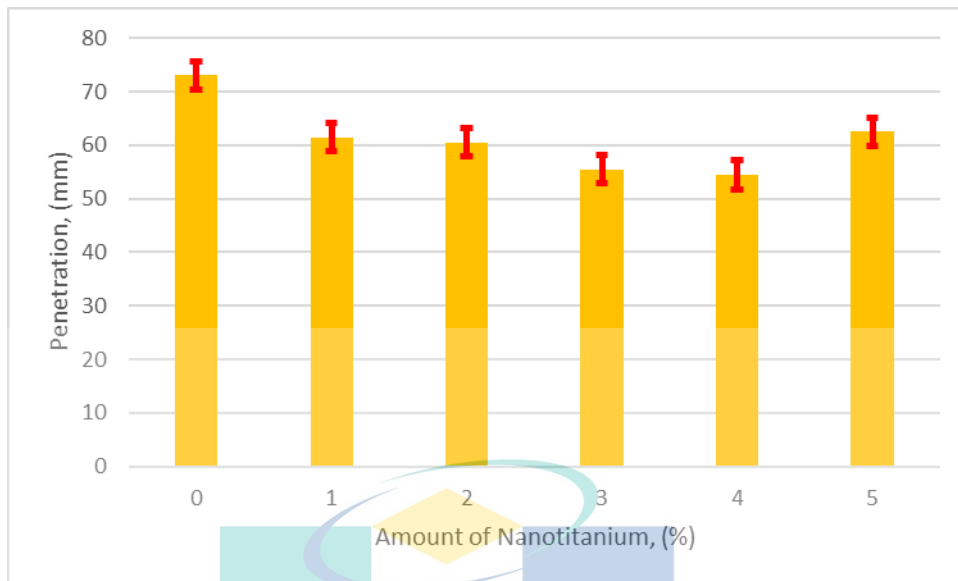


Figure 4.3 Penetration test results

#### 4.3.3 Rotational viscosity

Table 4.4 and Figure 4.4 show the viscosity values at 135°C and 165°C. The 3% nano titanium modified bitumen shows an improvement compared to the original. The modified sample shows a decreasing trend, but still has a greater value compared to the unmodified bitumen. Since nano titanium is sensitive to temperature, it could be seen that the same trend is observed at 165°C, but with decreasing values. However, even these values were still higher than the unmodified. The presence of nano titanium makes the binder stiffer and thus subsequently makes an improvement in the rutting behaviours. This shows overall that with the addition of nano titanium the binder is improved which is also supported by a study by (Ismael et al., 2021). The presence of these extremely small size particles will lead the binder to become more viscous as they increase the shear resistance to flow due to the higher relative surface of the dispersed colloidal particles. It is evident that with the presence of nano titanium in the binder, the binder is stiffer which makes it more resistant to permanent deformation.

Table 4.4 Rotational viscosity results

Temperature (°C)	Temperature (°C)	
	135	165
Nano titanium (%)		
0	1455	427
1	3824	725
2	879	436
3	1762	574
4	1400	460
5	1185	355

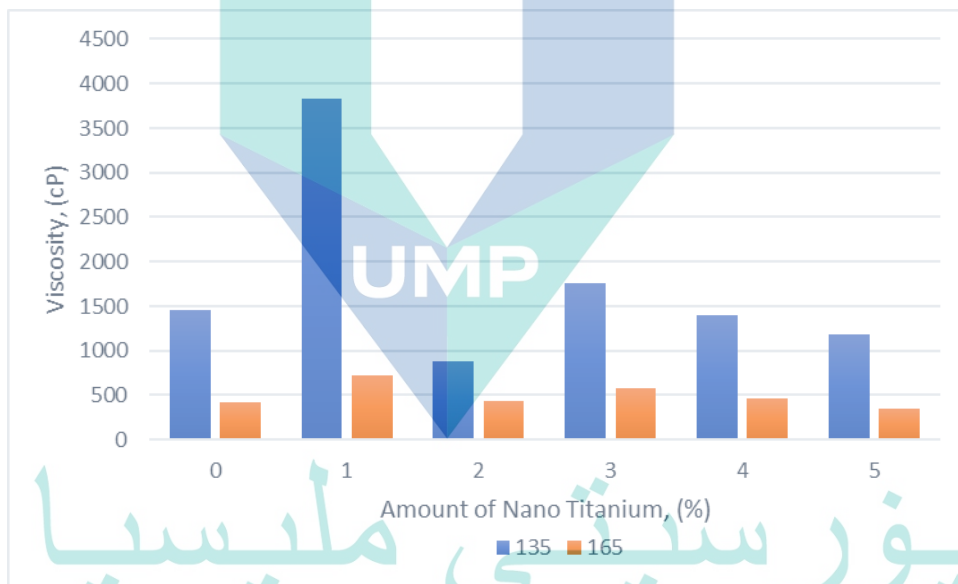


Figure 4.4 Rotational viscosity at 135 °C and 165 °C

# UNIVERSITI MALAYSIA PAHANG

## 4.4 Morphological and chemical properties

### 4.4.1 X-Ray Diffraction Analysis (XRD)

Figure 4.5 depicts the result of the XRD on the unmodified and modified with nano titanium bitumen samples. The peak for the original bitumen was observed between 20°-25°, which had peaks at 23.96 and 26.27. These peaks are due to the aliphatic chains

and layers of condensed saturated rings, since it is plain bitumen and is completely amorphous. A close check on the nano titanium powder was also done, which revealed that the nano titanium had a crystallized structure since sharp peaks were produced along the 25-75 peaks as shown in Figure 4.6.

After the addition of nano titanium to the bitumen, the position of  $2\theta$  at  $22.71^\circ$ ,  $44.31^\circ$ ,  $54.87^\circ$ , and  $62.95^\circ$  correspond to the rutile phase and matched well with the Original ICSD space group as reported by (Haider et al., 2017). The results were also similar with the other reports of rutile  $\text{TiO}_2$  by (Leal et al., 2017). It can be seen that the composition of the bitumen when assimilated with titanium dioxide does not disappear completely, nor is it changed thoroughly and the presence of the rutile phase is at a 3% addition of nano titanium.

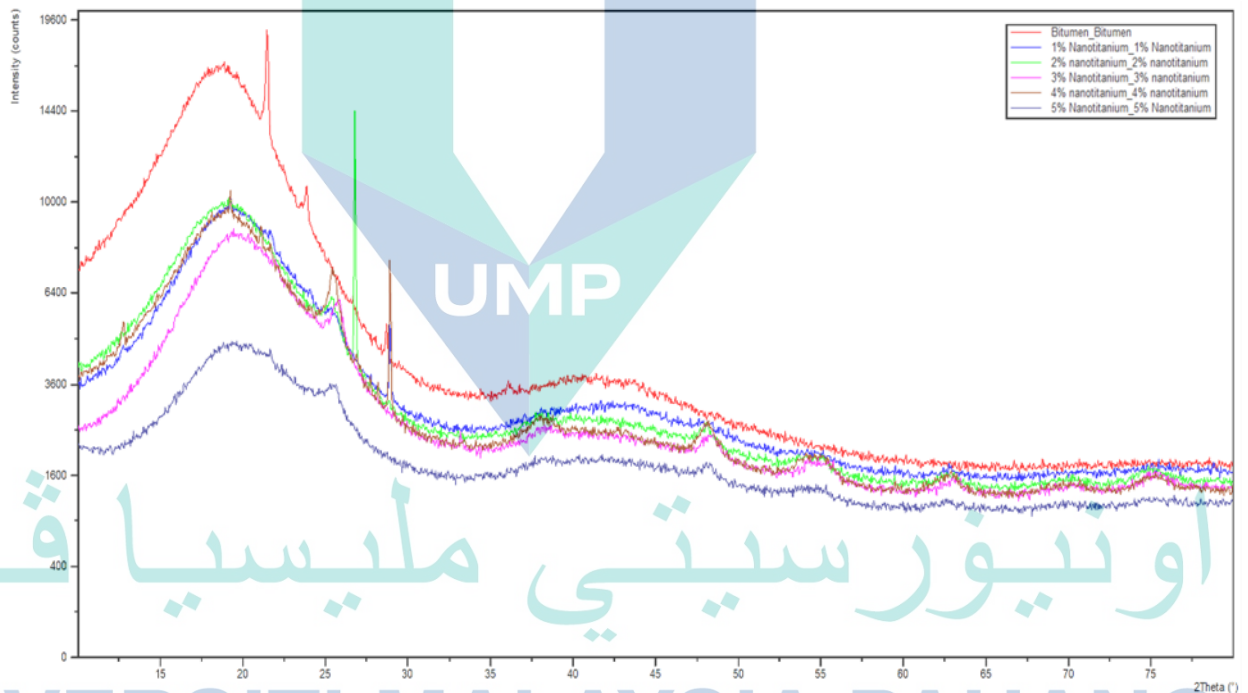


Figure 4.5 XRD graphs for nano titanium modified binder

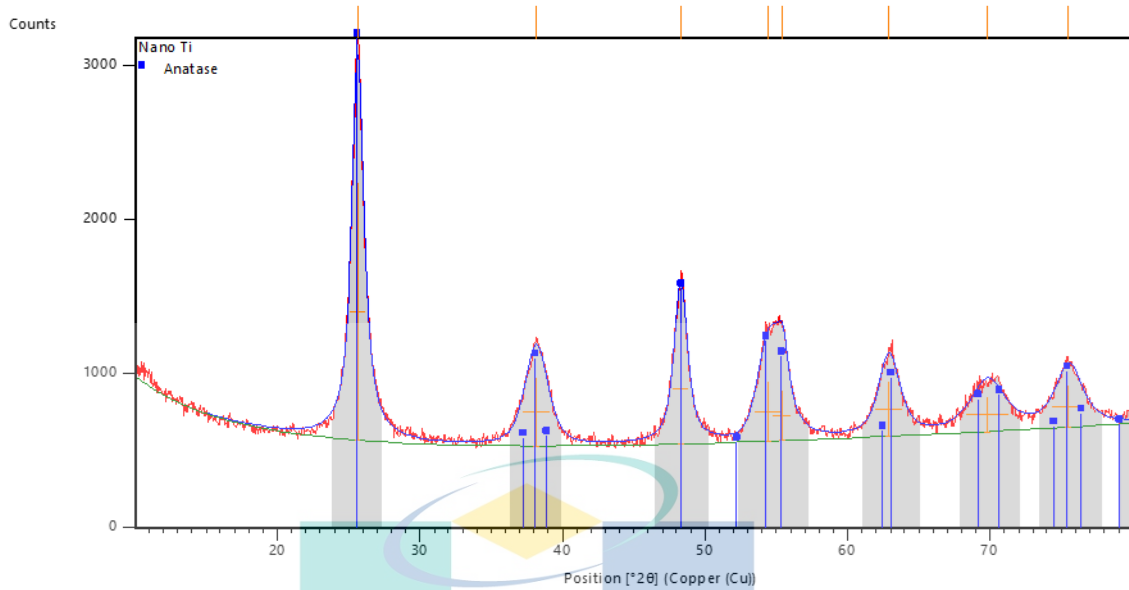


Figure 4.6 XRD graph for nano titanium powder

#### 4.4.2 Scanning Electron Microscope with Energy Dispersive X-Ray Analysis (SEM-EDX)

Figures 4.7 until 4.12 show the morphology of the bitumen both before and after being added with nano titanium powder. SEM was done to see the condition of the nano titanium when mixed with bitumen. From Figures 4.7 to 4.12, comparing the images of the 1%, 2%, 3%, 4% and 5% addition of nano titanium, the images generated show some nano titanium powder was still not blended well into the bitumen and there are some white spots present. It can be seen that with increasing amounts of nano titanium, the bitumen has difficulty blending well with the nano titanium, which then produces insoluble white lumps that are observed with increasing amounts of nano titanium powder as indicated by the red square boxes.

Next, EDX analysis was also carried out on the samples, from the elements observed from Table 4.5 and Figures 4.13 until 4.19. It is most likely that the white flakes or clumps observed were from the aluminium or calcium residues composed in the bitumen. The visibility of these elements is due to the amounts of those elements that still exist inside the nano titanium modified sample. The elements that can be seen from the

EDX results are carbon (C), aluminium (Al), oxygen (O<sub>2</sub>), sulphur (S), calcium (Ca), nano titanium (TiO<sub>2</sub>).

The unmodified bitumen shows all the elements which were mentioned before are present, but when nano titanium is added at various levels of content, the chemical composition changes according to the amount of nano titanium added. Hence, the highest nano titanium content is at 3% nano titanium modified bitumen, followed by 5%, 4%, 2% and 1% as shown in the Table 4.5 below. Only two elements are present, which are carbon and oxygen, which mainly make up the sample alongside with the nano titanium, showing that the nano titanium was mostly blended with the bitumen without having foreign influences or substances. Similarly, Li et al (2018) observed that nano titanium could fill the pores of the bitumen, making the bitumen denser. Overall, 3% nano titanium has the most influence on the changes of the chemical composition of the bitumen.

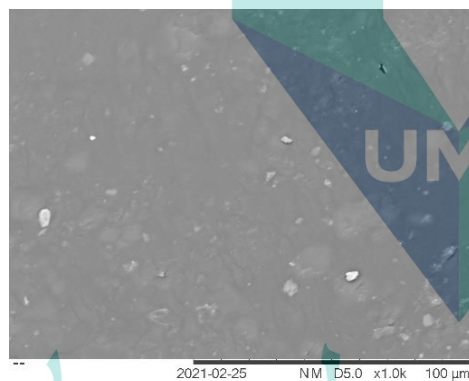


Figure 4.7 0% nano titanium modified bitumen

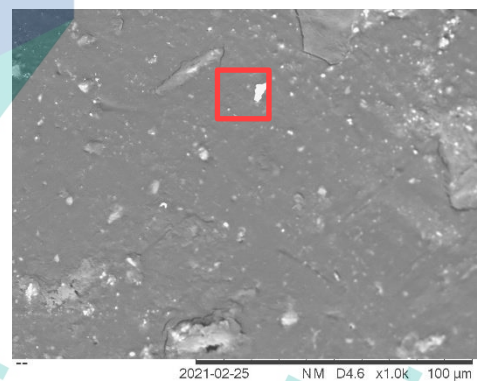


Figure 4.8 1% nano titanium modified bitumen

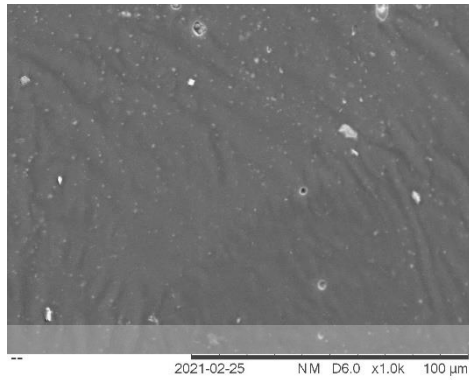


Figure 4.9  
bitumen

2% nano titanium modified

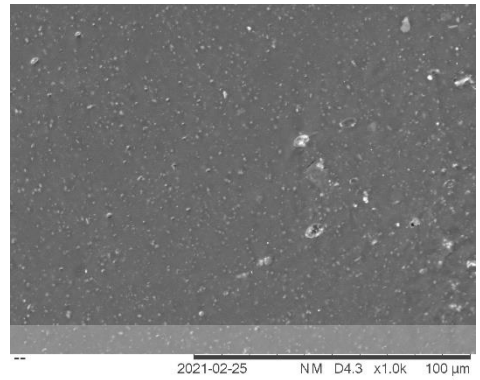


Figure 4.10  
bitumen

3% nano titanium modified

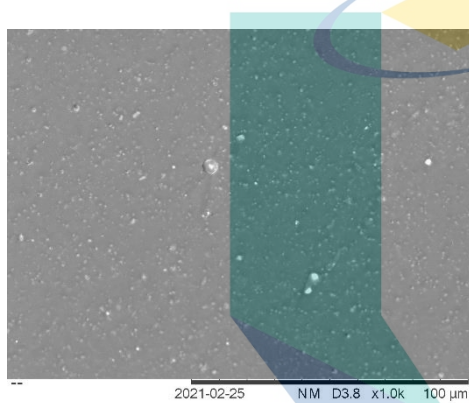


Figure 4.11  
bitumen

4% nano titanium modified

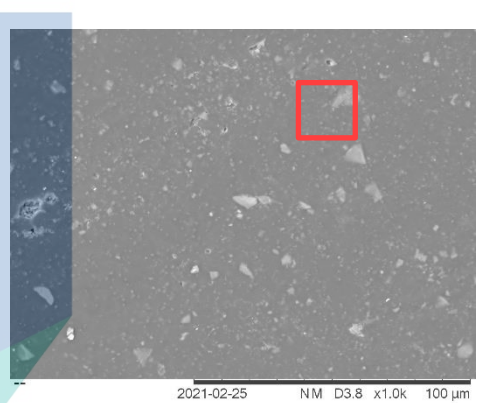


Figure 4.12  
bitumen

5% nano titanium modified

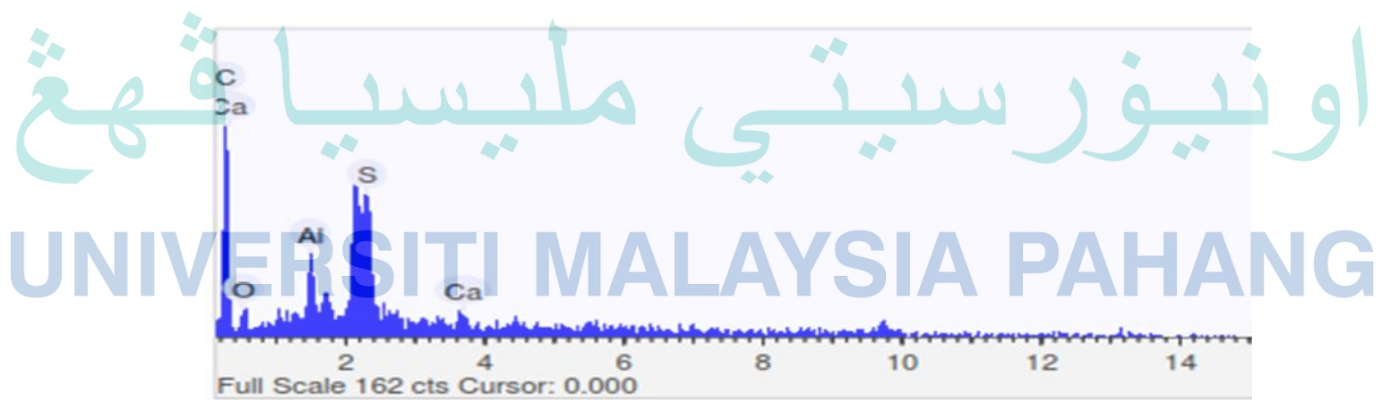


Figure 4.13

Control Sample



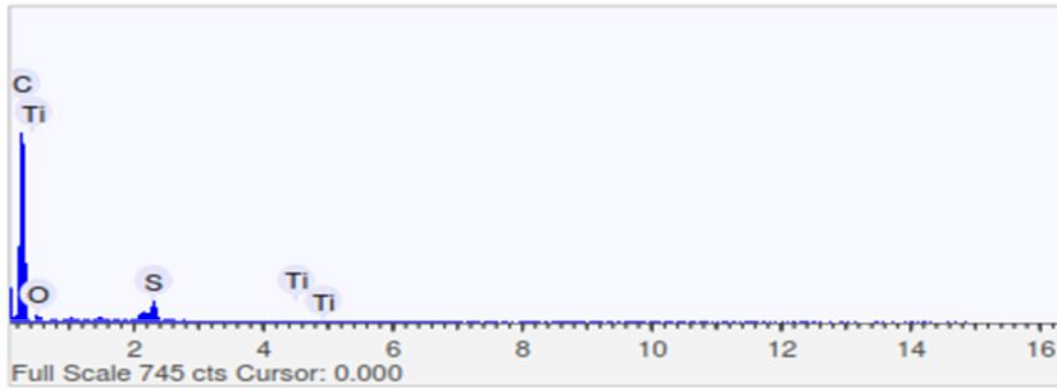


Figure 4.14 1% nano titanium modified bitumen

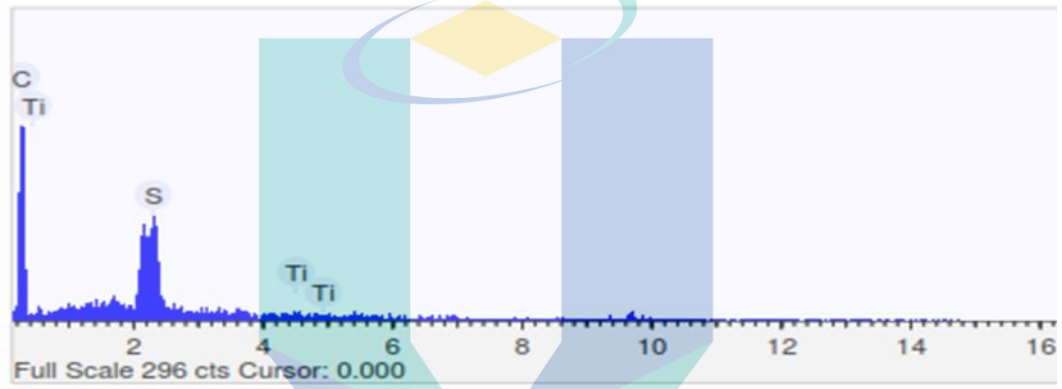


Figure 4.15 2% nano titanium modified bitumen

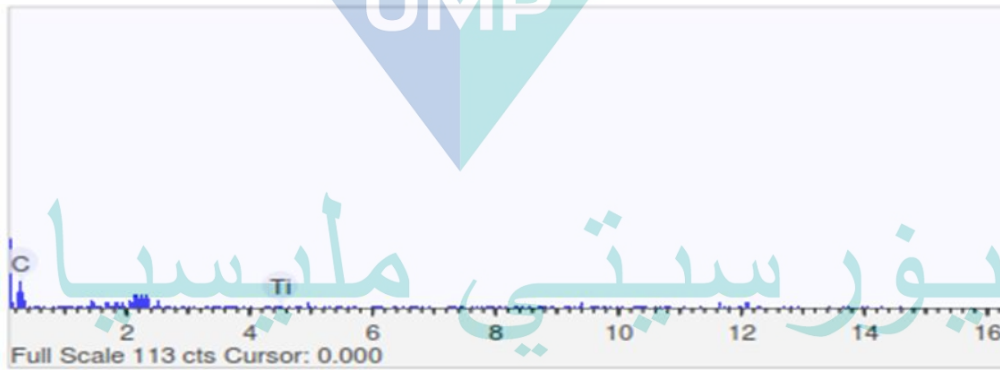


Figure 4.16 3% nano titanium modified bitumen

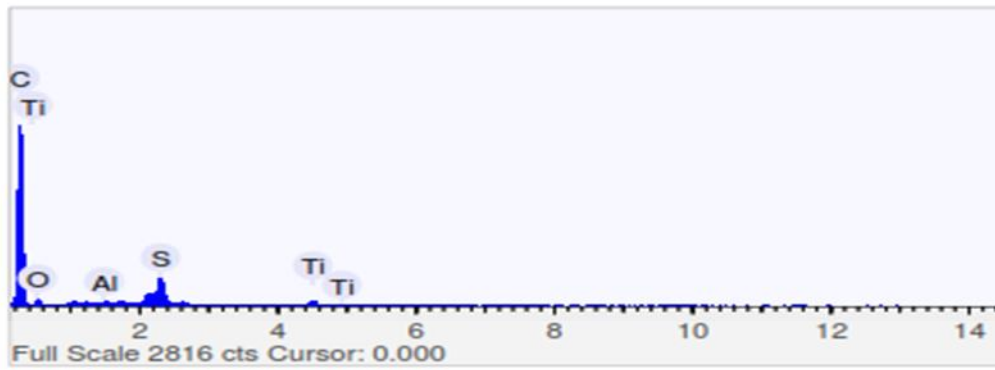


Figure 4.17 4% nano titanium modified bitumen

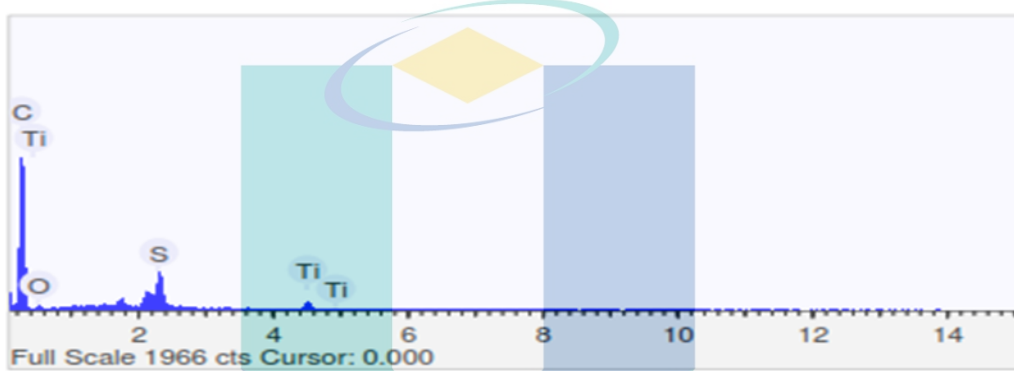


Figure 4.18 5% nano titanium modified bitumen

Table 4.5 Unmodified and modified bitumen elements

Nano titanium (%)	Carbon		Oxygen		Sulphur		Titanium	
	Weight (%)	Atomic (%)	Weight (%)	Atomic (%)	Weight (%)	Atomic (%)	Weight (%)	Atomic (%)
0 %	76.36	84.83	12.32	10.28	5.68	2.36	-	-
1 %	96.49	98.69	-	-	3.25	1.24	0.26	0.07
2 %	91.70	96.94	-	-	6.56	2.60	1.75	0.46
3 %	96.11	98.99	-	-	3.50	1.50	3.89	1.00
4 %	86.06	91.5	8.00	6.39	3.62	1.44	3.88	1.05
5 %	84.94	91.88	6.22	5.05	4.96	2.01	3.88	1.05

#### 4.4.3 Fourier Transform Infrared Spectroscopy (FTIR)

FTIR determines the functional chemical groups of materials. According to (Munajad et al., 2018) chemical functional groups are atomic groups that have an impact on different reactions of the compound. Figure 4.20 shows the chemical functional groups which exist in the bitumen like aliphatic primary amines, aliphatic hydrocarbons, and primary aliphatic alcohols. These chemical groups will later react with the nano titanium and produce new chemical reactions that will initiate a change in the molecular compound of the modified binder.

Figure 4.21 shows the IR spectrum of the original bitumen experience a N-H stretching at  $3395.75\text{cm}^{-1}$ . This peak is observed at the  $3100\text{-}3500\text{ cm}^{-1}$  region where it could be seen that it appears as a wide and broad shaped spectrum with medium strength. The spectrum then becomes longer and shorter as more nano titanium is added. The two peaks at  $2923.75\text{ cm}^{-1}$  and  $2852.09\text{ cm}^{-1}$  which later appears to be related to the C-H symmetric stretching (-CH<sub>2</sub>) and the C-H asymmetric vibrations (-CH<sub>3</sub> and -CH<sub>2</sub>) are due to the presence of hydrocarbon chain segments that usually exist in bitumen (Nivitha et al., 2019).

Next, from Figure 4.21 it shows all of the nano titanium modified bitumen samples have almost the same peaks, and the same results were observed by Ding et al. (2021) in his study. However, at 3% nano titanium modified bitumen, there is a new absorption bond that is observed. Thus, when nano titanium is included into the original region of  $3100\text{-}3500\text{ cm}^{-1}$ , then it makes the N-H bonds not appear anymore. It is instead replaced with the two peaks at the  $2851\text{-}3100\text{ cm}^{-1}$  region which are  $2923.14\text{ cm}^{-1}$  and  $2851.96\text{ cm}^{-1}$ . These peaks appear as there are interactions between the C-H and O-H bonds of the nano titanium with the bitumen mix, as these bonds are stretching with medium strength.

Going into the  $1700\text{cm}^{-1}$  region, a remarkable peak at  $1700.49\text{ cm}^{-1}$  is observed at the carboxylic region, indicating oxidation happens in this region and the carbonyl group (C=O) is present. Next, the two peaks observed at  $1462.37\text{ cm}^{-1}$  and  $1376.67\text{ cm}^{-1}$  are assigned to the O-H bond, which experiences bending with medium strength. It follows that this  $1376.67\text{cm}^{-1}$  peak is a response to the phenol group. Lastly, the  $721.20$

$\text{cm}^{-1}$  peak is due to the presence of a C double bond ( $\text{C}=\text{C}$ ) in the nano titanium modified bitumen sample. The bond is also observed in a study by (Al-sabaei et al., 2021).

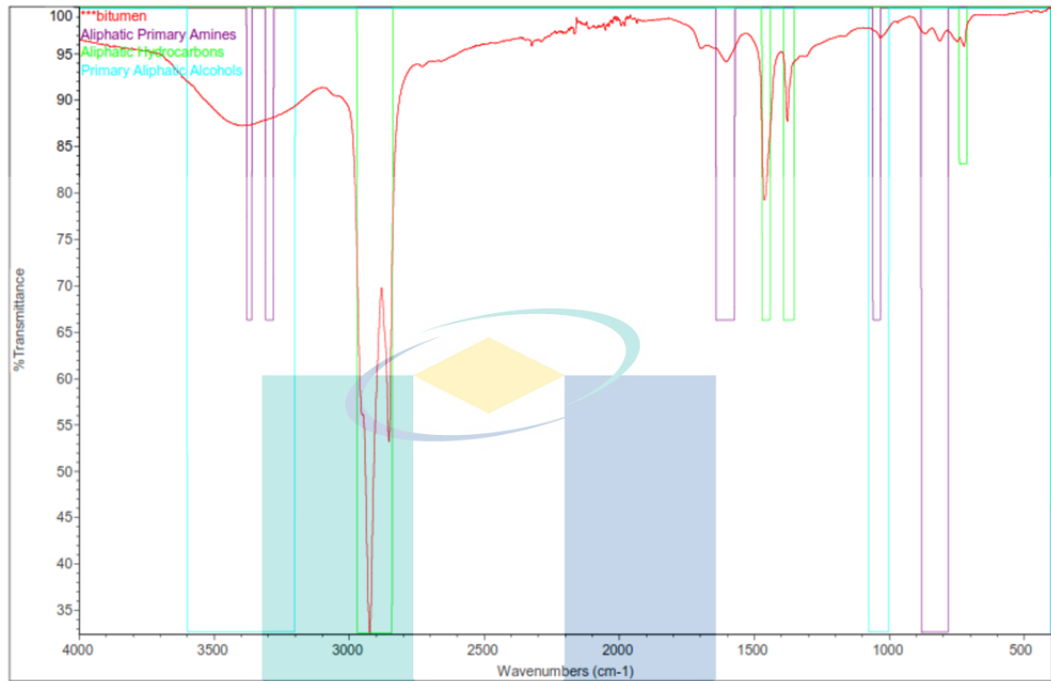


Figure 4.19 Transmittance (%) vs. wavenumbers ( $\text{cm}^{-1}$ ) spectral interpretation of unmodified bitumen.

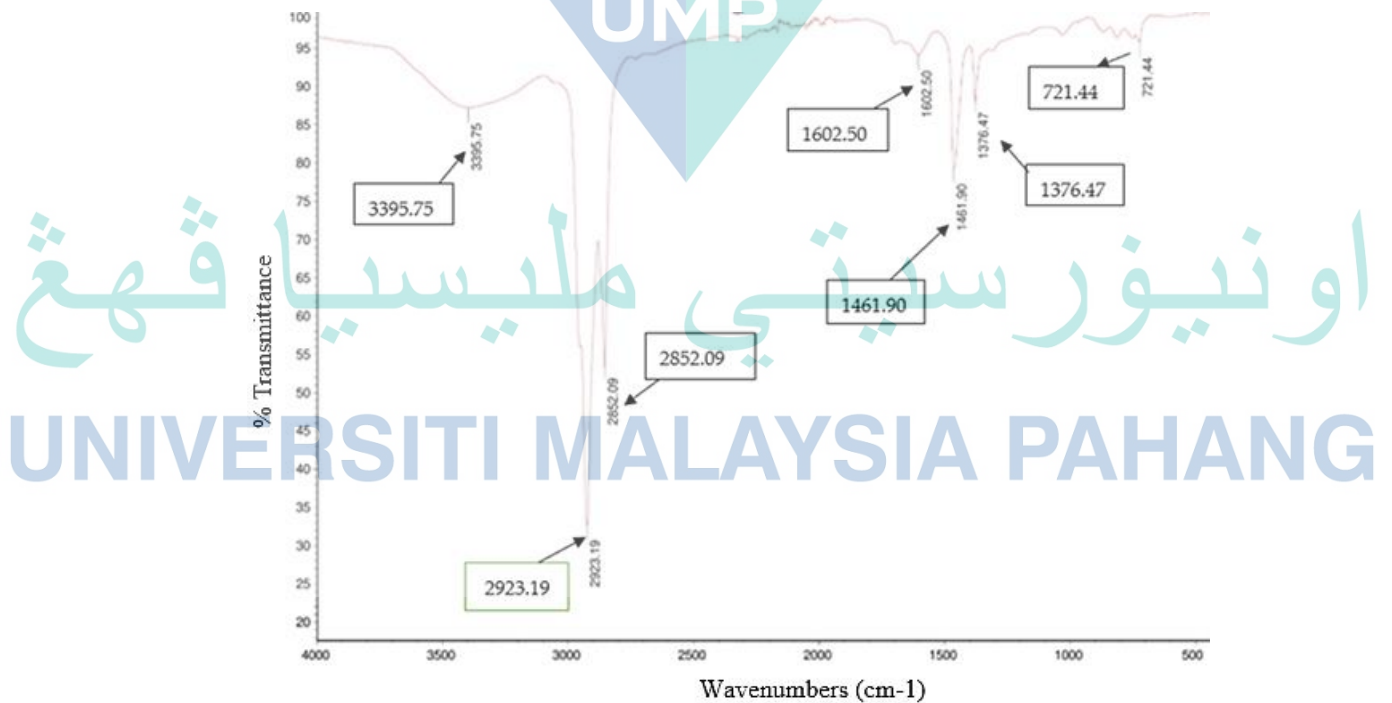


Figure 4.20 Transmittance peaks of unmodified bitumen.

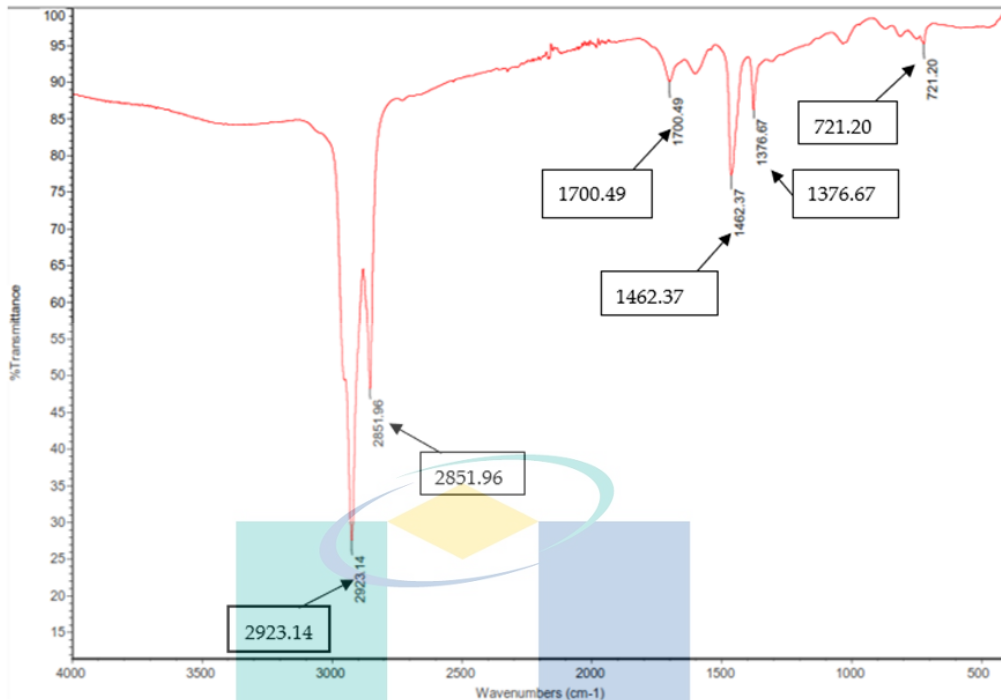


Figure 4.21 Transmittance peaks of 3% nano titanium modified bitumen

## 4.5 Volumetric properties of nano modified SMA

### 4.5.1 Stability

Figure 4.22 shows the density and stability of the modified binder against nano titanium percentages between 0% to 4%. The stability of the mixture is mostly influenced by the cohesion and internal friction of the matrix, which supports the coarse aggregates (Fauzi et al., 2020). For this particular sample, the density is 2.238 g/cm<sup>3</sup> while the maximum stability is 5945 N compared to 5879 N for a 0% nano titanium addition. Figure 4.23 shows the stability and flow for various nano titanium percentages. 0% nano titanium yields the highest flow, although the addition of further nano titanium actually reduces the flow value. It is found that increasing the nano titanium amount also increases the stability and density. However, nano titanium addition beyond 3% does not increase both parameters, and the same was reported by (Masri et al., 2020). The usage of 3% nano titanium in the SMA mixture is more effective in enhancing density and stability. Figure 4.24 shows the density  $R^2$  value which is 0.8531. An  $R^2$  value that is nearer to 1 is deemed as a good fit for the measured values, while lower values do not necessarily

mean that the model is not acceptable or cannot be used. Figure 4.25 shows the stability  $R^2$  value is at 0.5936. The lower value of flow may be due to other affecting reasons such as ageing, which has a significant impact on asphalt mixtures similar to what the samples in a study by (Rys et al., 2020) experienced.

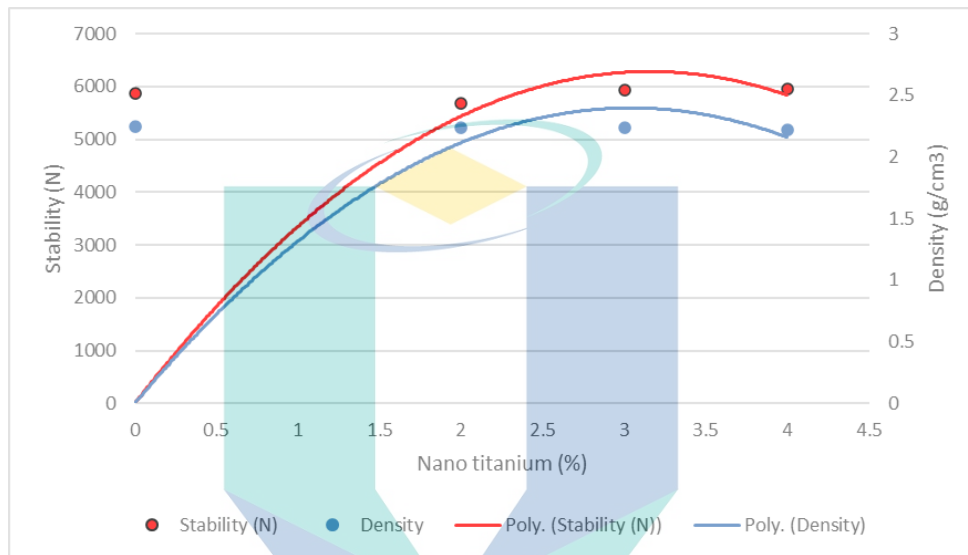


Figure 4.22 Stability and density against nano titanium percentages

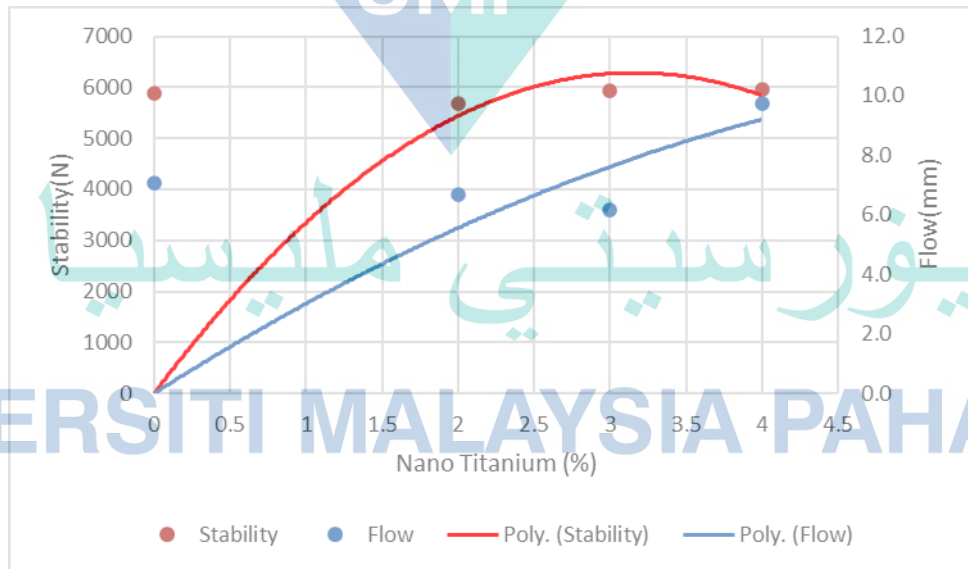


Figure 4.23 Stability and flow against nano titanium percentages



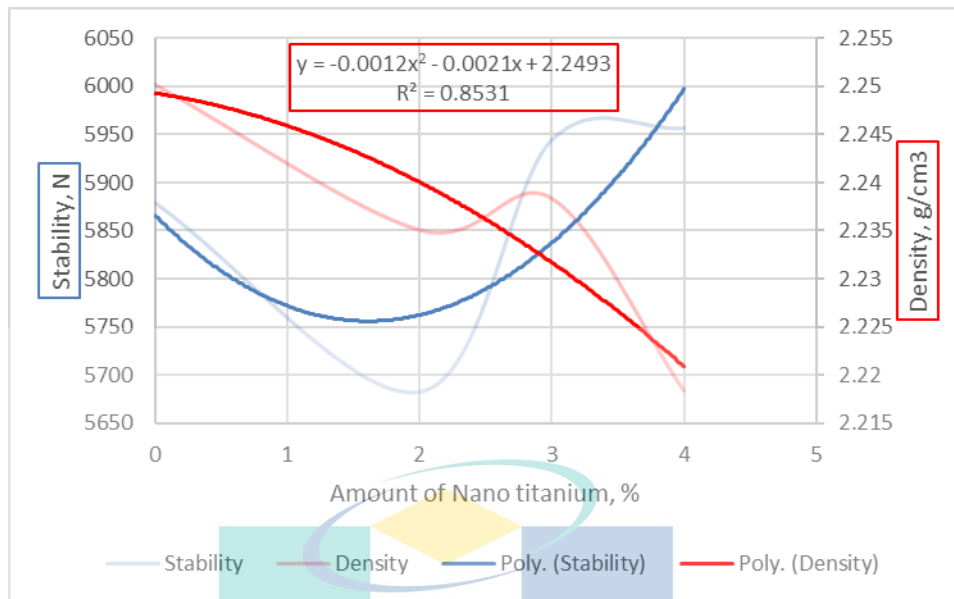


Figure 4.24 Stability and Density  $R^2$  values

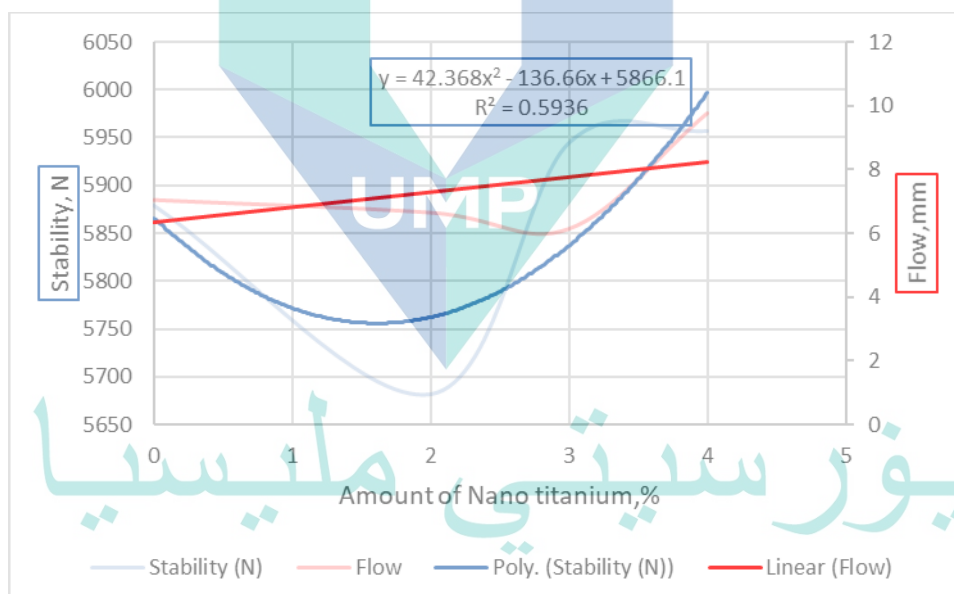


Figure 4.25 Stability and Flow  $R^2$  values

#### 4.5.2 Flow

Figures 4.26 and 4.27 show the flow performance of asphalt mixtures with different nano titanium percentages. The flow value indicates the flexibility of the asphalt

mixtures (Ahmad et al., 2019). The modified SMA20 mixture produces an inconsistent flow value with the inclusion of nano titanium. 0% nano titanium produces a relatively higher flow value (7 mm) than the requirement by the Public Work Department (between 3 to 5 mm). Meanwhile at 3%, the flow value is reduced, and although the flow value is not within the specification, the presence of nano titanium is seen to have an influence in reducing the flow value since the same issue was mentioned by (Yuan et al., 2021). Figure 4.28 shows the density  $R^2$  value, which is 0.8531. Figure 4.29 shows the stiffness  $R^2$  value of 0.6445. Since the density and stiffness are improved, some outside factors may be influencing the flow value. As mentioned earlier, it is not necessarily satisfactory, but there is a reliable value and it could be improvised further.

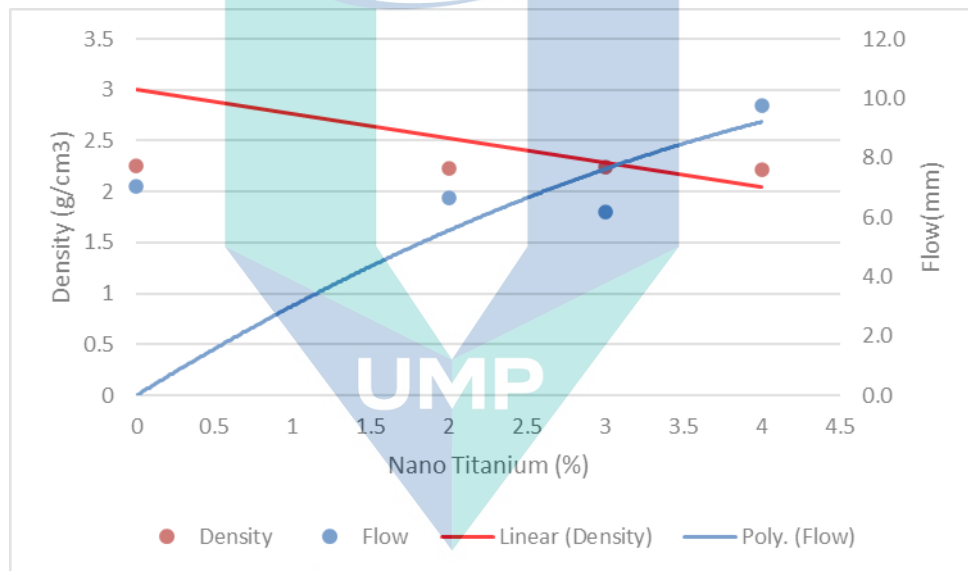


Figure 4.26 Density and Flow against nano titanium percentage

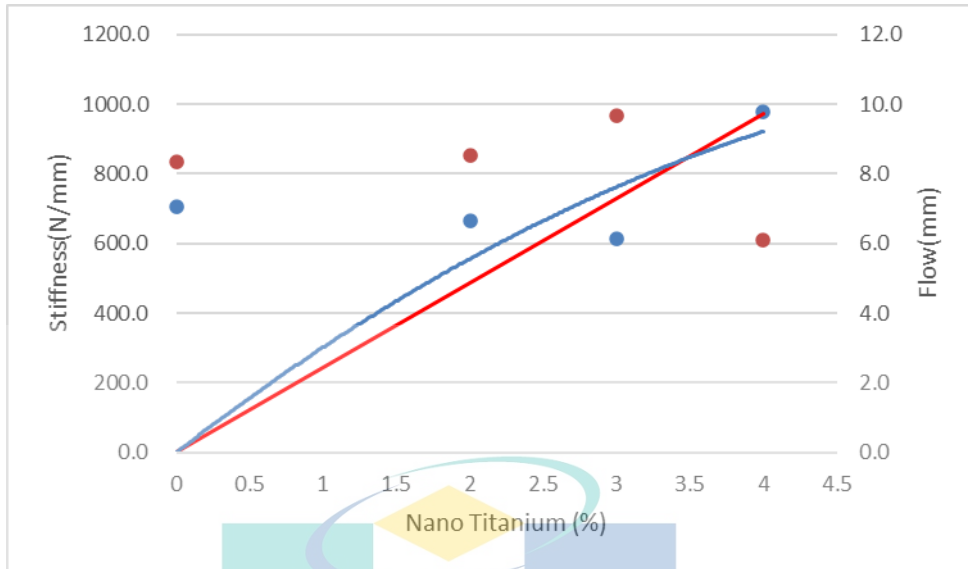


Figure 4.27 Flow and stiffness against nano titanium percentages

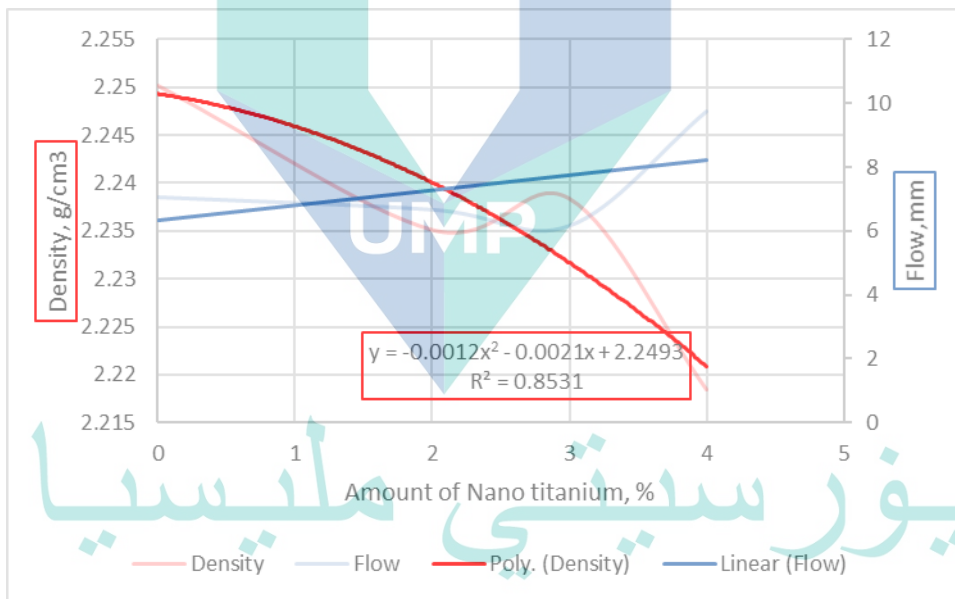


Figure 4.28 Density and Flow R<sup>2</sup> values

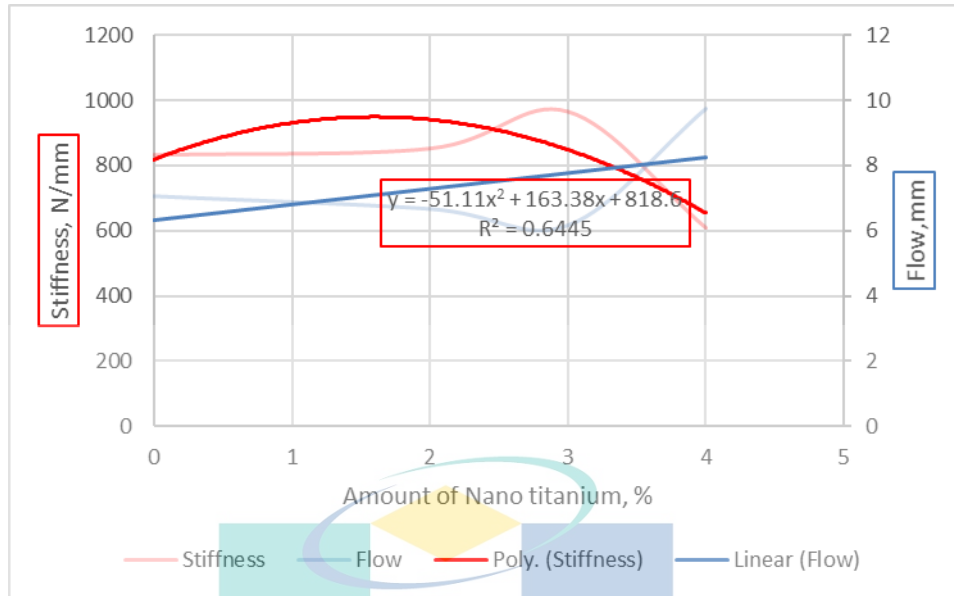


Figure 4.29 Stiffness and Flow  $R^2$  values

### 4.5.3 Stiffness

Figures 4.30 and 4.31 exhibit the stiffness of SMA mixtures against various nano titanium percentages. The highest stiffness value is obtained by the 3% nano titanium addition (965.67 N/mm), as compared to 833.3 N/mm for the 0% nano titanium, which is a 14.8% improvement. Stiffness is related to resistance and durability; thus, higher stiffness increases the mixtures resistance to ravelling and bleeding. This shows that the addition of nano titanium improves the stiffness characteristic of the asphalt mixture. The results are consistent with studies by (Arshad et al., 2019) and (Fauzi et al., 2020).

Figure 4.32 shows the density and stiffness  $R^2$  value of each of the graphs, which are 0.8531 and 0.6445. Figure 4.33 shows the stability and stiffness  $R^2$  values, which are both at 0.5936 and 0.6445 respectively. Both the density and stiffness reached above 50%  $R^2$  values, indicating that the addition of nano titanium influenced the stability and stiffness properties of the asphalt mix.

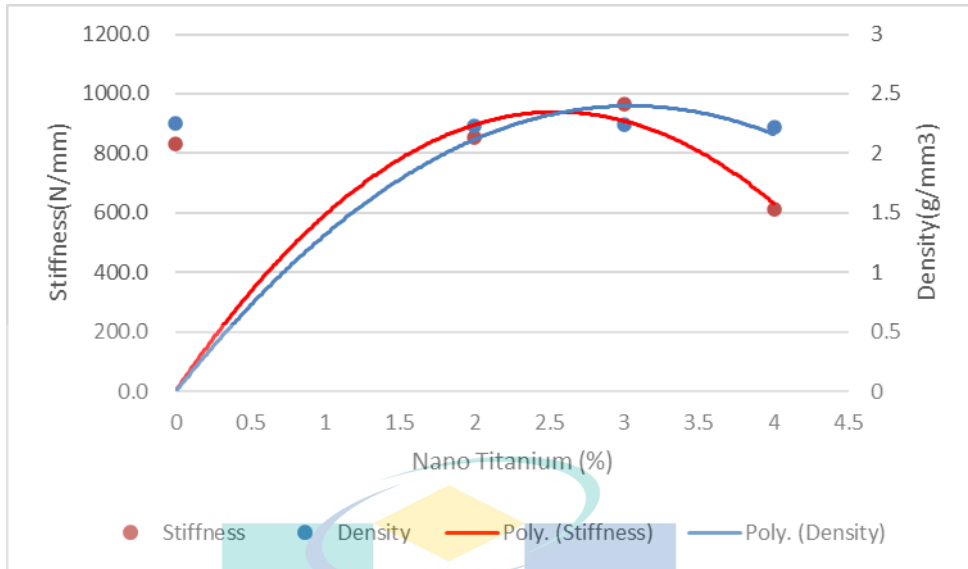


Figure 4.30 Stiffness and density against nano titanium percentages

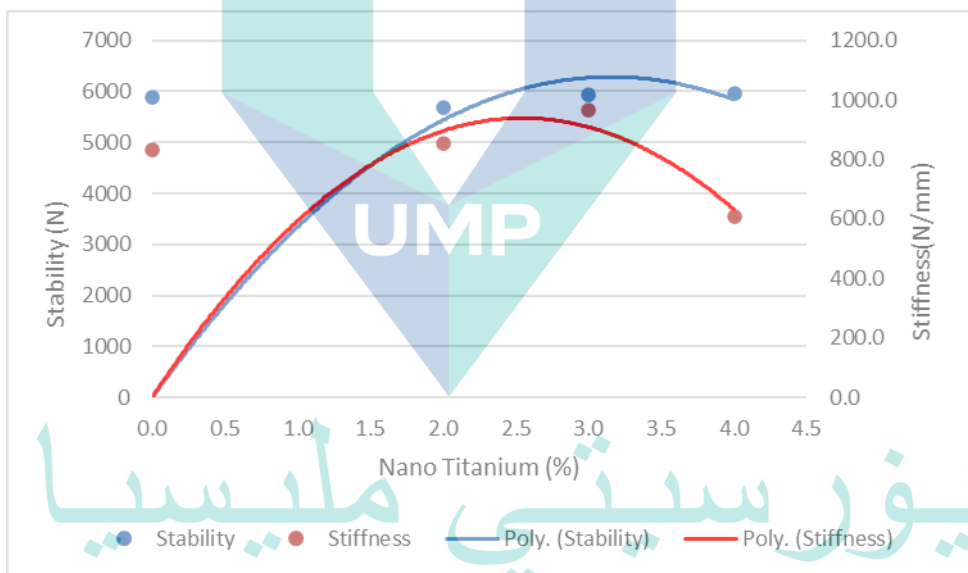


Figure 4.31 Stability and stiffness against nano titanium percentages

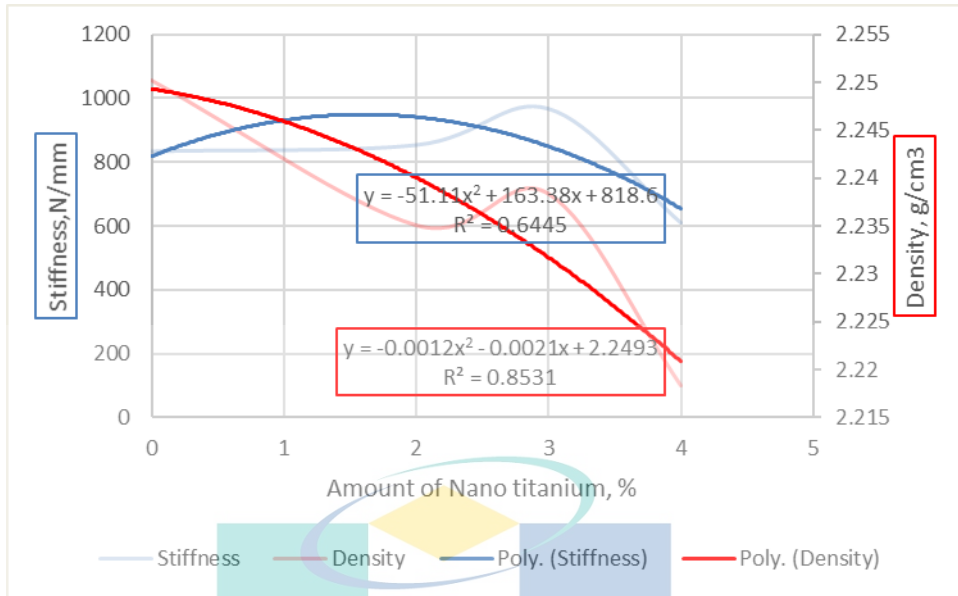


Figure 4.32 Stiffness and Density  $R^2$  values

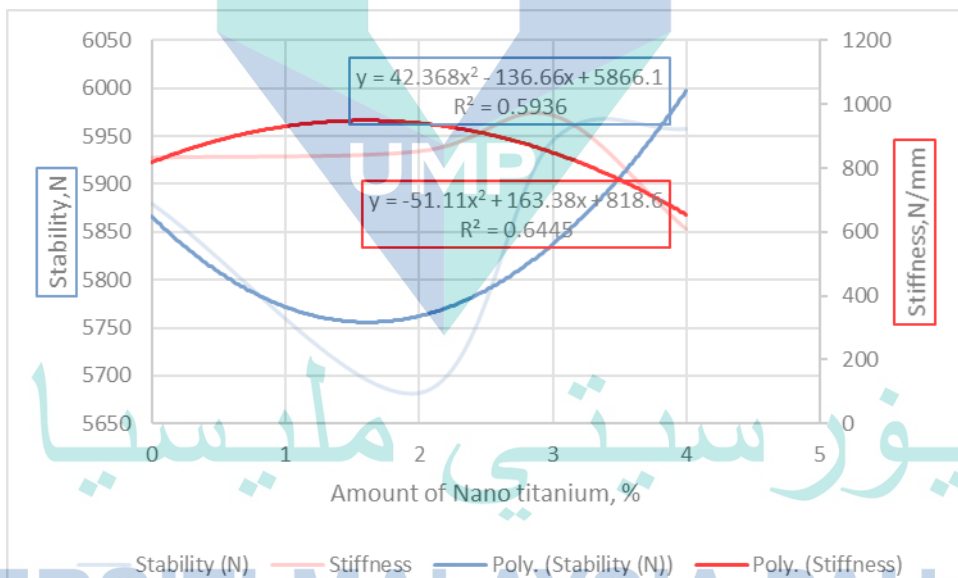


Figure 4.33 Stability and Stiffness  $R^2$  values



## 4.6 Mechanical properties of nano modified SMA

### 4.6.1 Resilient Modulus

The results of the resilient modulus at 25°C show an increasing trend when nano titanium is added. After reaching its optimum content however, the resilient modulus value of the sample showed a decreasing value. This trend is consistent with studies by (Fauzi et al., 2020) and (Radzi et al., 2020) in which the modification of the asphalt binder improved the resilient modulus values significantly. For the resilient modulus value of the nano titanium modified sample, the pulse repetition periods used were 1000, 2000 and 3000 ms respectively. From Figure 4.34, the sample with a 3% nano titanium modified binder has the highest resilient modulus with 1478 MPa as compared to the 0% sample with a 1473 MPa. The same is observed with the 2000 pulse repetition where the 3% sample is the highest with a 1903 MPa, while the 0% sample only reaches up to a 1311 MPa. When the 3000 pulse was applied, the values of the resilient modulus for 0% and 3% were 1424MPa and 1521 MPa respectively. The nano titanium helps the mixture to resist horizontal deformation. Not only that, but the presence of nano titanium could fill in the voids between the aggregates as they could make the bitumen harder, and could strengthen the mix. These results show that the resilient modulus values increased as compared to the control sample, thus proving the improvement of the resilient modulus of the sample.

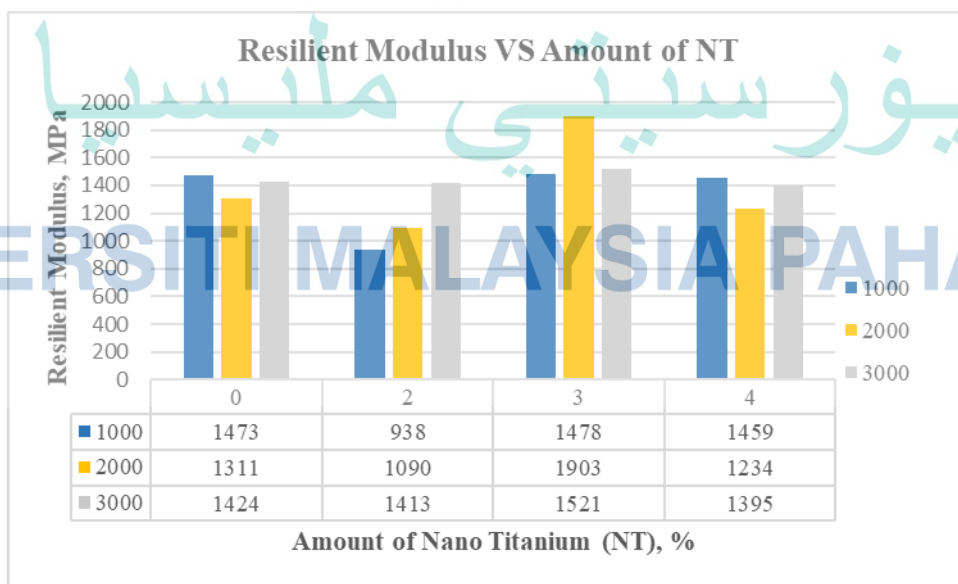


Figure 4.34 Resilient modulus vs Amount of Nano Titanium at 25°C

Next, Figure 4.35 display the resilient modulus of the samples, but at a temperature of 40°C. The strength of the samples with increasing temperatures is also related to a study by (Taherkhani & Tajdini, 2019). As can be seen, with each increasing addition of nano titanium, the strength also shows an increasing trend for each of the pulse repetition periods. The most significant one would be the 3% nano titanium modified sample. The resilient modulus value for 0% and 3% are 1453MPa and 2410MPa at an 1000 pulse repetition. Followed by 0% and 3% with 1438MPa and 2172 MPa, the resilient modulus values keep increasing up until the 3000 pulse repetition. This could be seen with their values of 2081MPa (0%) and 2248 MPa (3%). The highest value is observed for each of the pulses with the 3% nano titanium modified sample.

The temperature plays an important part in this, as it can be seen that by increasing the temperature, the resilient modulus also increases, but after adding more nano titanium, the strength decreases. This leads to the point which identifies that the modifier content and the temperature do have an effect on the resilient modulus value. This is also related with the temperature sensitivity aspect of the sample. Since the nano titanium is related to a higher specific surface area as it is a nano material, the interaction between the asphalt binder in the mix is greater when nano titanium is present as compared to when the bitumen is unmodified.

It shows that with the inclusion of 3% the resilient modulus of the sample is improved as compared to the control sample of the unmodified asphalt which had the lowest resilient modulus at 2081 MPa; meanwhile 3% modified asphalt is the highest with 2248 MPa. The increase in modifier content produces an improvement in the elastic properties in the asphalt mixture. The sample at 3% then showed that at a higher temperature the sample is more durable to damage, since the resilient modulus value increased, the elasticity increased and the sample had better resistance to damage such as rutting as compared to the unmodified sample.

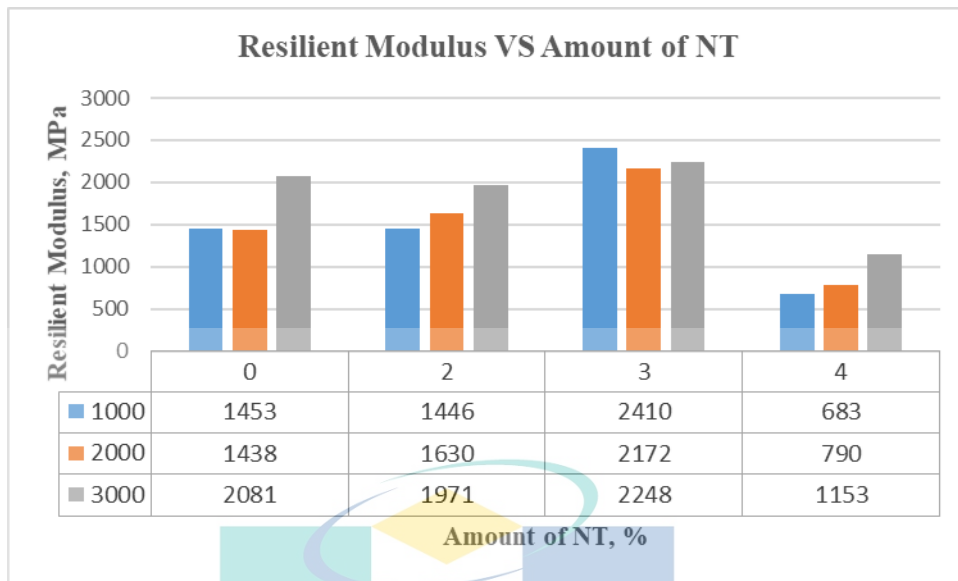


Figure 4.35 Resilient modulus vs Amount of Nano Titanium at 40°C

#### 4.6.2 Dynamic Creep

Figure 4.36 presents the permanent deformation as illustrated by the permanent strain vs cycles graph between modified and unmodified samples. It can be seen from the graphs that there are various differences between the amount of nano titanium content in the samples. There are three stages of creep which are the primary stage, the secondary stage and the tertiary stage. The samples observed show the primary stage up to the 1200 cycle where elastic strain occurs, and the secondary stage after the 2400 cycle where the viscoelastic strain by axial stress occurs.

The sample with 3% nano titanium shows a reduced resistance against plastic deformation as compared to the 2% nano titanium modified sample, since it might not have enough composition to resist deformation. At a 4% addition of nano titanium, the sample has a higher strain value as compared to the control sample. Dynamic creep is associated with permanent deformations such as rutting as seen in a study by (Jasni et al., 2020).

As for the result, it is seen that the lower the accumulated strain is, the higher the resistance to rutting. Thus, only the 3% addition of nano titanium produces a satisfactory

result, as at early strain it has less strain as compared to the control sample. It can be concluded that nano titanium does have a remarkable influence in the susceptibility of the mix to permanent deformation.

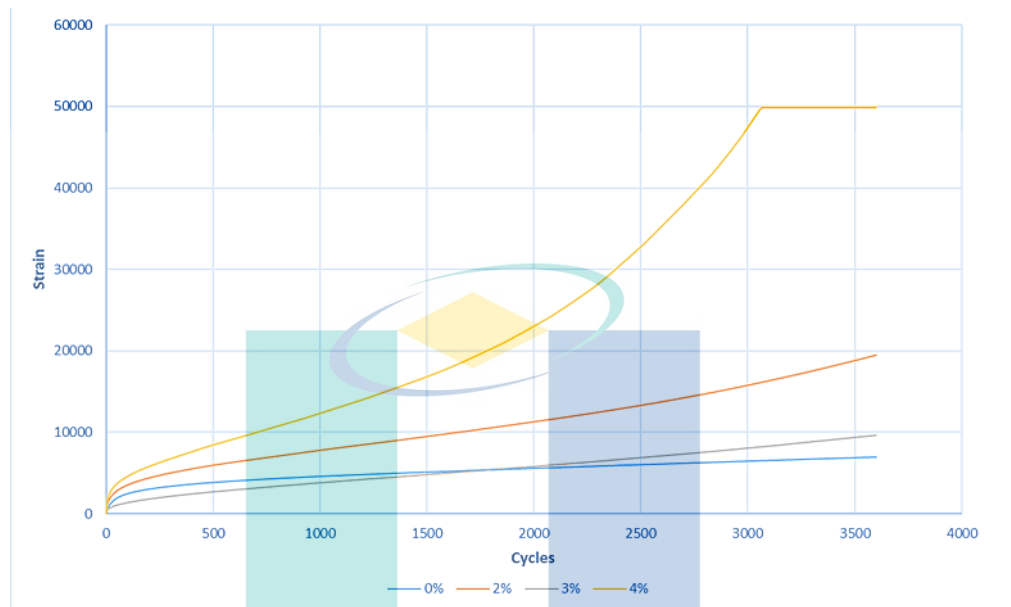


Figure 4.36 Permanent strain vs cycles

Figure 4.37 shows that the creep stiffness value obtained for 0% is 142kPa, 2% is 51 kPa, 3% is 103kPa and 4% is 20kPa. It does shows that all the mixture creep stiffness values have been lowered and this same trend was stumbled upon in a study by (Wazeri & Ali, 2017). The addition of nano titanium reduces the value of the slope, and this shows that at a higher temperature the nano modified samples have more resistance to failure. This is because the larger the creep stiffness value, the harder the material is, which makes its ability to resist creep also higher. In conclusion, the addition of nano titanium in the stone mastic asphalt samples is able to resist permanent deformation.

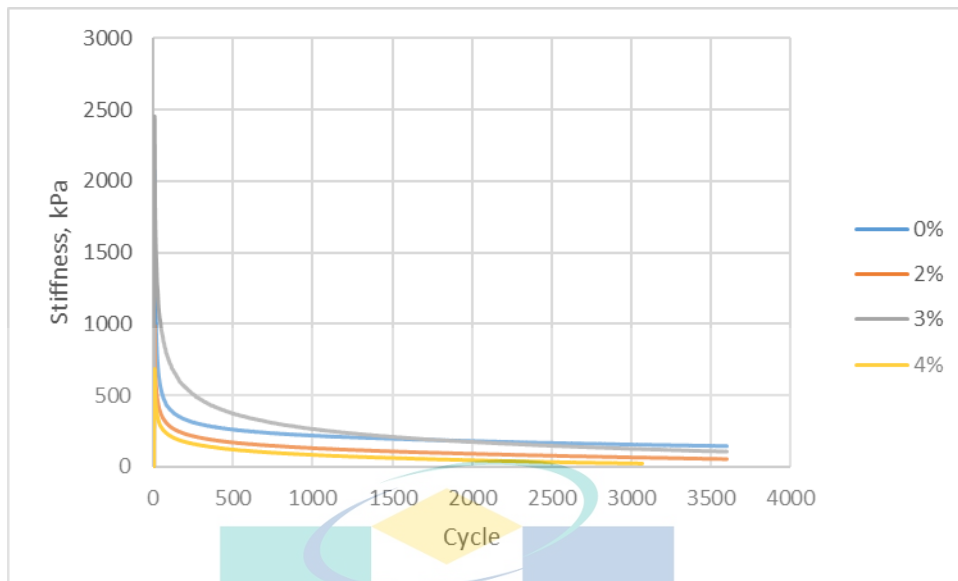


Figure 4.37 Creep stiffness values

#### 4.6.3 Moisture susceptibility

Moisture damage is one of the main sources of permanent damage that is usually encountered in asphalt. It also increases the possibility of binder drain down in samples. The indirect tensile strength test (ITS) and Tensile Strength Ratio (TSR) are used to evaluate moisture susceptibility. The ITS Value is calculated after the Maximum Applied Load from the Modified Lottman Test is obtained. Tensile strength represents the cracking resistance. The ability of a mix to withstand cracking would get better with higher tensile strength ((Fakhri & Shahryari, 2021)).

The values from dry conditions show more of an increase than the wet conditions, this has also been observed in studies by (Xing et al., 2020) and (Zhan et al., 2020). This is because the water acts as an agent that weakens the bonding force between the aggregates. Luckily, with the addition of nano particles that act as a hydrophilic agent, the mix is influenced in a positive way. From Figure 4.38, the highest ITS value for the dry condition is at 2% which is 276kPa, followed by 4% (264kPa) and 3% (174kPa). For the wet sample, the same trend is observed with 2% (226kPa), followed by 4% (195kPa) and 3% (189kPa). It is evident that by increasing the nano titanium content, both wet and dry samples are able to achieve more resistance to moisture.

Looking at the ITS value, it could be seen that the samples at wet conditions have less tensile strength than the samples at dry conditions, which means that there is a presence of moisture. With this, the tensile strength of the mix becomes less which makes it more susceptible to potential cracking. Since the mix possesses voids from its use of coarse aggregates, the gaps between them would enable moisture to seep into the mixture. This would influence the strength of the mixture, and it is seen that the presence of moisture does affect the performance of the mix.

As observed from the results, an increase in the percent of additives in mixtures caused an increase in the TSR index as compared with the control samples, which supported the findings of previous studies. For example, (Fakhri & Shahryari, 2021) reported that nano zinc oxide and nano reduced graphene oxide improved the interlocking and adhesion between bitumen and aggregates, which resulted in an excellent elastic system in the asphalt mix. As a result, this process increased the pull-off adhesion strength in dry and wet conditions and improved the TSR index. Figure 4.39 shows all of the TSR values managed to achieve more than 80%, and the 3% nano titanium modified mix recorded the highest TSR value. Moisture damage is related to the value of TSR and as the TSR value increases the moisture damage effect in bituminous mixes will be reduced.

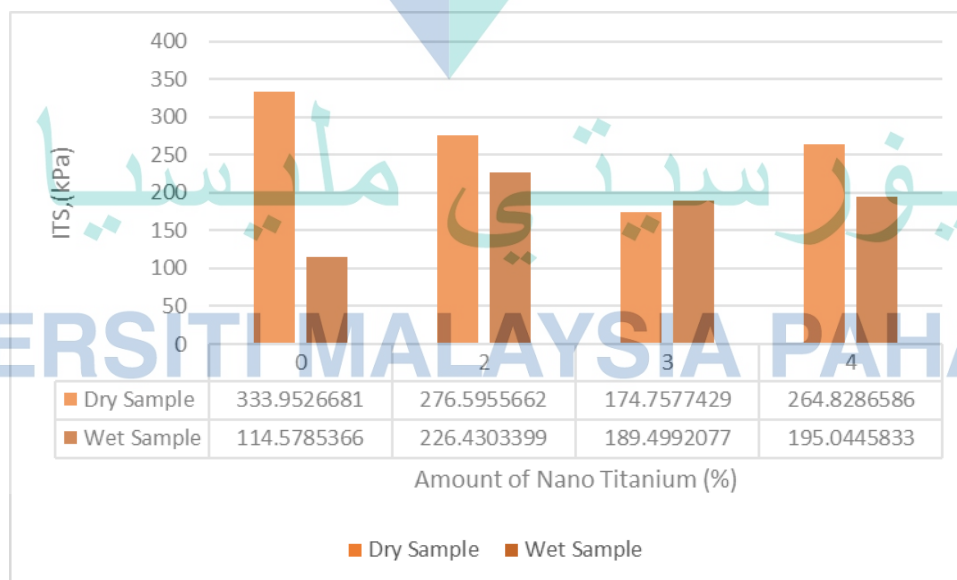


Figure 4.38 ITS value vs Amount of Nano Titanium



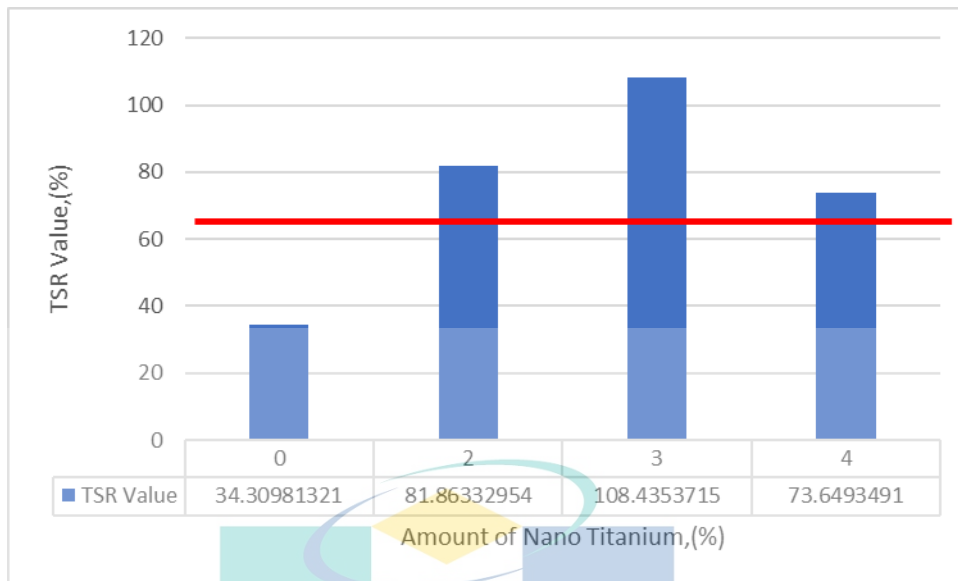


Figure 4.39 TSR value vs Amount of Nano Titanium

#### 4.7 Binder drain down

Figure 4.40 shows the binder drain down for each percentage of nano titanium modified bitumen, with 2% being the lowest binder drain down, followed by 4% and 3%. The binder drain down refers to the bitumen flowing out during the mixing of a mix. Since SMA has a high content of bitumen as a filler and has a gap graded composition, it is prone to binder drain down (Razavi & Kavussi, 2020). The 2% addition of nano titanium in the binder makes the binder less prone to flow out since the nano titanium has absorbed the solvent particles in the binder, making the nano titanium modified binder stiffer. This is due to the large interactions between the nano particles with the binder.

As seen on the 0% sample, there is quite a lot of excess bitumen flowing out during the mixing process, which could affect the condition of the mix. The nano titanium added into the bitumen would make the bitumen harder, making the particles of the bitumen more intact with each other and preventing them from easily flowing through the aggregates. This is because it will hold the aggregates more compactly and prevent excess draining of the bitumen, forestalling and even helping fill out the missing particles as mentioned by (Chegenizadeh et al., 2020). With the addition of nano titanium, the mix shows a significantly reduced amount of binder drain down.

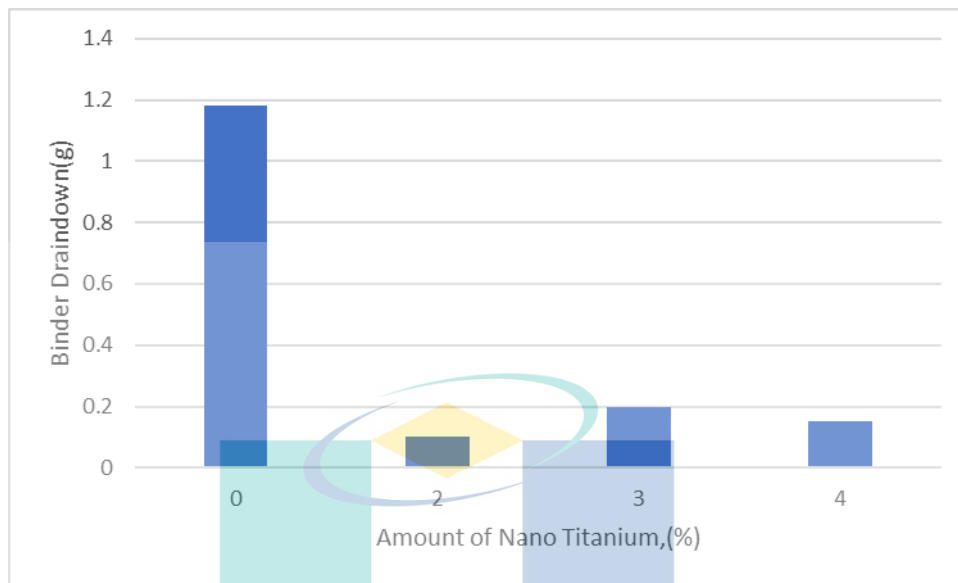


Figure 4.40 Binder drain down vs Amount of Nano Titanium

#### 4.8 Summary of results

From Tables 4.6 and 4.7 it can be seen that mostly the 3% addition of nano titanium had a positive influence on the properties of the bitumen and thus affects the 3% stone mastic asphalt mechanical performance as well.

The influence nano titanium has on the binder shows that the optimum content of nano titanium is 3%. The Table shows all the tests that have been done to each level of content of nano titanium. For the mechanical tests, only 2%, 3% and 4% nano titanium modified SMA were evaluated in terms of resilient modulus, dynamic creep, moisture susceptibility and binder drain down. They were then further ranked from the best to the average in comparison with the unmodified sample.

Table 4.6 and 4.7 shows the ranking in terms of the binder; the binder is evaluated from 1% to 5% inclusion of nano titanium. The tests involved were related to their physical, rheological, morphology and chemical properties.

Table 4.6 Ranking table for the mechanical tests on samples

Nano titanium (%)	0	2	3	4
Tests				
Binder Drain down	4	1	3	2
Resilient modulus @25°C	2	4	1	3
Resilient modulus @40°C	2	3	1	4
Dynamic Creep	2	3	1	4
Moisture Susceptibility	4	2	1	3
Total	14	13	7	16

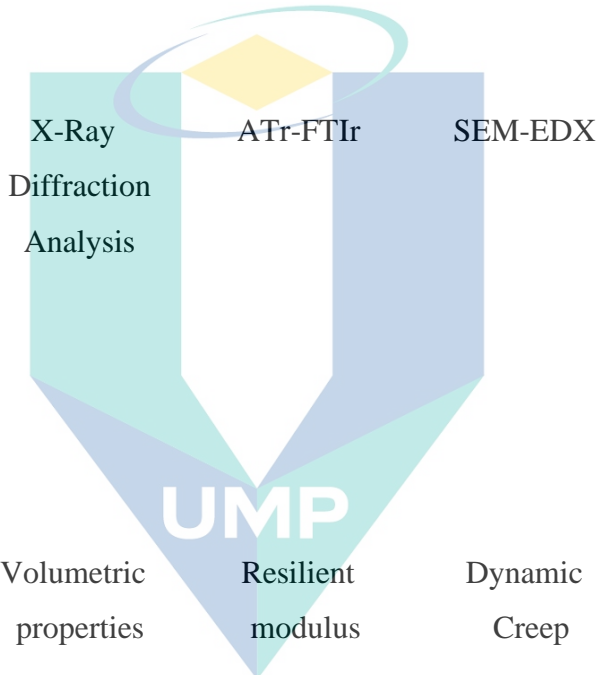
Table 4.7 Ranking table for the tests on binder samples

Nano titanium (%)	0	1	2	3	4	5
Tests						
Penetration test	6	4	3	2	1	5
Softening point	3	2	4	1	5	6
Rotational viscosity @ 135°C	3	1	6	2	4	5
Rotational viscosity @ 165°C	5	1	4	2	3	6
FTIR	6	3	5	1	2	4
XRD	6	5	2	1	3	4
EDX	6	5	4	1	3	2
SEM	6	5	4	1	3	2
Total	41	26	32	11	24	34

Table 4.8 shows the objective parameters which were related to the tests in order to assess the respective properties of the materials used. Starting from the binder itself, before the binder was added into the mixture, and evaluating the SMA samples after the binder modified with nano titanium was included in the SMA.

Table 4.8 Objective parameters

Objectives	Tests			
To determine the physical and rheological properties of nano titanium modified asphalt binder	Softening Point	Penetration test	Rotational viscosity	
To assess the morphology and chemical characteristics of nano titanium modified asphalt binder	X-Ray Diffraction Analysis	ATR-FTIR	SEM-EDX	
To evaluate the mechanical performance of nano titanium modified asphalt binder	Volumetric properties	Resilient modulus	Dynamic Creep	Moisture susceptibility



اونيورسيتي ملايسيا قهق  
 UNIVERSITI MALAYSIA PAHANG

## CHAPTER 5

### CONCLUSIONS

#### 5.1 Conclusion

Based on the overall findings, the nano titanium modified binder significantly improves the microstructural, chemical, and physical properties of the binder, as well as enhances the mechanical properties of the SMA mixture. The details are as follows:

- i. Overall, physical and rheological properties are improved with the addition of nano titanium. This can be seen because the softening point at 3% records the highest softening point, while the penetration values at 3% and 4% show that the bitumen is becoming more consistent as compared to the original bitumen which has lower viscosity. This is reflected in the viscosity test, which shows that the unmodified bitumen has lower viscosity as compared to the modified bitumen. For viscosity, a 1% addition of nano titanium for 135°C and 165°C is chosen. Hence, the nano titanium modified bitumen is able to influence both the physical and rheological properties to an improved state as compared to the unmodified bitumen.
- ii. The chemical bonds are improved. From the FTIR results, chemical bonds were observed at a certain wavelength and absorbance levels also peaked as compared to the normal binder. Whereas XRD analysis revealed no large peaks with consistent diffraction; the addition of nano titanium influenced the peaks observed in the XRD graphs. While SEM-EDX results showed well dispersed binder mixture particles, depending on the nano titanium percentages. The particles require a longer time to blend, hence they do not blend thoroughly at the earlier stage. Therefore, a mixing time of 60 minutes is chosen as suitable to ensure the mixture is well blended.

iii. The density, stability, flow, and stiffness properties of the 3% nano titanium addition mixture were better than the 0%. Additionally, improvements of the physical, morphological, and chemical characteristics of the binder also enhance the mechanical performance of SMA. The resilient modulus at 25°C shows that the sample with nano titanium included has better strength as compared to the control sample without nano titanium. The presence of 3% nano titanium in the mix influenced the strength of the SMA mix. The 40°C temperature represents the high temperature condition, and it also shows the same trend as the previous temperature, in which the resilient modulus value at 3% shows a better strength as compared to the sample without the presence of nano titanium. For dynamic creep, 3% is chosen as the permanent strain is acceptable as compared to 4%, which indicates that the sample undergoes failure. Then, ITS and TSR results show that at 3% the moisture susceptibility is improved. The presence of moisture is a prominent point, since the dry sample which had a large amount of strength earlier, has reduced strength after being exposed to moisture. Last, but not least, the binder drain down also shows a great improvement at 2% as the binder drain down is reduced to almost 91.5%.

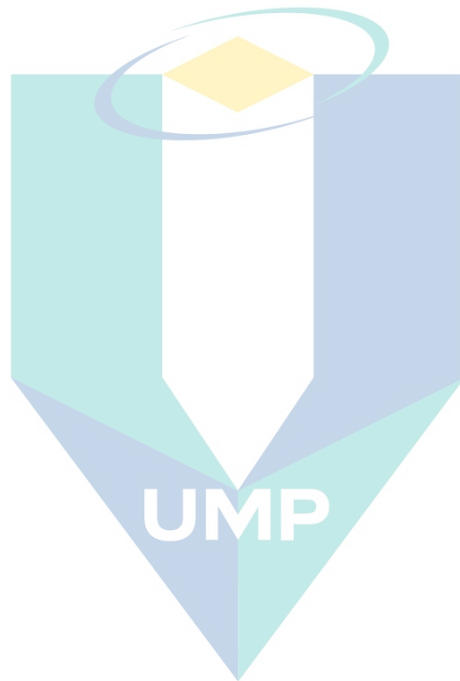
## 5.2 Recommendation

The following recommendations are made for further exploration into nanomaterials, whether it concerns the material itself, or even what aspect they will influence.

- a) Try a different mixing method or parameters in order to see whether there will be a different effect on the mixture when missing. Not only that, but also use a different content of nano titanium powder which includes more than 5%.
- b) For the resilient modulus and dynamic creep test, it is recommended to use only one temperature, which is 25°C. Since the apparatus itself may have different specifications, it is recommended to observe one temperature with several tries.



- c) Additional laboratory tests, such as Rotational viscosity test, FESEM, and AFM may be conducted. This is because these tests may reveal more applications and specifications.



اونيورسيتي مليسيا قهغ

UNIVERSITI MALAYSIA PAHANG

## REFERENCES

- Ahmad, M., Beddu, S., Hussain, S., Manan, A., & Itam, Z. binti. (2019). Mechanical properties of hot-mix asphalt using waste crumber rubber and phenol formaldehyde polymer. *AIMS Materials Science*, 6(6), 1164–1175. <https://doi.org/10.3934/MATERSCI.2019.6.1164>
- Alam, M. N., & Aggarwal, P. (2020). Effectiveness of anti stripping agents on moisture susceptibility of bituminous mix. *Construction and Building Materials*, 264. <https://doi.org/10.1016/j.conbuildmat.2020.120274>
- Alkaissi, Z. A. (2020). Effect of high temperature and traffic loading on rutting performance of flexible pavement. *Journal of King Saud University-Engineering Sciences*, 32(1), 1-4.
- Al-Sabaeei, A. M., Napiyah, M., Sutanto, M., Alaloul, W., Yusoff, N. I. M., Khan, M. I., & Saeed, S. M. (2021). Physicochemical, rheological and microstructural properties of Nano-Silica modified Bio-Asphalt. *Construction and Building Materials*, 297, 123772.
- Ameli, A., Babagoli, R., Khabooshani, M., AliAsgari, R., & Jalali, F. (2020). Permanent deformation performance of binders and stone mastic asphalt mixtures modified by SBS/montmorillonite nanocomposite. *Construction and Building Materials*, 239. <https://doi.org/10.1016/j.conbuildmat.2019.117700>
- Ameli, A., Hossein Pakshir, A., Babagoli, R., Norouzi, N., Nasr, D., & Davoudinezhad, S. (2020). Experimental investigation of the influence of Nano TiO<sub>2</sub> on rheological properties of binders and performance of stone matrix asphalt mixtures containing steel slag aggregate. *Construction and Building Materials*, 265. <https://doi.org/10.1016/j.conbuildmat.2020.120750>
- Ameli, A., Maher, J., Mosavi, A., Nabipour, N., Babagoli, R., & Norouzi, N. (2020). Performance evaluation of binders and stone matrix asphalt (SMA) mixtures modified by ground tire rubber (GTR), waste polyethylene terephthalate (PET) and anti stripping agents (ASAs). *Construction and Building Materials*, 251, 118932.
- Ameli, A., Nasr, D., Babagoli, R., Hossein Pakshir, A., Norouzi, N., & Davoudinezhad, S. (2020). Laboratory evaluation of rheological behavior of binder and performance of stone matrix asphalt (SMA) mixtures containing zycotherm nanotechnology, sasobit, and rheofalt warm mixture additives. *Construction and Building Materials*, 262. <https://doi.org/10.1016/j.conbuildmat.2020.120757>
- American Association of State Highway and Transportation Officials T 316 (AASHTO), (2019). Standard Method of Test for Viscosity Determination of Asphalt Binder Using Rotational Viscometer, 2019 Edition.
- American Society for Testing and Materials (ASTM) C131 / C131M-20. (2020). Standard Test Method for Resistance to Degradation of Small-Size Coarse Aggregate by Abrasion and Impact in the Los Angeles Machine, ASTM International, West Conshohocken, PA.
- American Society for Testing and Materials (ASTM) C136 / C136M-19. (2019). Standard Test Method for Sieve Analysis of Fine and Coarse Aggregates, ASTM International, West Conshohocken, PA.

- American Society for Testing and Materials (ASTM) D36 / D36M-14. (2020). Standard Test Method for Softening Point of Bitumen (Ring-and-Ball Apparatus), ASTM International, West Conshohocken, PA.
- American Society for Testing and Materials (ASTM) D4402 / D4402M-15. (2015). Standard Test Method for Viscosity Determination of Asphalt at Elevated Temperatures Using a Rotational Viscometer, ASTM International, West Conshohocken, PA.
- American Society for Testing and Materials (ASTM) D5 / D5M-20. (2020). Standard Test Method for Penetration of Bituminous Materials, ASTM International, West Conshohocken, PA.
- American Society for Testing and Materials (ASTM) D6927-15. (2015). Standard Test Method for Marshall Stability and Flow of Asphalt Mixtures, ASTM International, West Conshohocken, PA.
- American Society for Testing and Materials (ASTM) D704-15. (2015). Standard Test Method for Dynamic Creep of Asphalt Mixtures, ASTM International, West Conshohocken, PA.
- American Society for Testing and Materials (ASTM) D7369-20. (2020). Standard Test Method for Determining the Resilient Modulus of Asphalt Mixtures by Indirect Tension Test, ASTM International, West Conshohocken, PA.
- Amini, A., & Imaninasab, R. (2018). Investigating the effectiveness of Vacuum Tower Bottoms for Asphalt Rubber Binder based on performance properties and statistical analysis. *Journal of Cleaner Production*, 171, 1101-1110.
- Apostolidis, P., Liu, X., Erkens, S., & Scarpas, A. (2019). Evaluation of epoxy modification in bitumen. *Construction and Building Materials*, 208, 361-368. <https://doi.org/10.1016/j.conbuildmat.2019.03.013>
- Arshad, A. K., Masri, K. A., Ahmad, J., & Samsudin, M. S. (2017). Investigation on Moisture Susceptibility and Rutting Resistance of Asphalt Mixtures incorporating Nanosilica Modified Binder. *Pertanika Journal of Science & Technology*, 25.
- Arshad, A. K., Shaffie, E., Hashim, W., Ismail, F., & Masri, K. A. (2019). Evaluation of nanosilica modified stone mastic asphalt. *International Journal of Civil Engineering and Technology*, 10(2), 1508-1516.
- Bamigboye, G. O., Basse, D. E., Olukanni, D. O., Ngene, B. U., Adegoke, D., Odetoyan, A. O., ... & Nworgu, A. T. (2021). Waste materials in highway applications: An overview on generation and utilization implications on sustainability. *Journal of Cleaner Production*, 283. <https://doi.org/10.1016/j.jclepro.2020.124581>
- Blom, J., Soenen, H., & Van den Brande, N. (2021). New evidence on the origin of 'bee structures' on bitumen and oils, by atomic force microscopy (AFM) and confocal laser scanning microscopy (CLSM). *Fuel*, 303, 121265.
- Blom, J., Soenen, H., Katsiki, A., Van den Brande, N., Rahier, H., & van den Bergh, W. (2018). Investigation of the bulk and surface microstructure of bitumen by atomic force microscopy. *Construction and Building Materials*, 177, 158-169. <https://doi.org/10.1016/j.conbuildmat.2018.05.062>

- British Standard (BS) 812-110 (1990). Testing Aggregates. Method for determination of Aggregate Crushing Value. British Standards Institution.
- British Standard (BS) 812-112 (1990). Testing Aggregates. Method for determination of Aggregate Impact Value. British Standards Institution.
- Cadorin, N. D. A., de Melo, J. V. S., Broering, W. B., Manfro, A. L., & Barra, B. S. (2021). Asphalt nanocomposite with titanium dioxide: Mechanical, rheological and photoactivity performance. *Construction and Building Materials*, 289. <https://doi.org/10.1016/j.conbuildmat.2021.123178>
- Cao, Z., Chen, M., He, B., Han, X., Yu, J., & Xue, L. (2019). Investigation of ultraviolet aging resistance of bitumen modified by layered double hydroxides with different particle sizes. *Construction and Building Materials*, 196, 166-174. <https://doi.org/10.1016/j.conbuildmat.2018.11.125>
- Caputo, P., Porto, M., Angelico, R., Loise, V., Calandra, P., & Rossi, C. O. (2020). Bitumen and asphalt concrete modified by nanometer-sized particles: Basic concepts, the state of the art and future perspectives of the nanoscale approach. *Advances in Colloid and Interface Science*, 285. <https://doi.org/10.1016/j.cis.2020.102283>
- Chegenizadeh, A., Tokoni, L., Nikraz, H., & Dadras, E. (2021). Effect of ethylene-vinyl acetate (EVA) on stone mastic asphalt (SMA) behaviour. *Construction and Building Materials*, 272. <https://doi.org/10.1016/j.conbuildmat.2020.121628>
- Chen, J., Zhang, W., Shi, X., Yao, C., & Kuai, C. (2020). Use of PEG/SiO<sub>2</sub> phase change composite to control porous asphalt concrete temperature. *Construction and Building Materials*, 245. <https://doi.org/10.1016/j.conbuildmat.2020.118459>
- Chen, T., Ma, T., Huang, X., Guan, Y., Zhang, Z., & Tang, F. (2019). The performance of hot-recycling asphalt binder containing crumb rubber modified asphalt based on physiochemical and rheological measurements. *Construction and Building Materials*, 226, 83-93. <https://doi.org/10.1016/j.conbuildmat.2019.07.253>
- Cheraghian, G., & Wistuba, M. P. (2020). Ultraviolet aging study on bitumen modified by a composite of clay and fumed silica nanoparticles. *Scientific Reports*, 10(1), 1-17. <https://doi.org/10.1038/s41598-020-68007-0>
- Choudhary, J., Kumar, B., & Gupta, A. (2020). Utilization of solid waste materials as alternative fillers in asphalt mixes: A review. *Construction and Building Materials*, 234. <https://doi.org/10.1016/j.conbuildmat.2019.117271>
- Crucho, J. M. L., das Neves, J. M. C., Capitão, S. D., & de Picado-Santos, L. G. (2018). Mechanical performance of asphalt concrete modified with nanoparticles: Nanosilica, zero-valent iron and nanoclay. *Construction and Building Materials*, 181, 309-318. <https://doi.org/10.1016/j.conbuildmat.2018.06.052>
- Devulapalli, L., Kothandaraman, S., & Sarang, G. (2019). Evaluation of rejuvenator's effectiveness on the reclaimed asphalt pavement incorporated stone matrix asphalt mixtures. *Construction and Building Materials*, 224, 909-919.
- Ding, L., Wang, X., Zhang, M., Chen, Z., Meng, J., & Shao, X. (2021). Morphology and properties changes of virgin and aged asphalt after fusion. *Construction and Building*

*Materials*, 291, 123284.

- Enieb, M., & Diab, A. (2017). Characteristics of asphalt binder and mixture containing nanosilica. *International Journal of Pavement Research and Technology*, 10(2), 148-157.
- Eskandarsefat, S., Dondi, G., & Sangiorgi, C. (2019). Recycled and rubberized SMA modified mixtures: A comparison between polymer modified bitumen and modified fibres. *Construction and Building Materials*, 202, 681-691. <https://doi.org/10.1016/j.conbuildmat.2019.01.045>
- Fakhri, M. (2021). The effects of nano zinc oxide (ZnO) and nano reduced graphene oxide (RGO) on moisture susceptibility property of stone mastic asphalt (SMA). *Case Studies in Construction Materials*, 15. <https://doi.org/10.1016/j.cscm.2021.e00655>
- Fauzi, N. M., Masri, K. A., Ramadhansyah, P. J., Samsudin, M. S., Ismail, A., Arshad, A. K., ... & Hainin, M. R. (2020). Volumetric properties and resilient modulus of stone mastic asphalt incorporating cellulose fiber. In *IOP Conference Series: Materials Science and Engineering* (Vol. 712, No. 1, p. 012028). IOP Publishing.
- Fernandes, S. R., Silva, H. M., & Oliveira, J. R. (2019). Carbon dioxide emissions and heavy metal contamination analysis of stone mastic asphalt mixtures produced with high rates of different waste materials. *Journal of Cleaner Production*, 226, 463-470. <https://doi.org/10.1016/j.jclepro.2019.04.111>
- Ganji, M. R., Golroo, A., Sheikhzadeh, H., Ghelmani, A., & Bidgoli, M. A. (2019). Dense-graded asphalt pavement macrotexture measurement using tire/road noise monitoring. *Automation in Construction*, 106, 102887.
- Geçkil, T. (2019). Physical, chemical, microstructural and rheological properties of reactive terpolymer-modified bitumen. *Materials*, 12(6), 921. <https://doi.org/10.3390/ma12060921>
- Ghavami, M. S. M., Hosseini, M. S., Zavattieri, P. D., & Haddock, J. E. (2019). Flexible pavement drainage system effectiveness. *Construction and Building Materials*, 218, 99-107.
- Guo, R., Nian, T., & Zhou, F. (2020). Analysis of factors that influence anti-rutting performance of asphalt pavement. *Construction and Building Materials*, 254. <https://doi.org/10.1016/j.conbuildmat.2020.119237>
- Haider, A. J., AL-Anbari, R. H., Kadhim, G. R., & Salame, C. T. (2017). Exploring potential environmental applications of TiO<sub>2</sub> nanoparticles. *Energy Procedia*, 119, 332-345. <https://doi.org/10.1016/j.egypro.2017.07.117>
- He, H., Hu, J., Li, R., Shen, C., Pei, J., & Zhou, B. (2021). Study on rheological properties of silica nanofluids modified asphalt binder. *Construction and Building Materials*, 273. <https://doi.org/10.1016/j.conbuildmat.2020.122046>
- He, Y., Wang, Z., Wang, H., Wang, Z., Zeng, G., Xu, P., ... & Zhao, Y. (2021). Metal-organic framework-derived nanomaterials in environment related fields: Fundamentals, properties and applications. *Coordination Chemistry Reviews*, 429. <https://doi.org/10.1016/j.ccr.2020.213618>



- Hong, H., Zhang, H., & Zhang, S. (2020). Effect of multi-dimensional nanomaterials on the aging behavior of asphalt by atomic force microscope. *Construction and Building Materials*, 260. <https://doi.org/10.1016/j.conbuildmat.2020.120389>
- Huang, K., Onifade, I., & Birgisson, B. (2021). Rutting performance of flexible pavements using new energy-based potentials. *Construction and Building Materials*, 266, 120896.
- Irfan, M., Ali, Y., Ahmed, S., Iqbal, S., & Wang, H. (2019). Rutting and fatigue properties of cellulose fiber-added stone mastic asphalt concrete mixtures. *Advances in Materials Science and Engineering*, 2019. <https://doi.org/10.1155/2019/5604197>
- Ismael, M. Q., Fattah, M. Y., & Jasim, A. F. (2021). Improving the rutting resistance of asphalt pavement modified with the carbon nanotubes additive. *Ain Shams Engineering Journal*, 12(4), 3619-3627. <https://doi.org/10.1016/j.asej.2021.02.038>
- Jabatan Kerja Raya (JKR). (2008). JKR/SPJ/2008-S4 Standard Specification for Road Works Part4 Flexible Pavement.
- Jain, S., Singh, H., & Chopra, T. (2020). Laboratory investigations and performance evaluation of stone matrix asphalt as a wearing course using three different fibers. *International Journal of Applied Science and Engineering*, 17(4), 411-418. [https://doi.org/10.6703/IJASE.202012\\_17\(4\).411](https://doi.org/10.6703/IJASE.202012_17(4).411)
- Jameel, Z. N., Mahmood, O. A., & Ahmed, F. L. (2019). Studying the effect of synthesized nano-titanium dioxide via two phases on the Pseudomonas aeruginosa and portus bacteria as antimicrobial agents. *International Journal of Nanoelectronics and Materials*, 12, 329-338.
- Jasni, N. E., Masri, K. A., Ramadhansyah, P. J., Arshad, A. K., Shaffie, E., Ahmad, J., & Norhidayah, A. H. (2020). Mechanical performance of stone mastic asphalt incorporating steel fiber. In *IOP Conference Series: Materials Science and Engineering* (Vol. 712, No. 1, p. 012026). IOP Publishing.
- Jayaraman, J., Dey, K., Arunkumar, T., Appavu, P., & Joy, N. (2021). Investigation on titanium oxide nano particles as additives for operating biodiesel fuelled engine. *Materials Today: Proceedings*, 44, 3525-3529.
- Jin, J., Chen, B., Liu, L., Liu, R., Qian, G., Wei, H., & Zheng, J. (2019). A study on modified bitumen with metal doped nano-TiO<sub>2</sub> pillared montmorillonite. *Materials*, 12(12). <https://doi.org/10.3390/ma12121910>
- Khedmati, M., Khodaii, A., & Haghshenas, H. F. (2017). A study on moisture susceptibility of stone matrix warm mix asphalt. *Construction and Building Materials*, 144, 42-49. <https://doi.org/10.1016/j.conbuildmat.2017.03.121>
- Korayem, A. H., Ziari, H., Hajiloo, M., Abarghoie, M., & Karimi, P. (2020). Laboratory evaluation of stone mastic asphalt containing amorphous carbon powder as filler material. *Construction and Building Materials*, 243. <https://doi.org/10.1016/j.conbuildmat.2020.118280>
- Kumar, N. K., & Ravitheja, A. (2019). Characteristics of stone matrix asphalt by using natural fibers as additives. *Materials today: proceedings*, 19, 397-402. <https://doi.org/10.1016/j.matpr.2019.07.624>



- Leal, J. H., Cantu, Y., Gonzalez, D. F., & Parsons, J. G. (2017). Brookite and anatase nanomaterial polymorphs of TiO<sub>2</sub> synthesized from TiCl<sub>3</sub>. *Inorganic Chemistry Communications*, 84, 28-32. <https://doi.org/10.1016/j.inoche.2017.07.014>
- Li, J., Liu, J., Zhang, W., Liu, G., & Dai, L. (2019). Investigation of thermal asphalt mastic and mixture to repair potholes. *Construction and Building Materials*, 201, 286-294. <https://doi.org/10.1016/j.conbuildmat.2018.12.153>
- Li, Z., Ding, S., Yu, X., Han, B., & Ou, J. (2018). Multifunctional cementitious composites modified with nano titanium dioxide: A review. *Composites Part A: Applied Science and Manufacturing*, 111, 115-137. <https://doi.org/10.1016/j.compositesa.2018.05.019>
- Lima, M. S., & Thives, L. P. (2020). Evaluation of red mud as filler in Brazilian dense graded asphalt mixtures. *Construction and Building Materials*, 260, 119894.
- Lin, P., Yan, C., Huang, W., Li, Y., Zhou, L., Tang, N., ... & Lv, Q. (2019). Rheological, chemical and aging characteristics of high content polymer modified asphalt. *Construction and Building Materials*, 207, 616-629. <https://doi.org/10.1016/j.conbuildmat.2019.02.086>
- Liu, Y., Su, P., Li, M., You, Z., & Zhao, M. (2020). Review on evolution and evaluation of asphalt pavement structures and materials. *Journal of Traffic and Transportation Engineering (English Edition)*, 7(5), 573-599. <https://doi.org/10.1016/j.conbuildmat.2017.06.062>
- Masri, K. A., Arshad, A. K., & Samsudin, M. S. (2016). Mechanical properties of porous asphalt with nanosilica modified binder. *Jurnal Teknologi*, 78(7-2). <https://doi.org/10.11113/jt.v78.9509>
- Masri, K. A., Jaya, R. P., Arshad, A. K., & Mahmud, M. Z. H. (2020). Morphological and physical characteristic of stone mastic asphalt mixture incorporating nano silica. *The Open Civil Engineering Journal*, 14(1). <https://doi.org/10.2174/1874149502014010113>
- Mazari, S. A., Ali, E., Abro, R., Khan, F. S. A., Ahmed, I., Ahmed, M., ... & Shah, A. (2021). Nanomaterials: Applications, waste-handling, environmental toxicities, and future challenges—A review. *Journal of Environmental Chemical Engineering*, 9(2). <https://doi.org/10.1016/j.jece.2021.105028>
- Miranda, H. M. B., Batista, F. A., de Lurdes Antunes, M., & Neves, J. (2020). Influence of laboratory aggregate compaction method on the particle packing of stone mastic asphalt. *Construction and Building Materials*, 259. <https://doi.org/10.1016/j.conbuildmat.2020.119699>
- Mirsepahi, M., Tanzadeh, J., & Ghanoon, S. A. (2020). Laboratory evaluation of dynamic performance and viscosity improvement in modified bitumen by combining nanomaterials and polymer. *Construction and Building Materials*, 233, 117183.
- Mohammed, B. S., Adamu, M., & Liew, M. S. (2018). Evaluating the effect of crumb rubber and nano silica on the properties of high volume fly ash roller compacted concrete pavement using non-destructive techniques. *Case studies in construction materials*, 8, 380-391. <https://doi.org/10.1016/j.cscm.2018.03.004>
- Munajad, A., & Subroto, C. (2018). Fourier transform infrared (FTIR) spectroscopy analysis of transformer paper in mineral oil-paper composite insulation under accelerated thermal aging. *Energies*, 11(2), 364. <https://doi.org/10.3390/en11020364>

- Nciri, N., Kim, N., & Cho, N. (2021). From Street to Road: An Innovative Approach to Explore Discarded Chewing Gum as a Performance-Enhancing Modifier for Road Pavement Applications. *Polymers*, 13(12), 1963.
- Nivitha, M. R., Prasad, E., & Krishnan, J. M. (2019). Transitions in unmodified and modified bitumen using FTIR spectroscopy. *Materials and Structures*, 52(1), 1-11. <https://doi.org/10.1617/s11527-018-1308-7>
- Nobakht, M., Zhang, D., Sakhaeifar, M. S., & Lytton, R. L. (2020). Characterization of the adhesive and cohesive moisture damage for asphalt concrete. *Construction and Building Materials*, 247. <https://doi.org/10.1016/j.conbuildmat.2020.118616>
- Orešković, M., Pires, G. M., Bressi, S., Vasconcelos, K., & Presti, D. L. (2020). Quantitative assessment of the parameters linked to the blending between reclaimed asphalt binder and recycling agent: A literature review. *Construction and Building Materials*, 234. <https://doi.org/10.1016/j.conbuildmat.2019.117323>
- Ozdemir, D. K., Topal, A., & McNally, T. (2021). Relationship between microstructure and phase morphology of SBS modified bitumen with processing parameters studied using atomic force microscopy. *Construction and Building Materials*, 268. <https://doi.org/10.1016/j.conbuildmat.2020.121061>
- Parimita, P. (2020, November). Influence of Natural Fibers as Additive on Characteristics of Stone Mastic Asphalt. In *IOP Conference Series: Materials Science and Engineering* (Vol. 970, No. 1, p. 012021). IOP Publishing.
- Peng, J., Zhang, J., Li, J., Yao, Y., & Zhang, A. (2020). Modeling humidity and stress-dependent subgrade soils in flexible pavements. *Computers and Geotechnics*, 120, 103413.
- Perera, S., Arulrajah, A., Wong, Y. C., Horpibulsuk, S., & Maghool, F. (2019). Utilizing recycled PET blends with demolition wastes as construction materials. *Construction and building materials*, 221, 200-209.
- Picado-Santos, L. G., Capitão, S. D., & Neves, J. M. (2020). Crumb rubber asphalt mixtures: A literature review. *Construction and Building Materials*, 247. <https://doi.org/10.1016/j.conbuildmat.2020.118577>
- Pipintakos, G., Hasheminejad, N., Lommaert, C., Bocharova, A., & Blom, J. (2021). Application of Atomic Force (AFM), Environmental Scanning Electron (ESEM) and Confocal Laser Scanning Microscopy (CLSM) in bitumen: a review of the ageing effect. *Micron*, 147. <https://doi.org/10.1016/j.micron.2021.103083>
- Qian, N., Wang, D., Li, D., & Shi, L. (2020). Three-dimensional mesoscopic permeability of porous asphalt mixture. *Construction and Building Materials*, 236, 117430.
- Radzi, N. A. M., Masri, K. A., Ramadhansyah, P. J., Jasni, N. E., Arshad, A. K., Ahmad, J., ... & Yaacob, H. (2020). Stability and Resilient Modulus of Porous Asphalt Incorporating Steel Fiber. In *IOP Conference Series: Materials Science and Engineering* (Vol. 712, No. 1, p. 012027). IOP Publishing.
- Rahmad, S., Rosyidi, S. A. P., Memon, N. A., Badri, K. H., Widyatmoko, I., Arshad, A. K., ... & Hainin, M. R. (2021). Physical, thermal and micro-surface characteristics of PG76 binder incorporated with liquid chemical WMA additive. *Construction and Building*

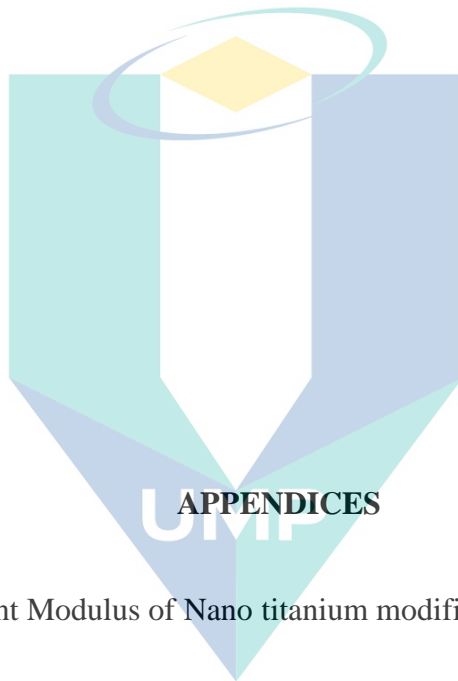
*Materials*, 272, 121626.

- Rahman, M. T., Mohajerani, A., & Giustozzi, F. (2020). Possible use of cigarette butt fiber modified bitumen in stone mastic asphalt. *Construction and Building Materials*, 263, 120134. <https://doi.org/10.1016/j.conbuildmat.2020.120134>
- Ramadhansyah, P. J., Masri, K. A., Norhidayah, A. H., Hainin, M. R., Naquiddin, M. M., Haryati, Y., ... & Juraidah, A. (2020). Nanoparticle in Asphalt Binder: A State-of-The-Art Review. In *IOP Conference Series: Materials Science and Engineering* (Vol. 712, No. 1, p. 012023). IOP Publishing.
- Rawtani, D., Rao, P. K., & Hussain, C. M. (2020). Recent advances in analytical, bioanalytical and miscellaneous applications of green nanomaterial. *TrAC Trends in Analytical Chemistry*, 133. <https://doi.org/10.1016/j.trac.2020.116109>
- Razavi, S. H., & Kavussi, A. (2020). The role of nanomaterials in reducing moisture damage of asphalt mixes. *Construction and Building Materials*, 239. <https://doi.org/10.1016/j.conbuildmat.2019.117827>
- Ren, S., Liu, X., Li, M., Fan, W., Xu, J., & Erkens, S. (2020). Experimental characterization of viscoelastic behaviors, microstructure and thermal stability of CR/SBS modified asphalt with TOR. *Construction and Building Materials*, 261. <https://doi.org/10.1016/j.conbuildmat.2020.120524>
- Rodríguez-Fernández, I., Baheri, F. T., Cavalli, M. C., Poulidakos, L. D., & Bueno, M. (2020). Microstructure analysis and mechanical performance of crumb rubber modified asphalt concrete using the dry process. *Construction and Building Materials*, 259. <https://doi.org/10.1016/j.conbuildmat.2020.119662>
- Rosyidi, S. A. P., Rahmad, S., Yusoff, N. I. M., Shahrir, A. H., Ibrahim, A. N. H., Ismail, N. F. N., & Badri, K. H. (2020). Investigation of the chemical, strength, adhesion and morphological properties of fly ash based geopolymer-modified bitumen. *Construction and Building Materials*, 255. <https://doi.org/10.1016/j.conbuildmat.2020.119364>
- Rys, D., Jaczewski, M., Pszczola, M., Jaskula, P., & Bankowski, W. (2020). Effect of bitumen characteristics obtained according to EN and Superpave specifications on asphalt mixture performance in low-temperature laboratory tests. *Construction and Building Materials*, 231, 117156. <https://doi.org/10.1016/j.conbuildmat.2019.117156>
- Saboo, N., Ranjeesh, R., Gupta, A., & Suresh, M. (2019). Development of hierarchical ranking strategy for the asphalt skeleton in semi-flexible pavement. *Construction and Building Materials*, 201, 149-158.
- Sadeghnejad, M., & Shafabakhsh, G. (2017). Use of Nano SiO<sub>2</sub> and Nano TiO<sub>2</sub> to improve the mechanical behaviour of stone mastic asphalt mixtures. *Construction and Building Materials*, 157, 965-974. <https://doi.org/10.1016/j.conbuildmat.2017.09.163>
- Shafabakhsh, G. A., Sadeghnejad, M., Ahoor, B., & Taheri, E. (2020). Laboratory experiment on the effect of nano SiO<sub>2</sub> and TiO<sub>2</sub> on short and long-term aging behavior of bitumen. *Construction and Building Materials*, 237. <https://doi.org/10.1016/j.conbuildmat.2019.117640>
- Snehal, K., Das, B. B., & Akanksha, M. (2020). Early age, hydration, mechanical and

- microstructure properties of nano-silica blended cementitious composites. *Construction and Building Materials*, 233. <https://doi.org/10.1016/j.conbuildmat.2019.117212>
- Soenen, H., Vansteenkiste, S., & Kara De Maeijer, P. (2020). Fundamental approaches to predict moisture damage in asphalt mixtures: State-of-the-art review. *Infrastructures*, 5(2), 20.
- Taherkhani, H., & Tajdini, M. (2019). Comparing the effects of nano-silica and hydrated lime on the properties of asphalt concrete. *Construction and Building Materials*, 218, 308-315. <https://doi.org/10.1016/j.conbuildmat.2019.05.116>
- UN Environment Programme (UNEP). (2018). Single-use plastic: a roadmap for sustainability. In: United Nation Environment Programme. Retrieved from. <https://www.unenvironment.org/resources/report/single-use-plastics-roadmap-sustainability>
- Wang, R., Xiong, Y., Yue, M., Hao, M., & Yue, J. (2020). Investigating the effectiveness of carbon nanomaterials on asphalt binders from hot storage stability, thermodynamics, and mechanism perspectives. *Journal of Cleaner Production*, 276. <https://doi.org/10.1016/j.jclepro.2020.124180>
- Wang, S., Mallick, R. B., & Rahbar, N. (2020). Toughening mechanisms in polypropylene fiber-reinforced asphalt mastic at low temperature. *Construction and Building Materials*, 248. <https://doi.org/10.1016/j.conbuildmat.2020.118690>
- Wang, X., Ji, G., Zhang, Y., Guo, Y., & Zhao, J. (2021). Research on high-and low-temperature characteristics of bitumen blended with waste eggshell powder. *Materials*, 14(8). <https://doi.org/10.3390/ma14082020>
- Wazeri, A., & Ali, T. (2017). Creep Stiffness and Permanent Deformation of Rubberized Asphalt. February 2015.
- Woodward, D., Millar, P., Lantieri, C., Sangiorgi, C., & Vignali, V. (2016). The wear of Stone Mastic Asphalt due to slow speed high stress simulated laboratory trafficking. *Construction and Building Materials*, 110, 270-277. <https://doi.org/10.1016/j.conbuildmat.2016.02.031>
- Xing, C., Liu, L., Cui, Y., & Ding, D. (2020). Analysis of base bitumen chemical composition and aging behaviors via atomic force microscopy-based infrared spectroscopy. *Fuel*, 264. <https://doi.org/10.1016/j.fuel.2019.116845>
- Xu, X., Guo, H., Wang, X., Zhang, M., Wang, Z., & Yang, B. (2019). Physical properties and anti-aging characteristics of asphalt modified with nano-zinc oxide powder. *Construction and Building Materials*, 224, 732-742. <https://doi.org/10.1016/j.conbuildmat.2019.07.097>
- Yan, K., Sun, H., You, L., & Wu, S. (2020). Characteristics of waste tire rubber (WTR) and amorphous poly alpha olefin (APAO) compound modified porous asphalt mixtures. *Construction and Building Materials*, 253.
- Yang, B., Li, H., Zhang, H., Xie, N., & Zhou, H. (2019). Laboratorial investigation on effects of microscopic void characteristics on properties of porous asphalt mixture. *Construction and Building Materials*, 213, 434-446.



- Yang, C., Zhu, B., Wang, J., & Qin, Y. (2019). Structural changes and nano-TiO<sub>2</sub> migration of poly (lactic acid)-based food packaging film contacting with ethanol as food simulant. *International journal of biological macromolecules*, 139, 85-93. <https://doi.org/10.1016/j.ijbiomac.2019.07.151>
- Yang, W. E., & Huang, H. H. (2019). Multiform TiO<sub>2</sub> nano-network enhances biological response to titanium surface for dental implant applications. *Applied Surface Science*, 471, 1041-1052. <https://doi.org/10.1016/j.apsusc.2018.11.244>
- You, L., Man, J., Yan, K., Wang, D., & Li, H. (2020). Combined Fourier-wavelet transforms for studying dynamic response of anisotropic multi-layered flexible pavement with linear-gradual interlayers. *Applied Mathematical Modelling*, 81, 559-581.
- Yuan, L., Masri, K. A., Ramadhansyah, P. J., Razelan, I. S. M., Norhidayah, A. H., & Warid, M. M. (2021, February). Performance of asphalt mixture incorporated with tin ore tailing. In *IOP Conference Series: Earth and Environmental Science* (Vol. 682, No. 1, p. 012057). IOP Publishing.
- Yusoff, N. I. M., Alhamali, D. I., Ibrahim, A. N. H., Rosyidi, S. A. P., & Hassan, N. A. (2019). Engineering characteristics of nanosilica/polymer-modified bitumen and predicting their rheological properties using multilayer perceptron neural network model. *Construction and Building Materials*, 204, 781-799. <https://doi.org/10.1016/j.conbuildmat.2019.01.203>
- Yusoff, N. I. M., Breem, A. A. S., Alattug, H. N., Hamim, A., & Ahmad, J. (2014). The effects of moisture susceptibility and ageing conditions on nano-silica/polymer-modified asphalt mixtures. *Construction and Building Materials*, 72, 139-147.
- Zhan, Y., Xie, J., Wu, Y., & Wang, Y. (2020). Synergetic Effect of Nano-ZnO and Trinidad Lake Asphalt for Antiaging Properties of SBS-Modified Asphalt. *Advances in Civil Engineering*, 2020. <https://doi.org/10.1155/2020/3239793>
- Zhang, H., Wang, Y., Yu, T., & Liu, Z. (2020). Microstructural characteristics of differently aged asphalt samples based on atomic force microscopy (AFM). *Construction and Building Materials*, 255. <https://doi.org/10.1016/j.conbuildmat.2020.119388>
- Zhang, Y., Luo, X., Deng, Y., Hou, S., Shi, X., & Lytton, R. L. (2020). Evaluation of rutting potential of flexible pavement structures using energy-based pseudo variables. *Construction and Building Materials*, 247, 1-13. <https://doi.org/10.1016/j.conbuildmat.2020.118391>
- Zhou, J., Yang, T., Chen, J., Wang, C., Zhang, H., & Shao, Y. (2020). Two-dimensional nanomaterial-based plasmonic sensing applications: Advances and challenges. *Coordination Chemistry Reviews*, 410, 213218.



## APPENDICES

Appendix A: Resilient Modulus of Nano titanium modified binder of SMA mix at 25°C & 40°C.

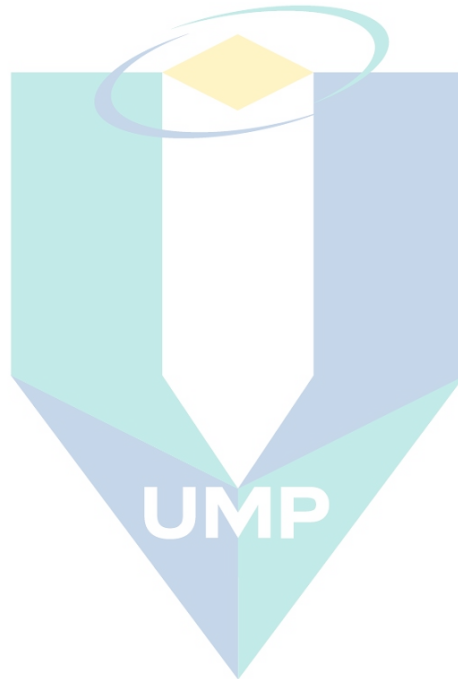
Resilient Modulus of Nano titanium modified binder of SMA mix at 25°C

% NT	Revised Resilient Modulus, Mpa		
	1000	2000	3000
0	1473	1311	1424
2	938	1090	1413
3	1478	1903	1521
4	1459	1234	1395



Resilient Modulus of Nano titanium modified binder of SMA mix at 40°C

% NT	Revised Resilient Modulus, Mpa		
	1000	2000	3000
0	1453	1438	2081
2	1446	1630	1971
3	2410	2172	2248
4	683	790	1153

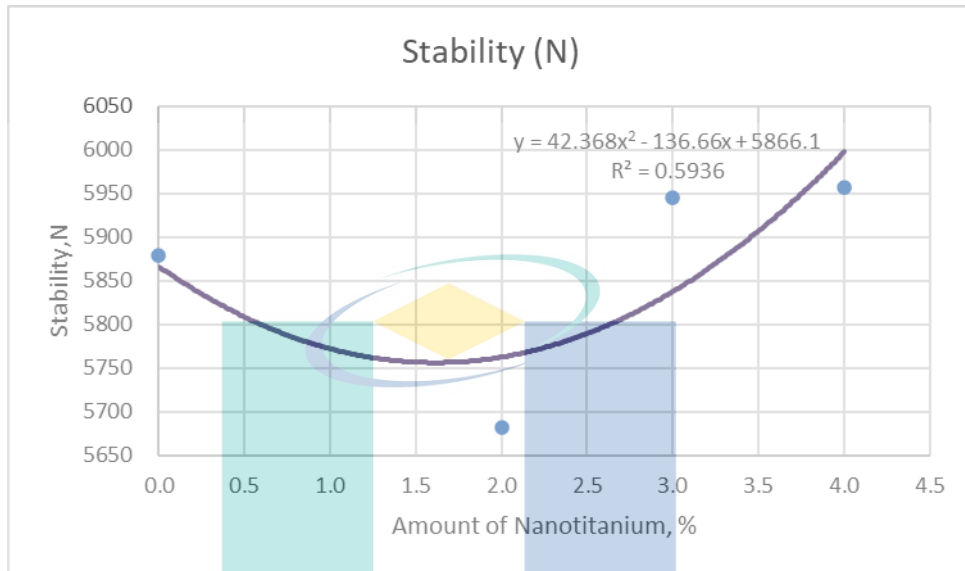


اونيورسيتي ملايسيا قهغ

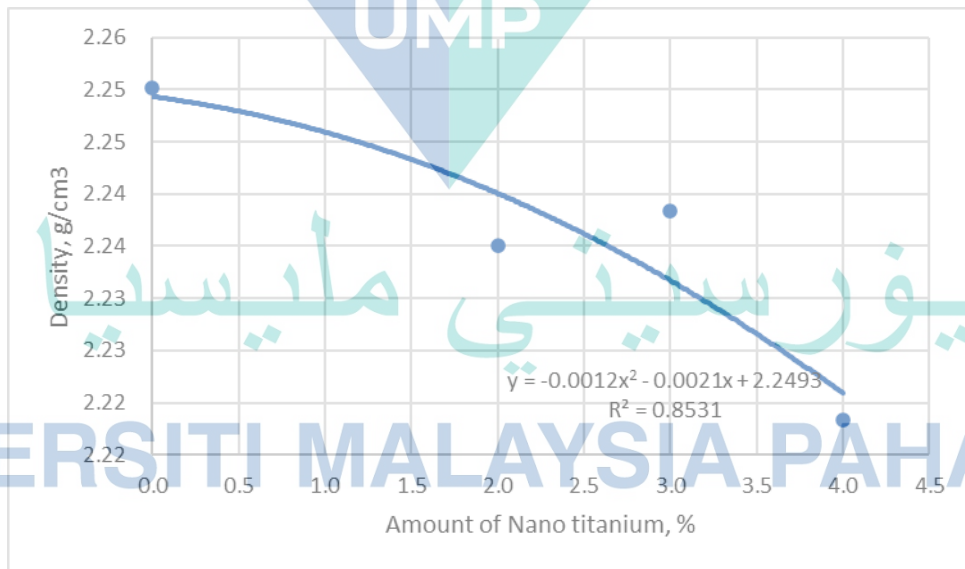
UNIVERSITI MALAYSIA PAHANG

Appendix B: Graphs of Marshall properties

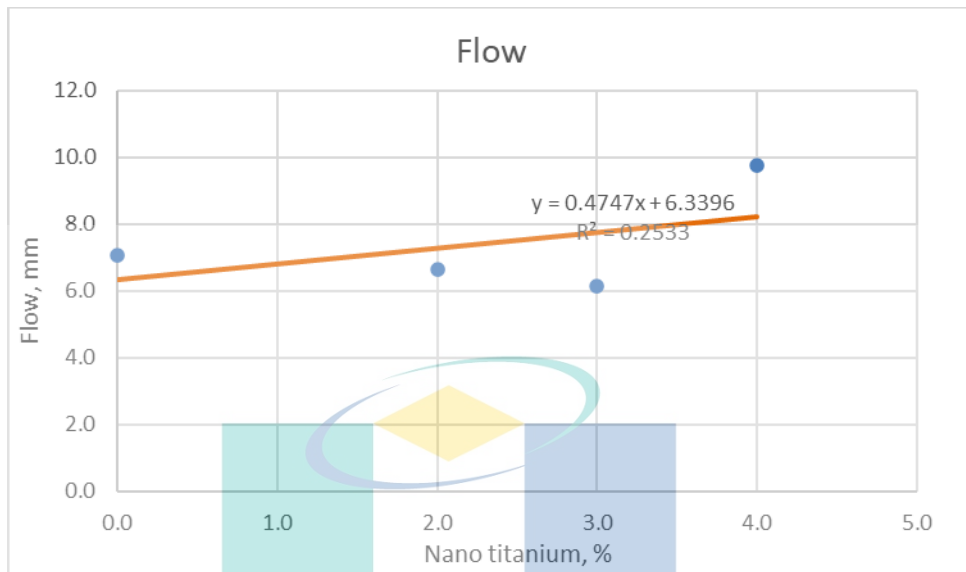
B 1: Amount of Nano titanium vs Stability



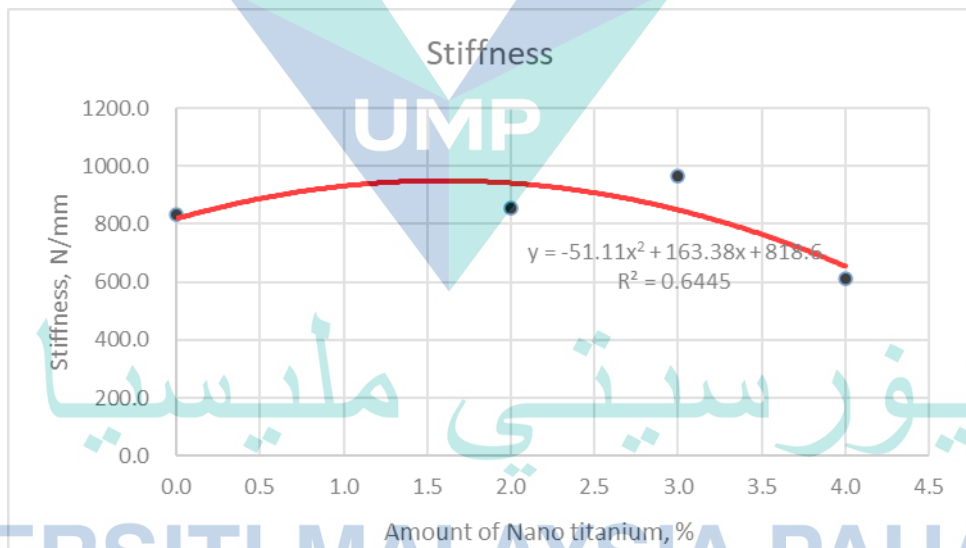
B 2: Amount of Nano titanium vs Density



B 3: Amount of Nano titanium vs Flow



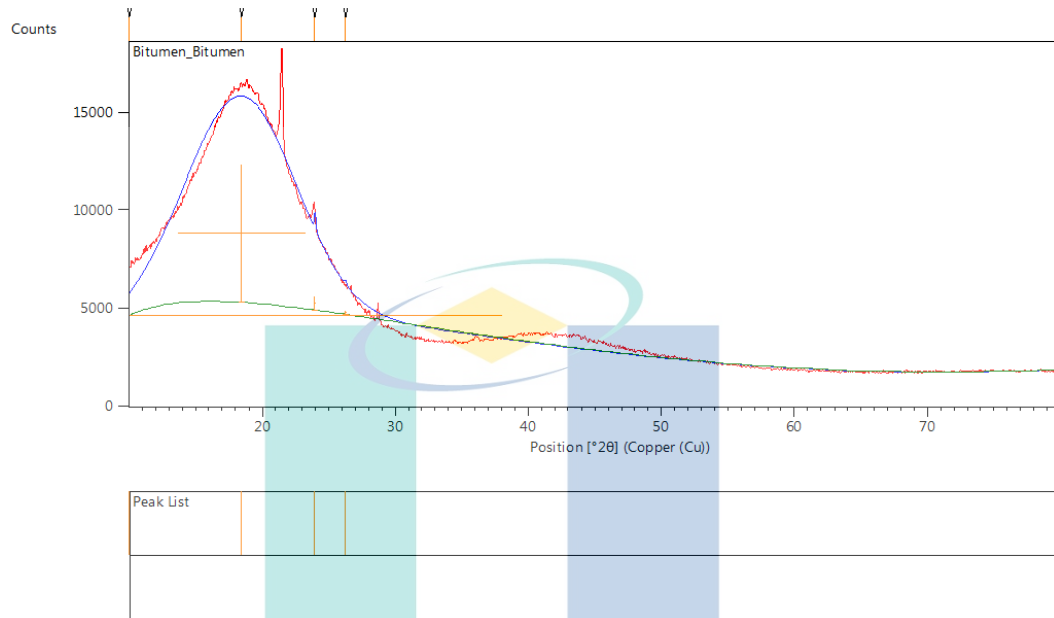
B 4: Amount of Nano titanium vs Stiffness



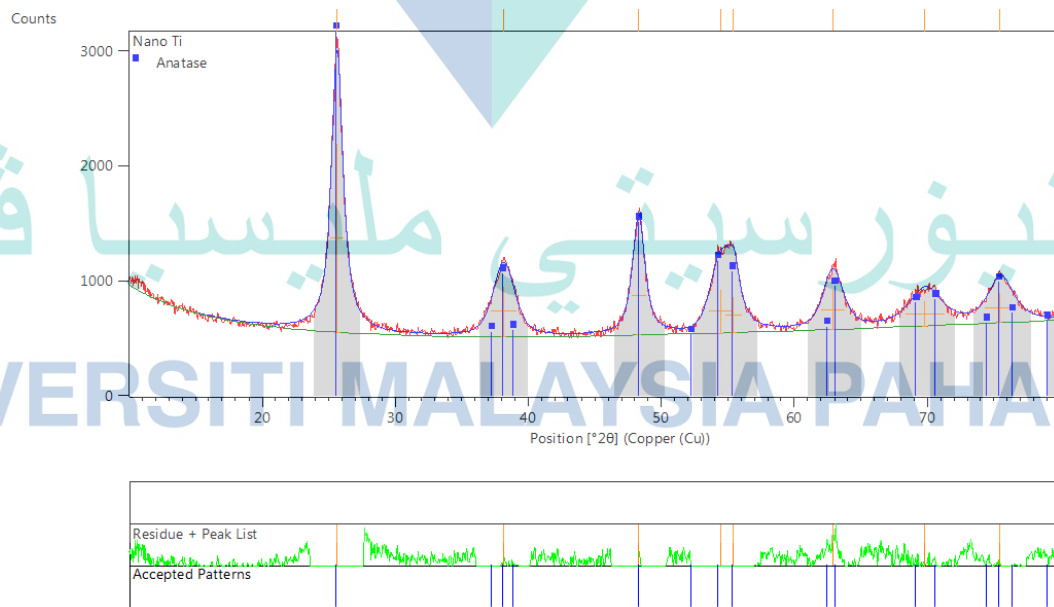
اونیورسیتی ملیسیا قهق  
UNIVERSITI MALAYSIA PAHANG

## Appendix C: Graphs of Marshall properties

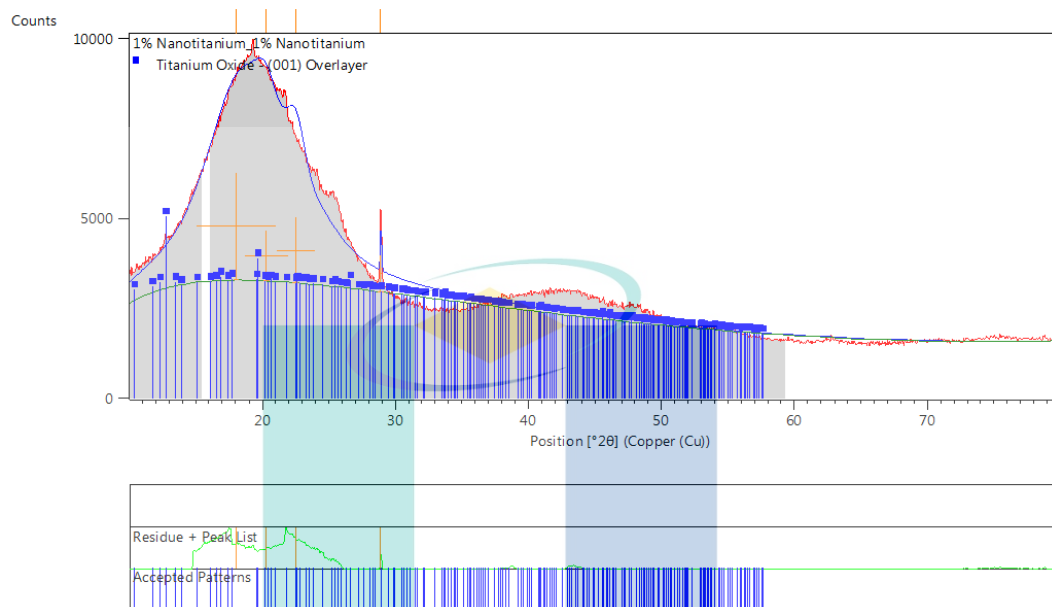
### C 1: XRD peaks for bitumen



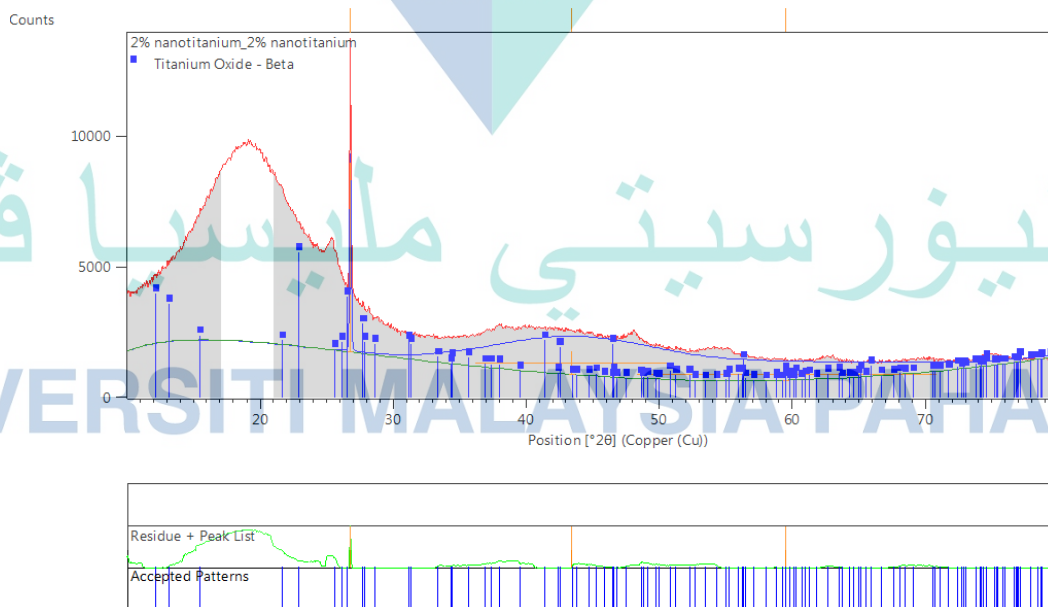
### C 2: XRD peaks for nano titanium



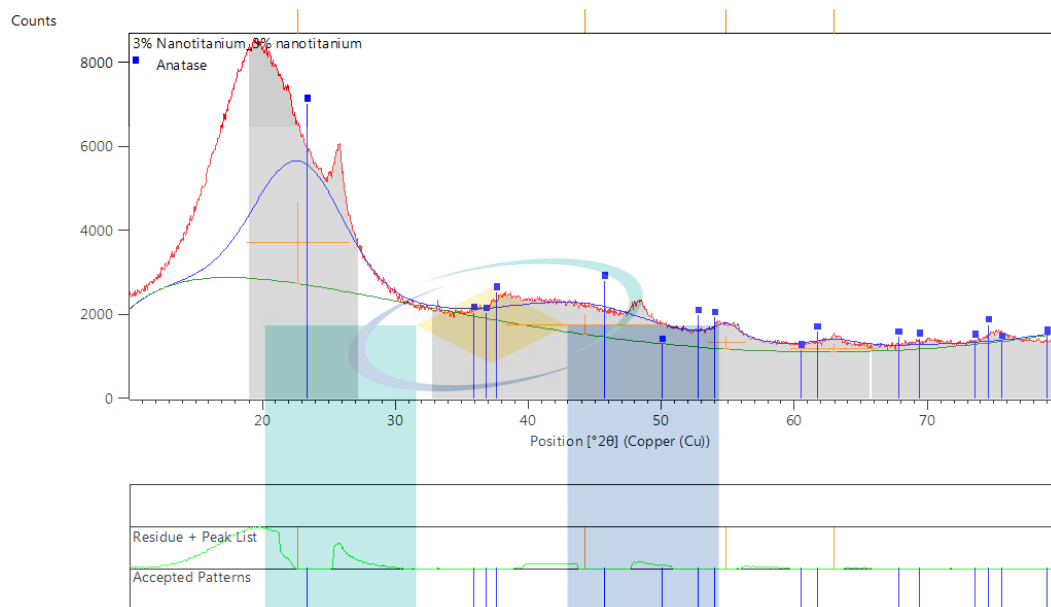
### C 3: XRD peaks for 1 % nano titanium



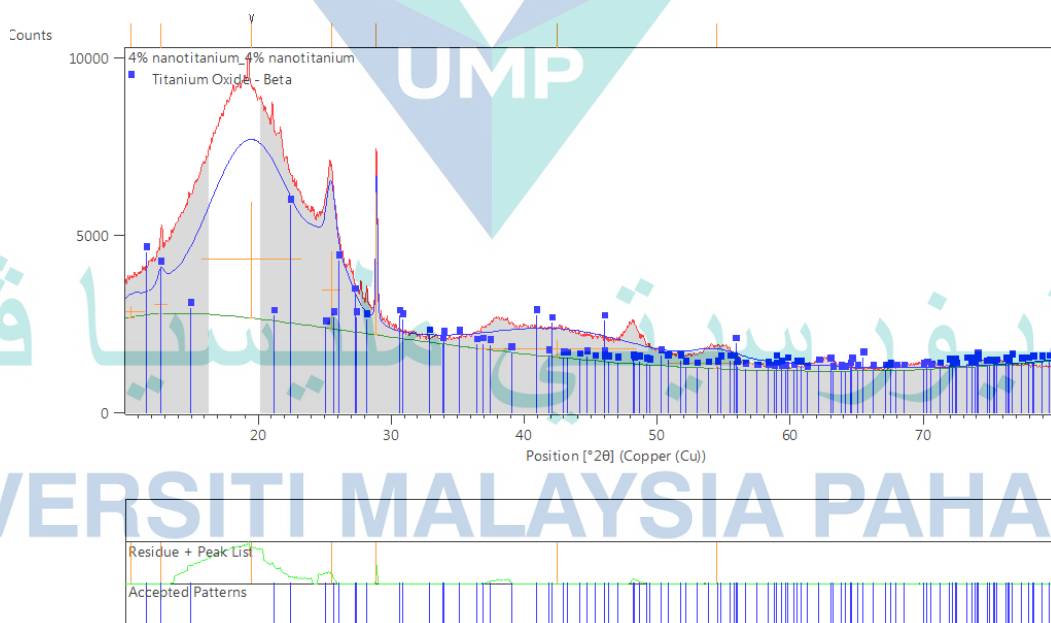
### C 4: XRD peaks for 2% nano titanium



### C 5: XRD peaks for 3% nano titanium

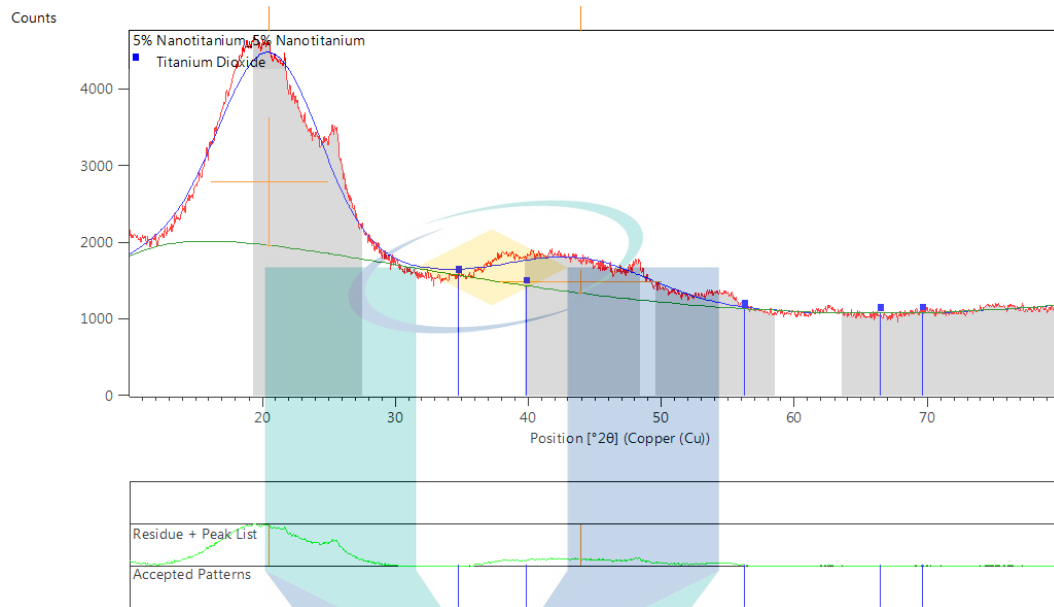


### C 6: XRD peaks for 4% nano titanium





C 7: XRD peaks for 5% nano titanium



UMP

اونيورسيتي ملايسيا قهغ

UNIVERSITI MALAYSIA PAHANG

Appendix D: Images from scanning electron microscope (SEM) of unmodified bitumen



Appendix E: Images from scanning electron microscope (SEM) of 1% NT modified bitumen





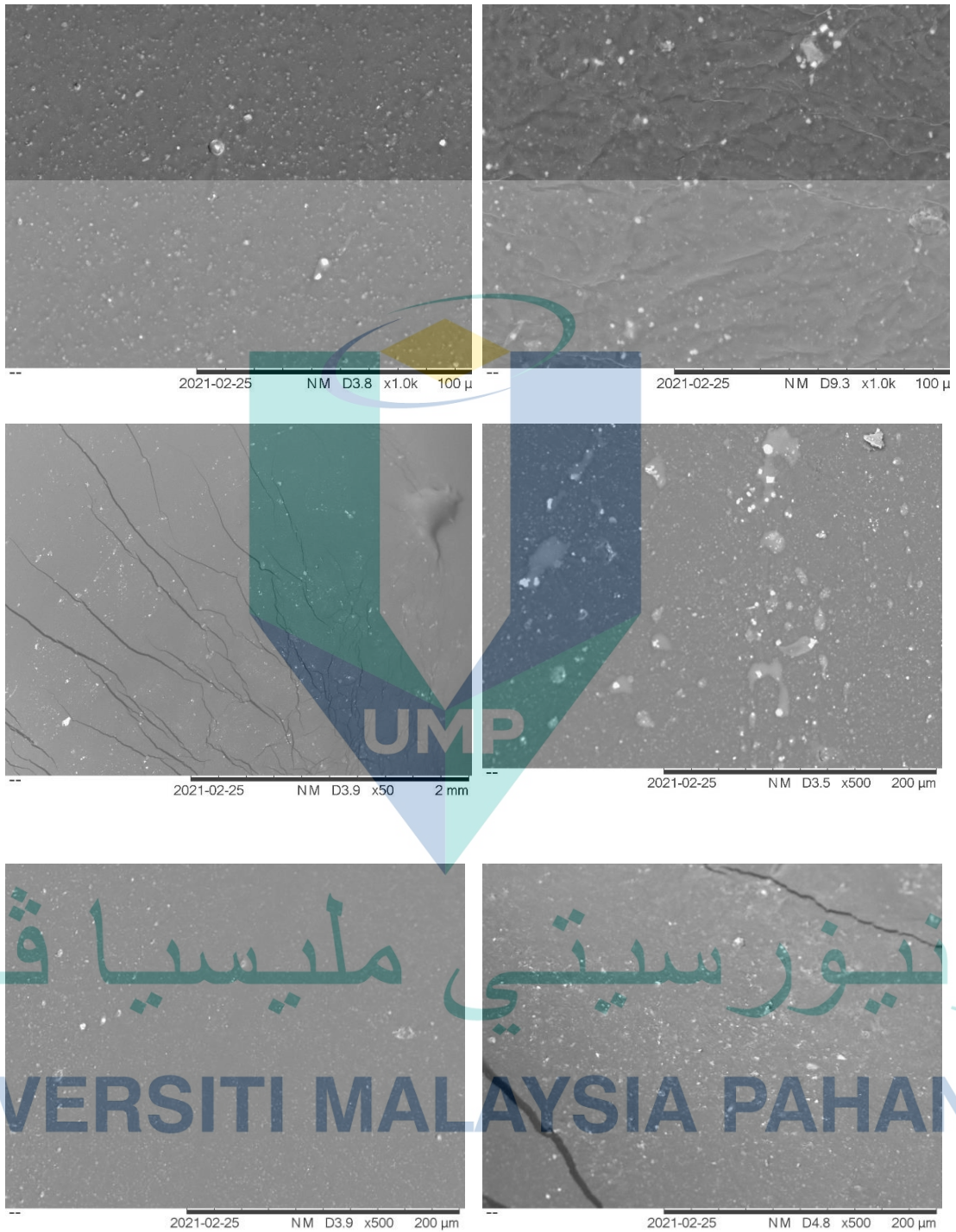
Appendix F: Images from scanning electron microscope (SEM) of 2% NT modified bitumen



Appendix G: Images from scanning electron microscope (SEM) of 3% NT modified bitumen

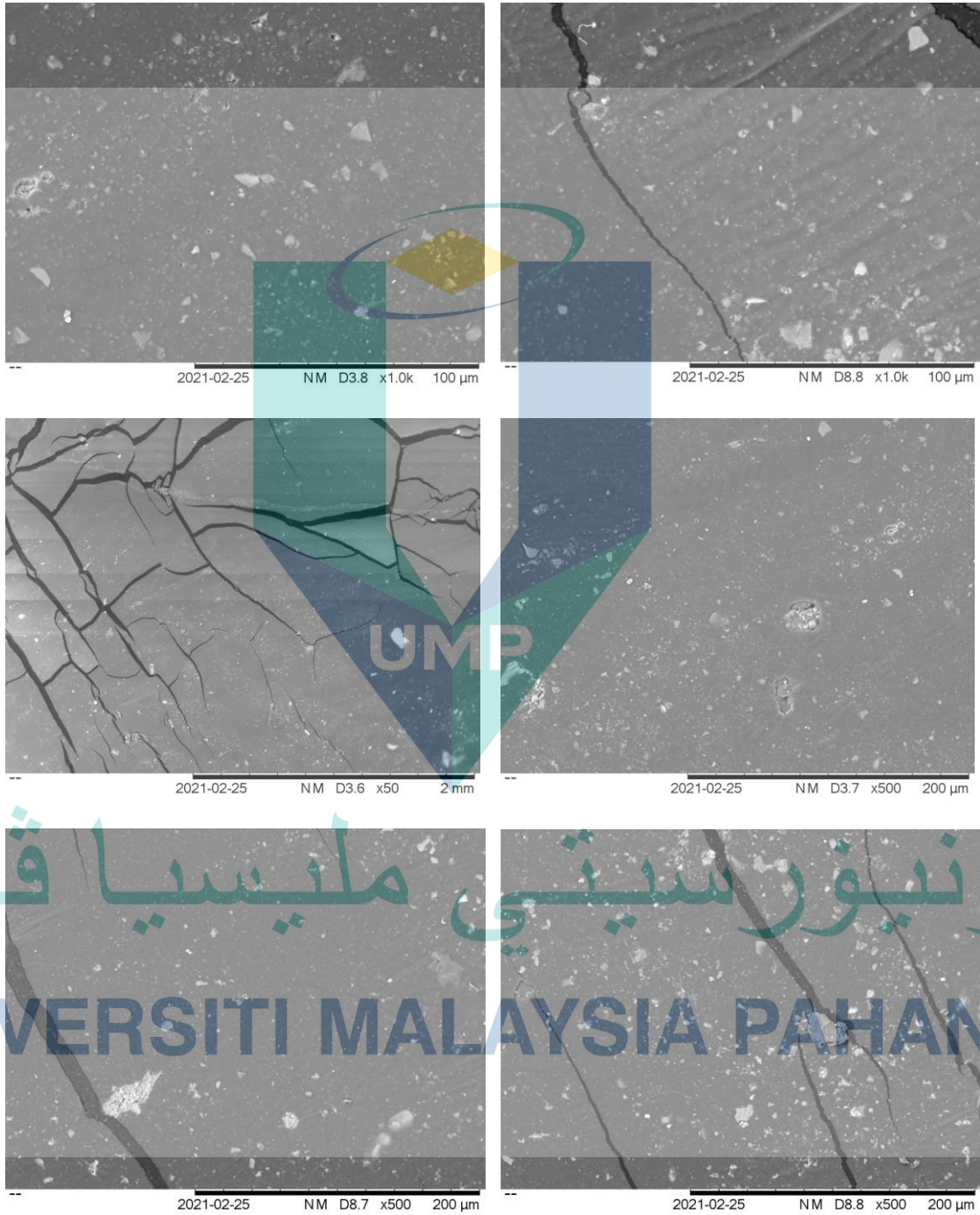


Appendix H: Images from scanning electron microscope (SEM) of 4% NT modified bitumen

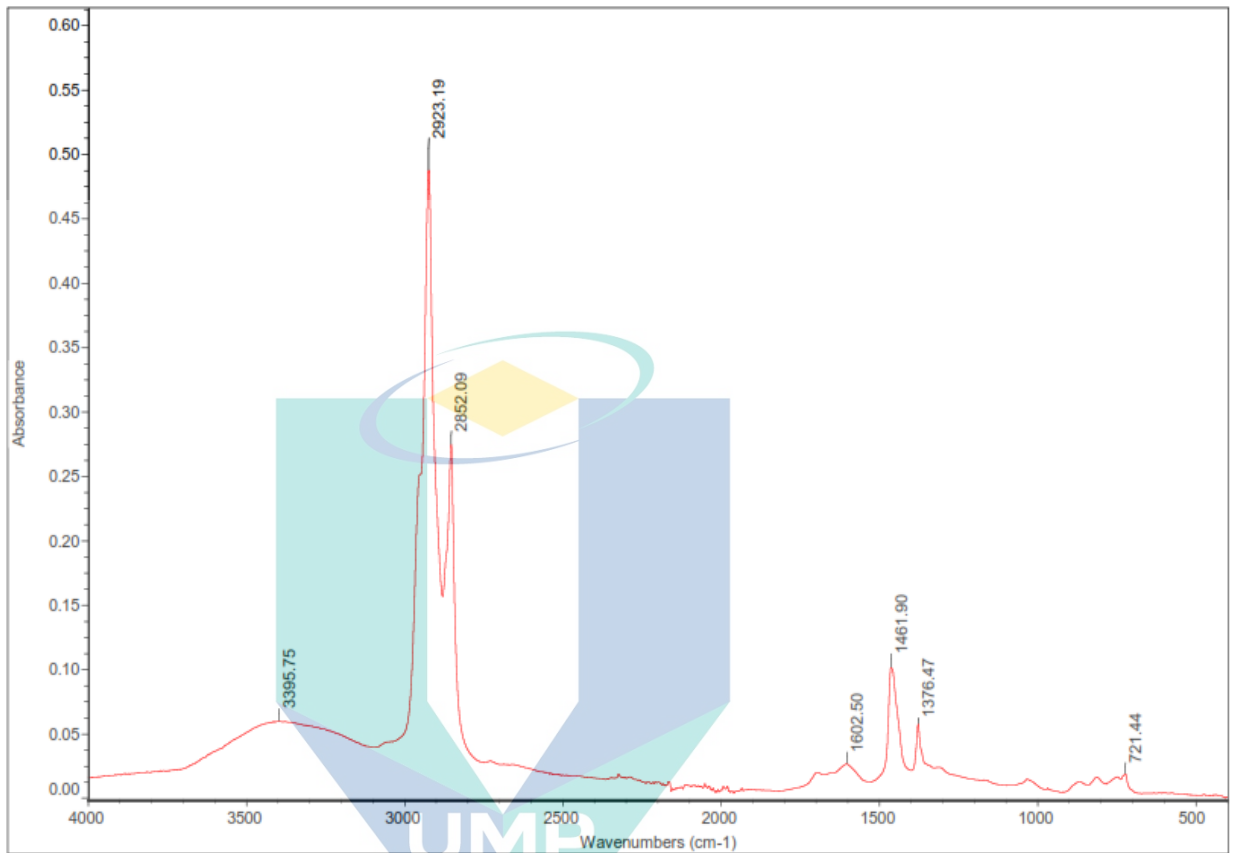




Appendix I: Images from scanning electron microscope (SEM) of 5% NT modified bitumen

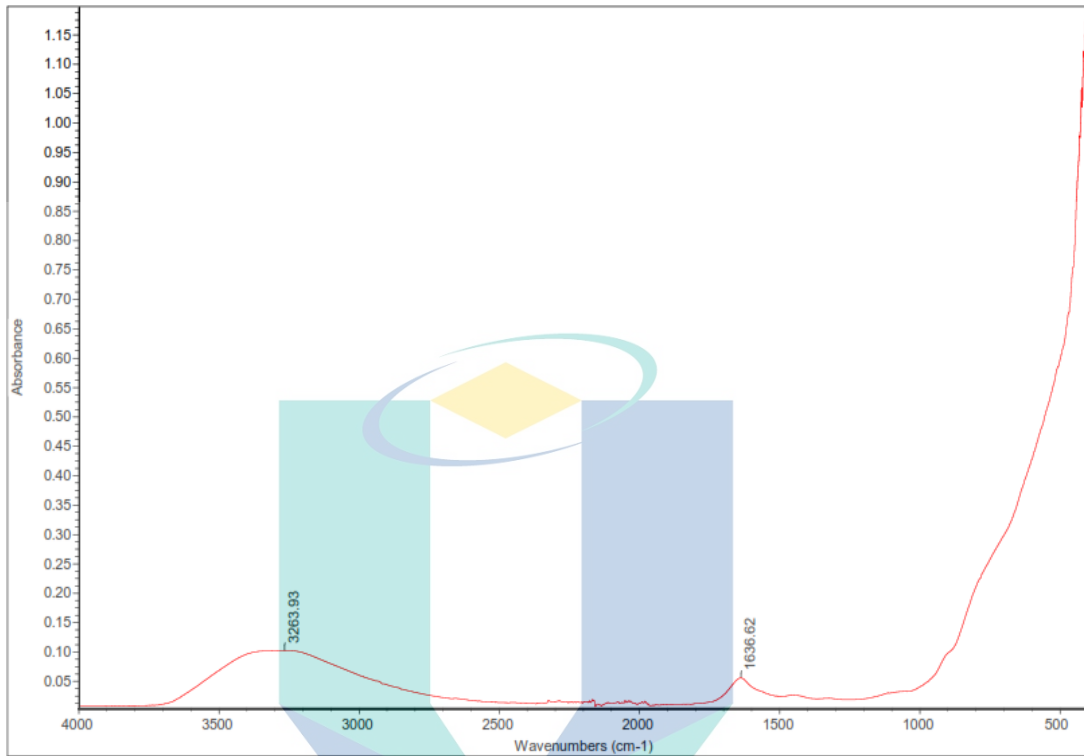


Appendix J: FTIR Absorbance peaks for bitumen



اونيورسيتي ملايسيا قهق  
UNIVERSITI MALAYSIA PAHANG

Appendix K: FTIR Absorbance peaks for nano titanium

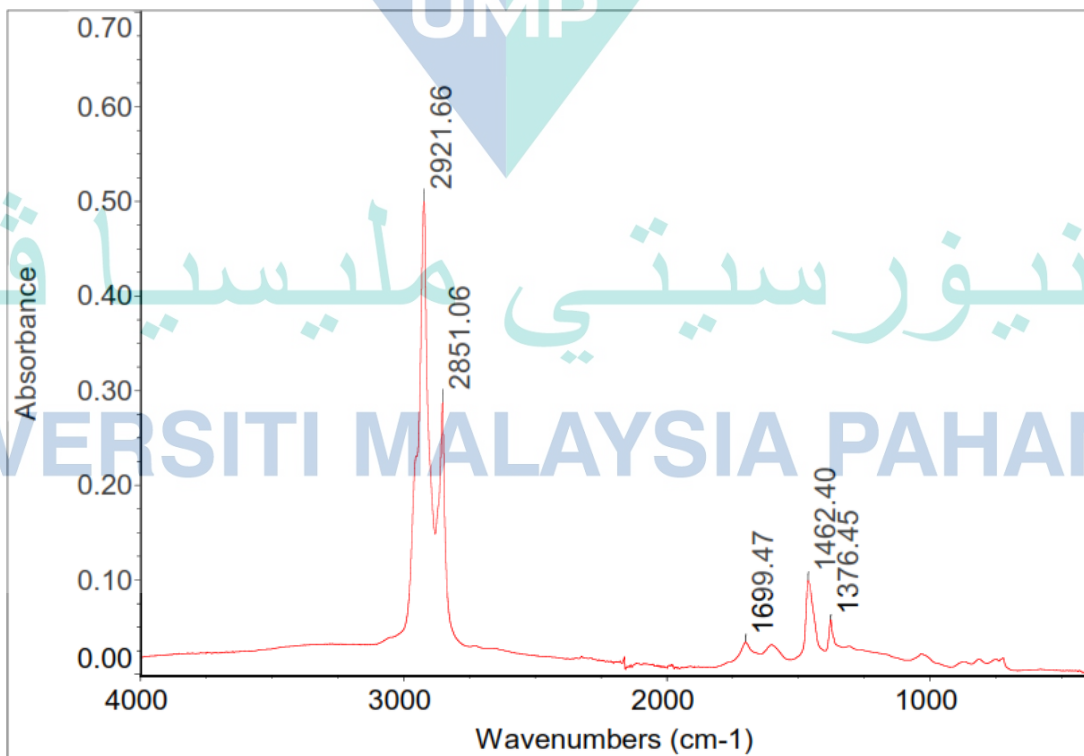
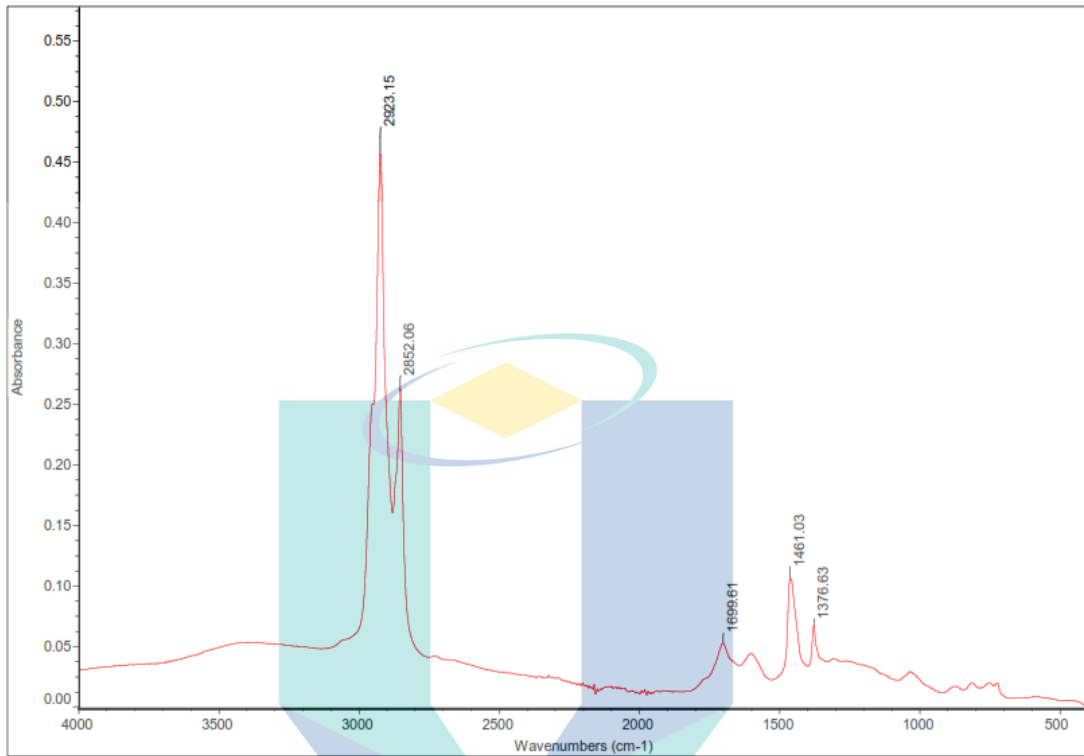


UMP

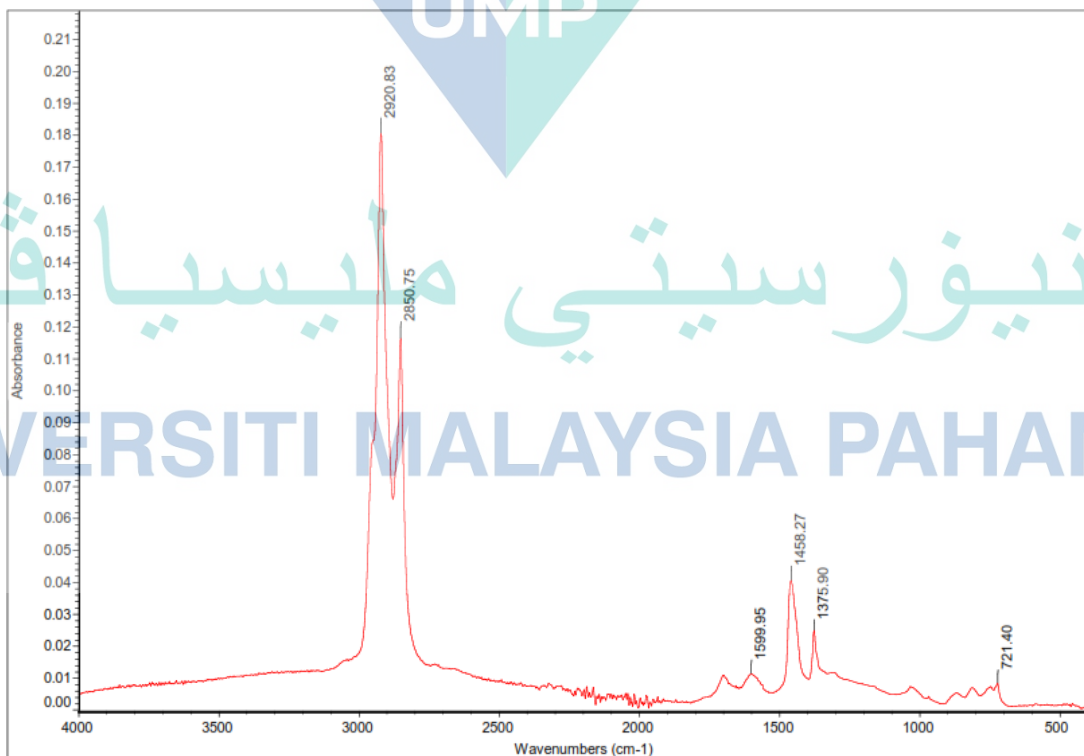
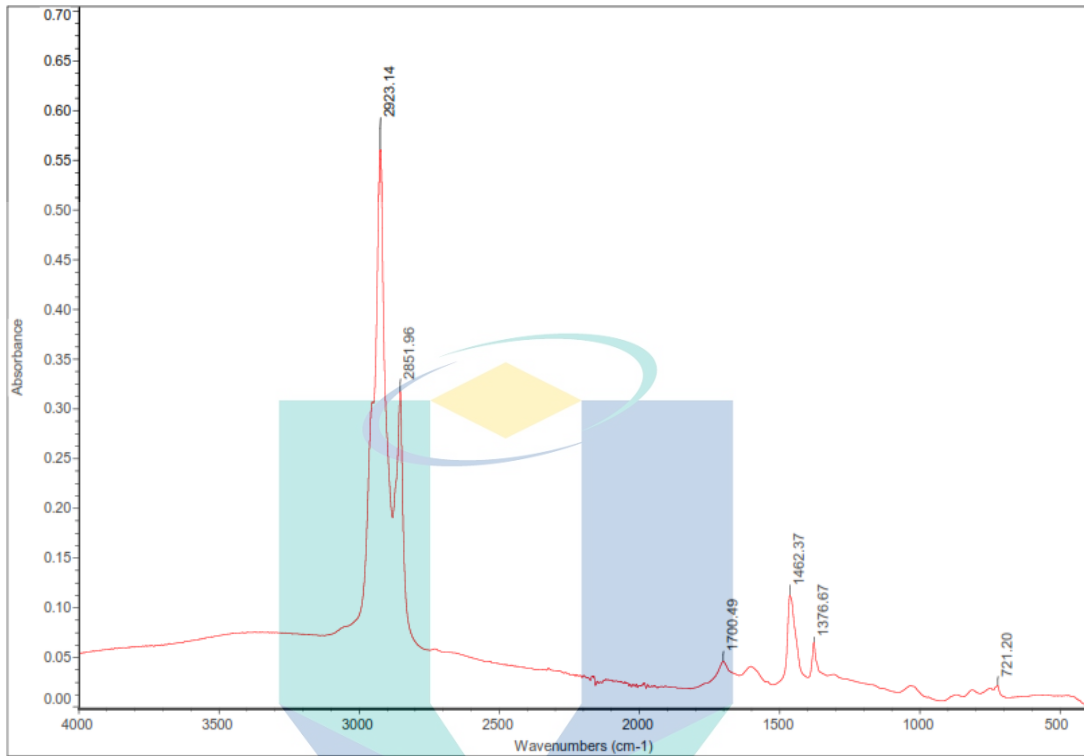
اونيورسيتي ملايسيا قهق

UNIVERSITI MALAYSIA PAHANG

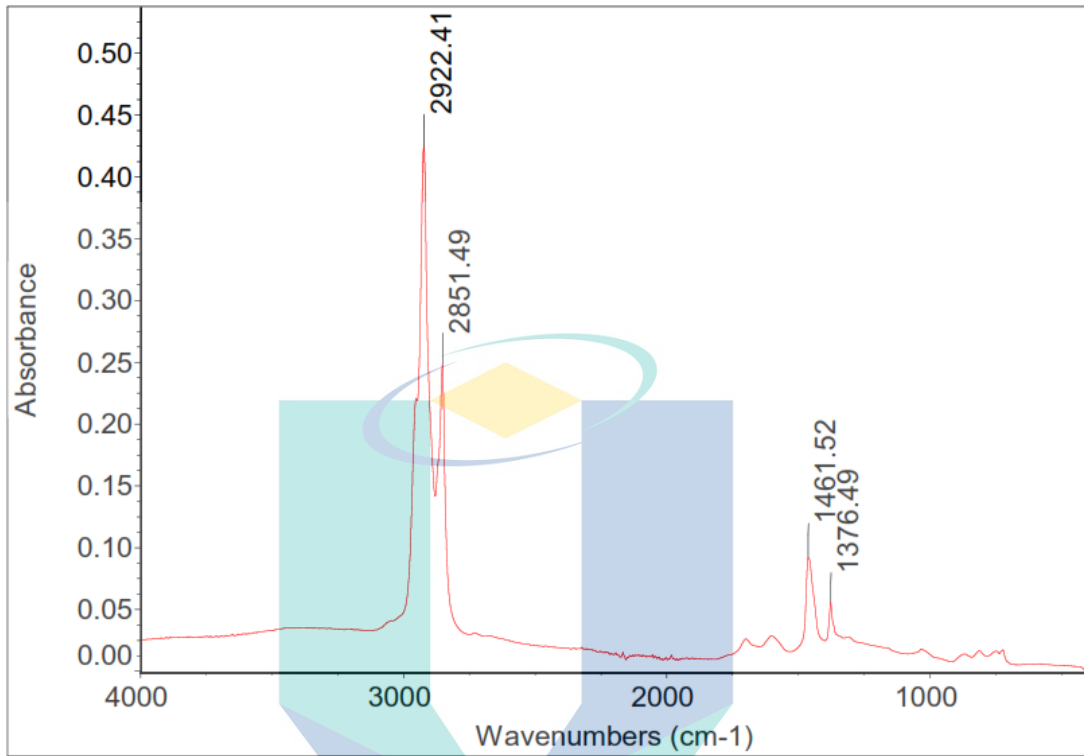
Appendix L: FTIR Absorbance peaks for 1% and 2%



Appendix M: FTIR Absorbance peaks for 3% and 4%



Appendix N: FTIR Absorbance peaks for 5%



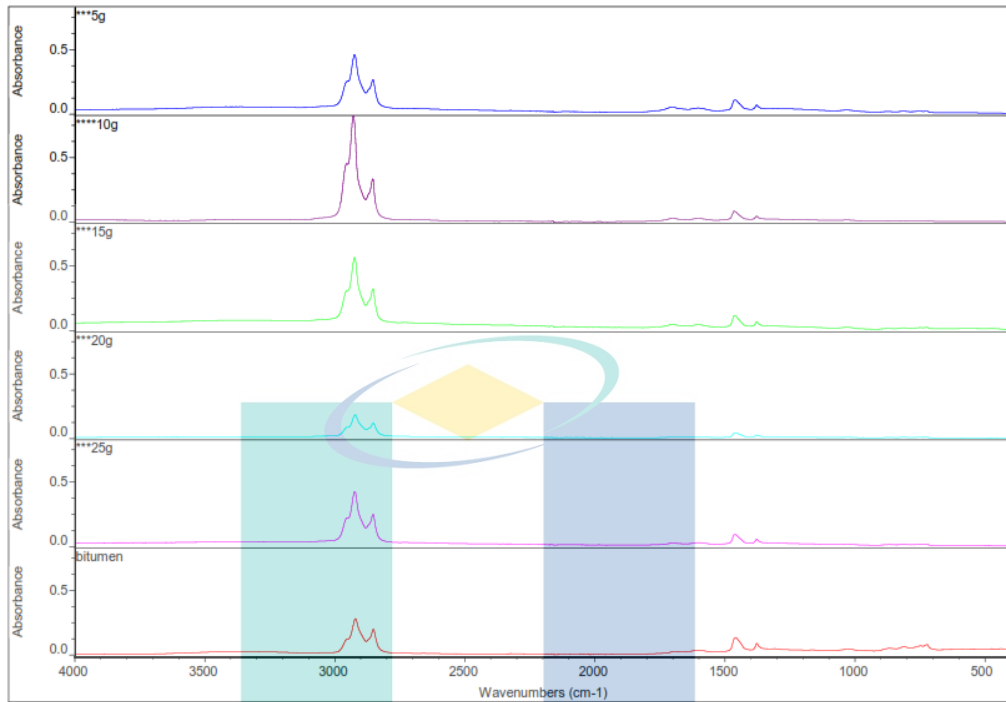
UMP

اونيورسيتي ملايسيا قهق

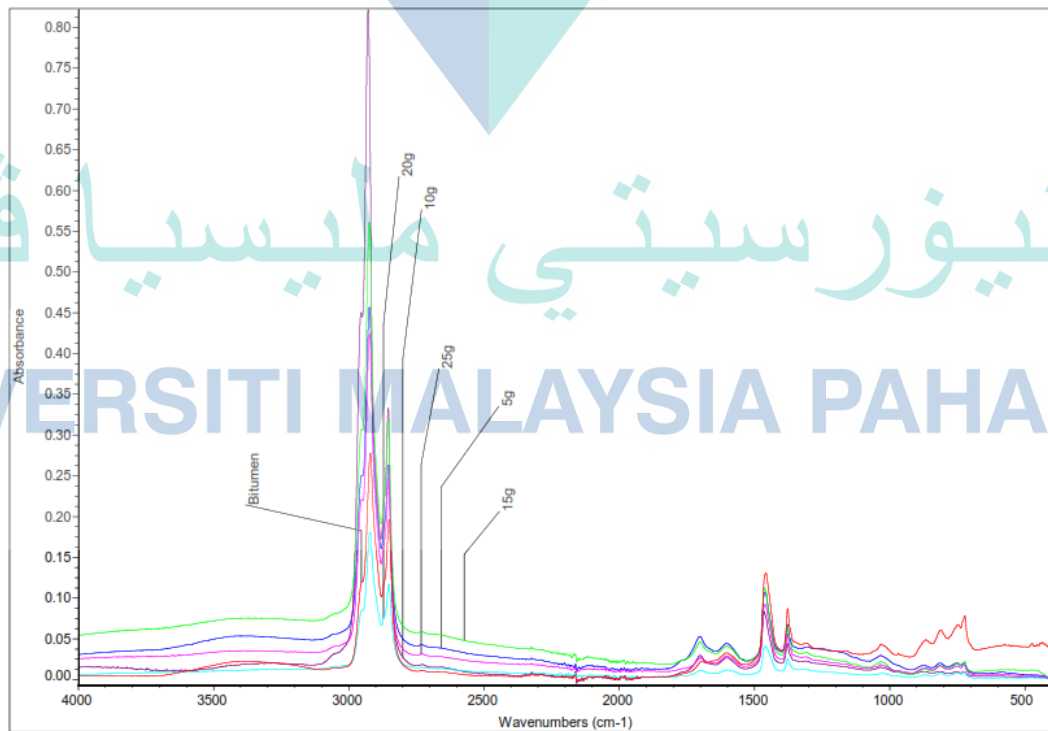
UNIVERSITI MALAYSIA PAHANG



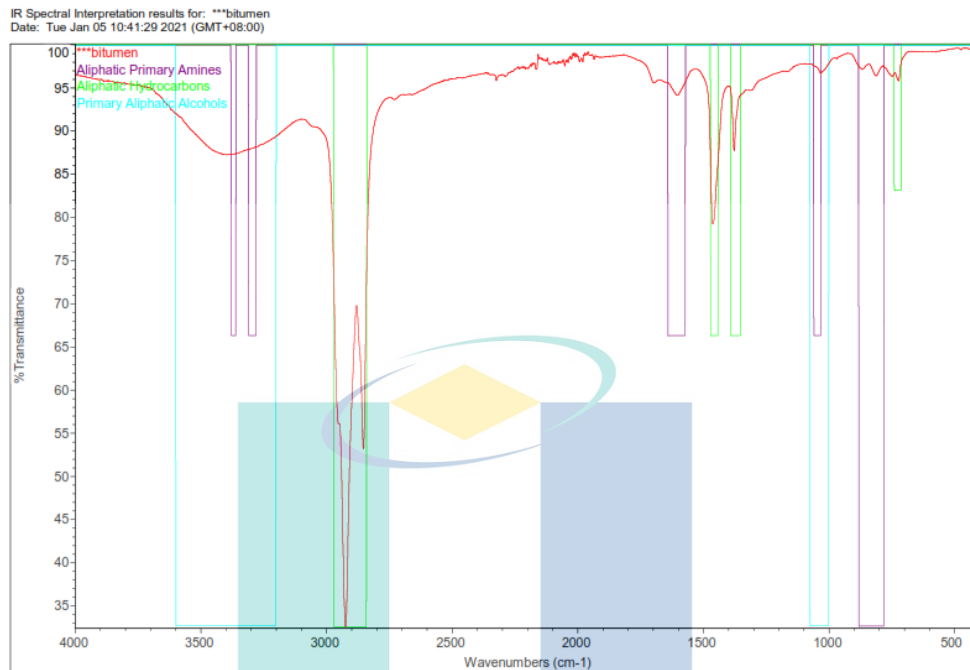
Appendix O: FTIR Absorbance peaks stacking



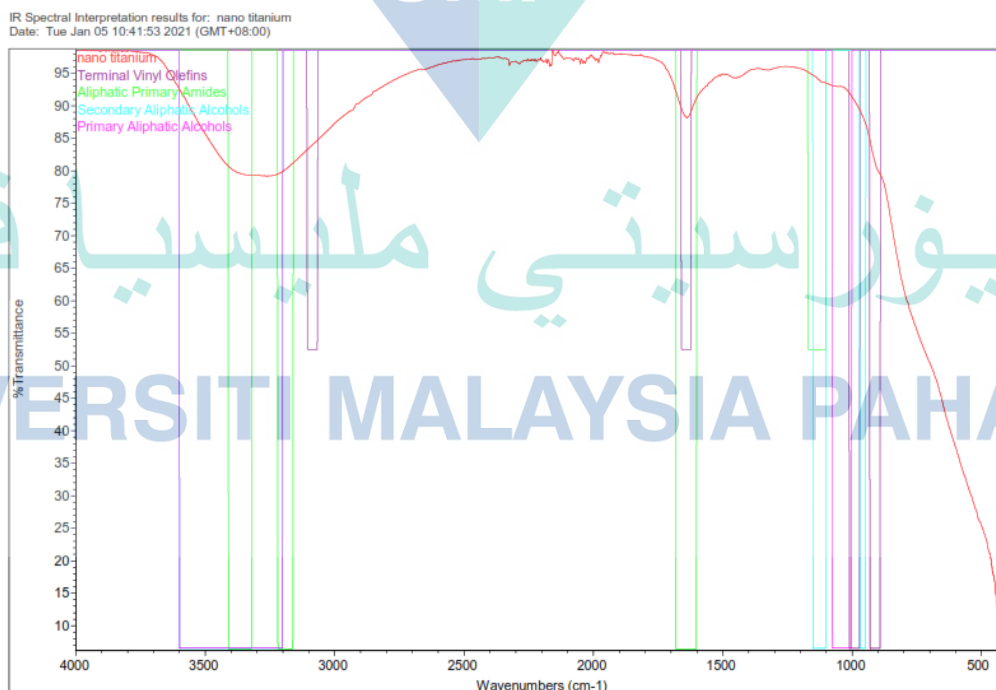
Appendix P: FTIR Absorbance peaks overlay



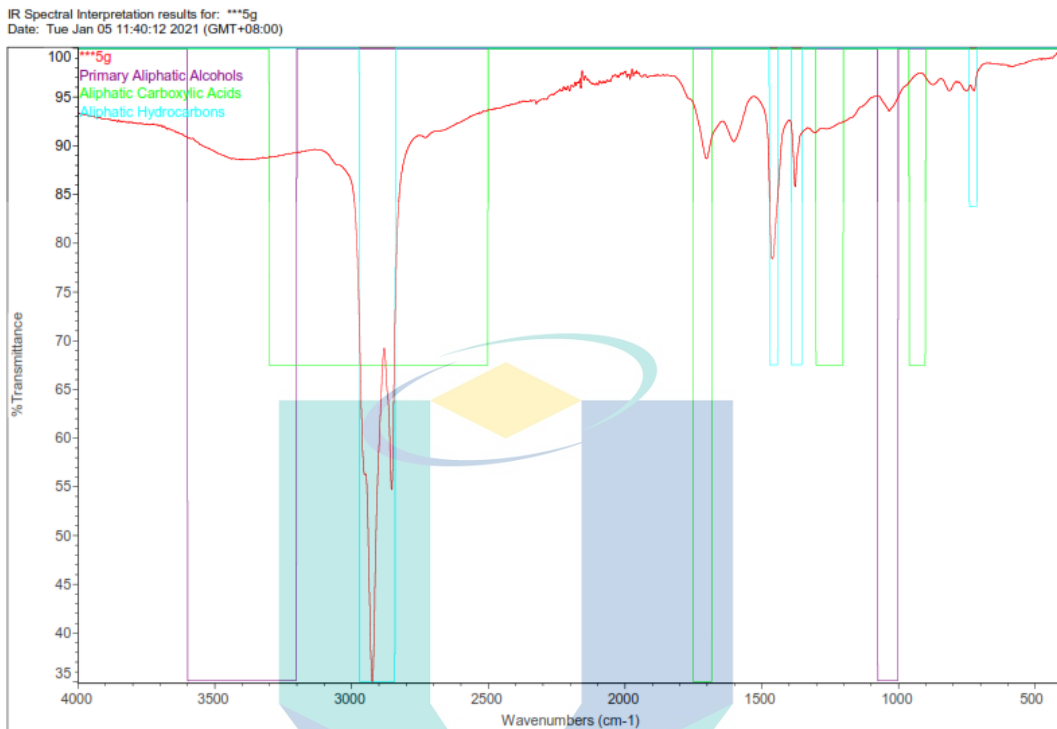
## Appendix Q: Spectral interpretation of bitumen



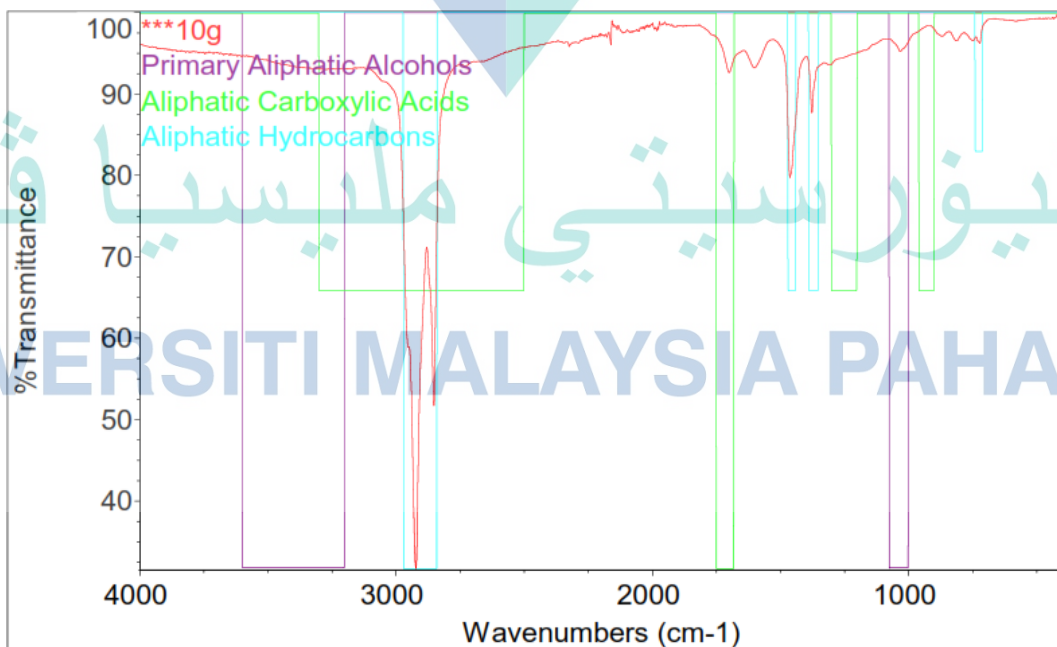
## Appendix R: Spectral interpretation of nano titanium



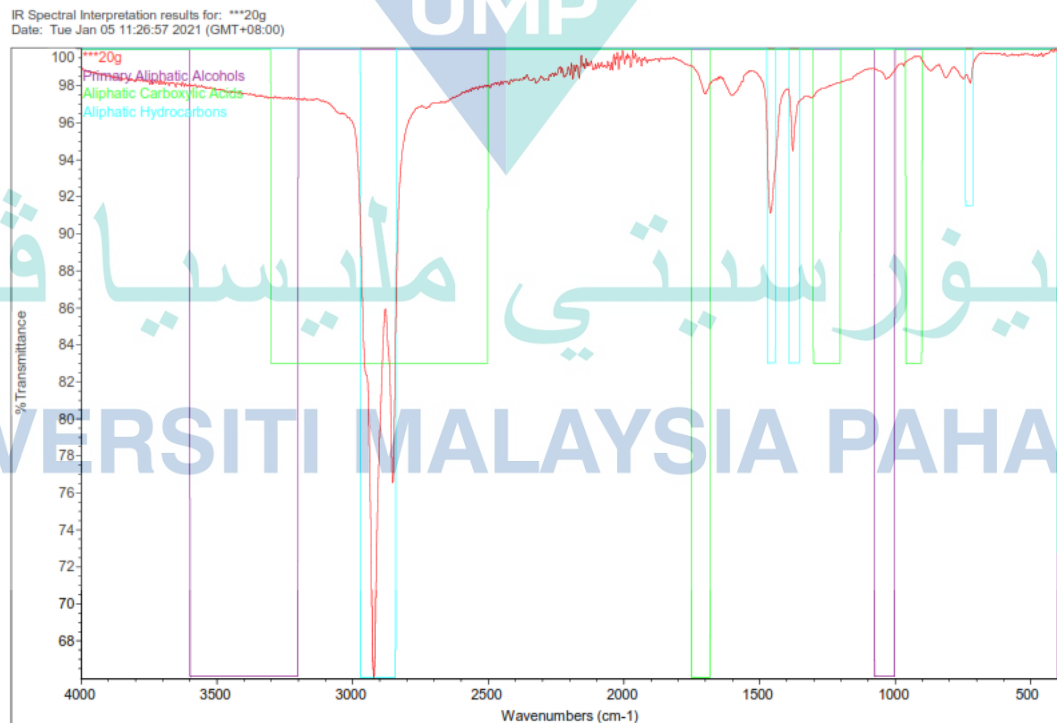
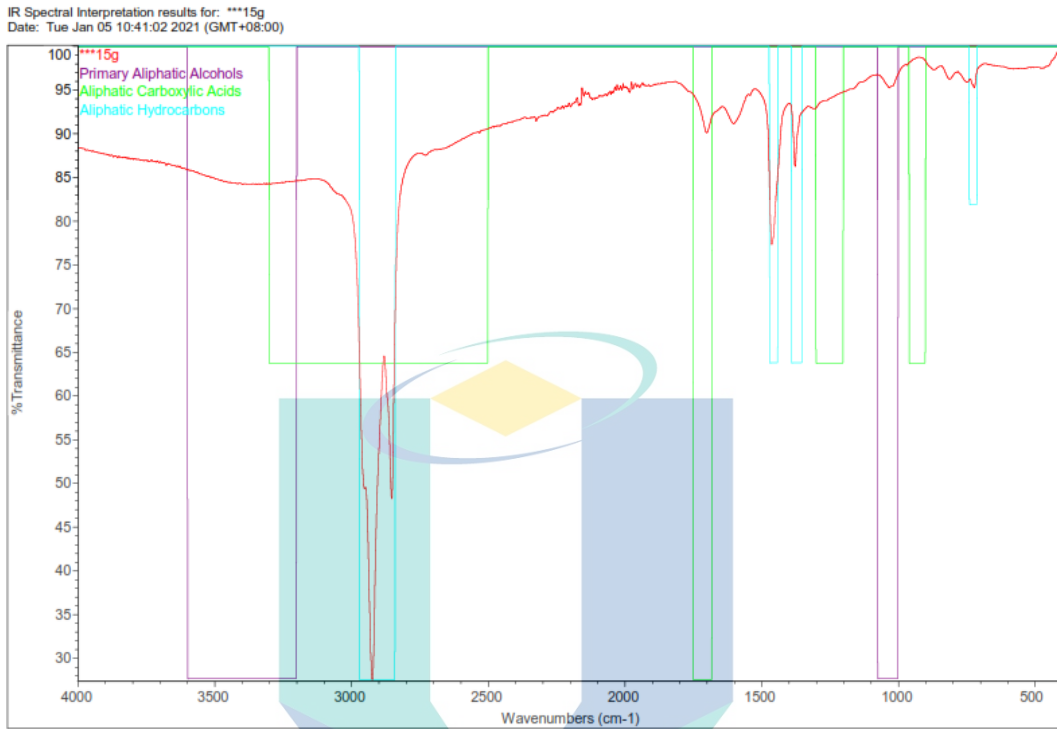
Appendix S: Spectral interpretation 1% and 2%



IR Spectral Interpretation results for: \*\*\*10g  
Date: Tue Jan 05 11:47:50 2021 (GMT+08:00)



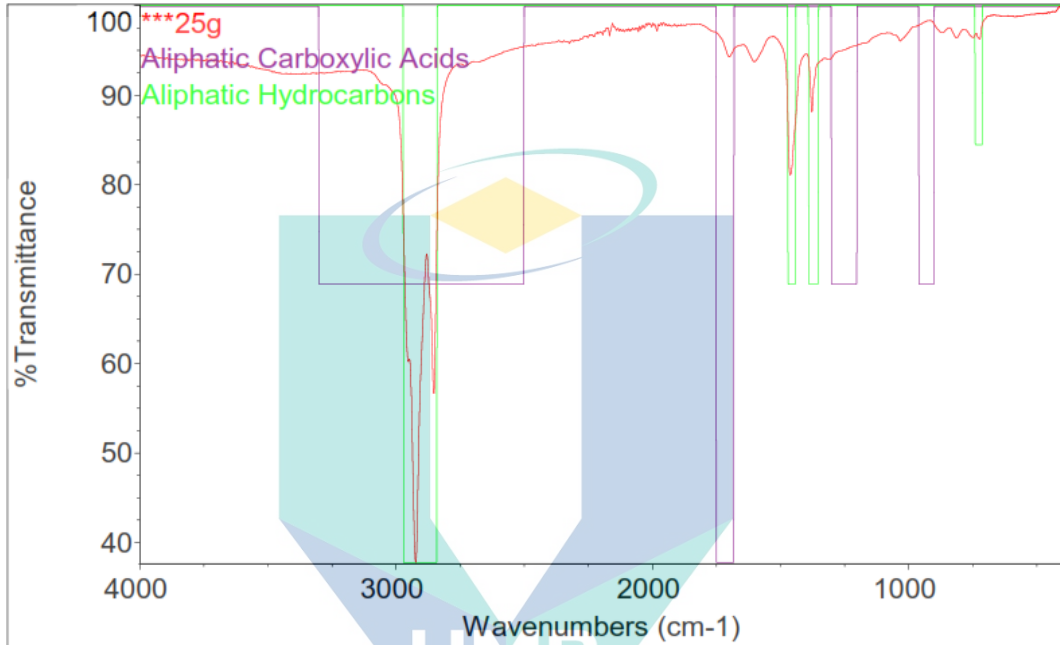
Appendix T: Spectral interpretation 3% and 4%



اونيفورسيتي ملايسيا قهق  
UNIVERSITI MALAYSIA PAHANG

Appendix U: Spectral interpretation 5%

IR Spectral Interpretation results for: \*\*\*25g  
Date: Tue Jan 05 11:52:47 2021 (GMT+08:00)



اونيورسيتي ملايسيا قهق  
UNIVERSITI MALAYSIA PAHANG